1-1-2011

Pelvic Shape, Hip Abductor Mechanics and Locomotor Energetics in Extinct Hominins and Modern Humans

Anna Warrener
Washington University in St. Louis

WASHINGTON UNIVERSITY IN ST. LOUIS

Department of Anthropology

Dissertation Examination Committee:
Herman Pontzer, co-Chair
Erik Trinkaus, co-Chair
Glenn Conroy
Charles Hildebolt
Richard Smith
Lewis Wall

Pelvic Shape, Hip Abductor Mechanics and Locomotor Energetics in Extinct Hominins and Modern Humans

by

Anna Gabriella Warrener

A dissertation presented to the
Graduate School of Arts and Sciences
of Washington University in
partial fulfillment of the
requirements for the degree
of Doctor of Philosophy

December 2011
St. Louis, Missouri

ABSTRACT

PELVIC SHAPE, HIP ABDUCTOR MECHANICS AND LOCOMOTOR ENERGETICS IN EXTINCT HOMININS AND MODERN HUMANS

by

Anna Gabriella Warrener

Habitual bipedal locomotion in hominins required major alterations in pelvic shape, particularly the recruiting of the minor gluteal muscles to act as abductors, stabilizing the pelvis during walking and running. However, significant disagreement has emerged regarding the effect of variation in pelvic breadth, in both extinct hominins and in modern humans, on hip abductor mechanics and locomotor energetics. The purpose of this dissertation was to test whether skeletal measures of pelvic width are correlated with relevant mechanical dimensions during locomotion, and how hip abductor mechanics may influence locomotor cost. Twenty-seven individuals participated in biomechanics testing, including kinematics, force plate and oxygen consumption trials. In addition, subject specific anatomical data was obtained through Magnetic Resonance Imaging.

Using an inverse dynamics approach, joint moments, effective mechanical advantage, muscle force and active muscle volume of the hip abductors, hip extensors, knee extensors and ankle plantarflexors was determined. The results show that pelvic width (biacetabular) is poorly correlated with the moment arm of ground reaction force in the coronal plane during locomotion, and therefore, hip abductor mechanics are difficult to predict from skeletal measures alone. In addition, hip abductor moments are large during both walking and running and this muscle group contributes a substantial portion

to total lower limb force production and active muscle volume. Additionally, the abductor muscle group accounts for approximately 10% of metabolic demand during locomotion. Comparisons of lower limb mechanics in males and females show few differences in effective mechanical advantage or mass-specific force production in the lower limb, although females tend to have slightly lower hip abductor effective mechanical advantage during most locomotor conditions. However, overall locomotor cost does not differ between the sexes. These results call into question the effectiveness of using pelvic skeletal dimensions to predict hip abductor mechanics in extinct hominins, and the assumption that a tradeoff exists between locomotion and parturition in females.

ACKNOWLEDGEMENTS

The work to produce this document would not have been possible without the guidance and support of many people. I am very grateful to Glenn Conroy for bringing me to Washington University and supporting me through a major academic transition and change of focus in my work. I would also like to thank Lewis Wall for giving me my first opportunity to produce a manuscript for publication, and Richard Smith for taking the time to go through my dissertation research in detail and being an important intellectual mentor both early in my graduate career and at its conclusion.

Erik Trinkaus has been a very important and supportive advisor, intellectually, logistically and emotionally. I am grateful to him for taking me on as a student in my last year of graduate work and for investing his time and energy into my research as he does with all his students. I have enjoyed many positive conversations, both on the specifics of my dissertation research and broader anthropological questions, where he has always greatly enhanced my knowledge.

I would particularly like to thank Herman Pontzer who opened an entirely new, and unknown door of intellectual inquiry for me. He has been patient as I stumbled through the beginnings of biomechanics, always respecting my intellectual capacity while I learned new material. I have learned a great deal by watching his process of inquiry and particularly through his clear and succinct style of communication. His willingness to question and investigate new territory without fear has been an important example for

me. Although I became his student somewhat by chance, I feel our collaboration has been very fruitful and I hope to continue it in the future.

I must also acknowledge the tireless work and kind support of Elaine Beffa, Kathleen Cook and Carrie Asmar-O'Guin who have all been instrumental in keeping me on track and accountable to the various agencies and institutions who provided me important funds and services to complete my research. I would also like to thank Glen Foster and Scott Love at the Center for Clinical Imaging Research for helping me to complete MRI data acquisition and always giving me a good laugh in the process. I am grateful to Campbell Rolian and David Raichlen for sharing the MatLab code they created, and to Tom Erez who dedicated many hours and provided technical expertise so that I could adapt the program for my needs. Also, my lab assistants Christina Williams, Samantha Huo and Mathew Manginni made it possible for me to collect and analyze my data. I'm also indebted to Julia Maki and Cara Ocobock for their technical and emotional support while working in the biomechanics lab.

I am very grateful to the National Science Foundation, The Leakey Foundation and the Wenner-Gren Foundation for financial support of this project. Without their generosity, this project would not have been possible.

I would like to thank my friends and family. Mercedes Gutierrez and Kate Grillo have been the best of friends. Throughout my graduate school career they have cared for my children and for me when I needed support. I feel they have given me so much, I hope now I can return their kindness and devotion. My husband's family, Cade, Tim, Grandmere, Corinne and Caitlin have also been so supportive, giving my boys and Ben

entertainment and care when I was unable to be with them. I also must thank Samuel A. Trufant (Grandpere) who saw me as both a good wife to his grandson, mother to his great grandchildren, and an important intellect. I miss talking anatomy, politics and healthcare with him. When at Washington University, I liked knowing I was walking in his footsteps in some way or another.

Finally, I must try to express my thankfulness for my parents, Ben, Clark and Aubrey. To my boys, because you love me no matter what, I could keep putting one foot in front of the other each day. I hope as you grow older, my achievement is something that will make you proud, and that you will understand the sacrifice we all made for it. To Ben, I thank you for your loyalty, understanding and constant belief in my ability, even when I didn't believe in myself. To my Mom Juliet Wittman and my Dad Bill Blackburn, you have always trusted me. You let me follow all my paths wherever they took me and believed that I would weave together a good life. Each part of my nature you have understood and helped to develop and grow. I would never have made it through without you both.

This manuscript is dedicated to

Clark Warrener and Aubrey Warrener

For reminding me that asking questions is human nature

TABLE OF CONTENTS

LIST OF FIGURES

LIST OF TABLES

CHAPTER 1
PELVIC SHAPE AND HIP BIOMECHANICS

1.1 Introduction

The distinctive architecture of the human pelvis reflects the mechanical demands of habitual bipedal locomotion, the defining adaptation of the hominin lineage. Compared to anthropoid primates, and quadrupeds in general, the human pelvis is short and broad and the iliac blades have been reoriented so that the external surface faces laterally on the body (Reynolds, 1931; Dart, 1949). This pelvic rearrangement places the minor gluteal muscles (gluteus medius and gluteus minimus) in a position to act as abductors of the lower limb instead of extensors as in other quadrupedal mammals. The abduction function of these muscles is critical for pelvic stabilization and proper gait mechanics during bipedal locomotion (Inman, 1947; Saunders et al., 1954).

During normal walking and running, gravity acts to pull the body center of mass (COM) downwards, while the muscles of the lower limb act to support and accelerate the COM upwards (Pontzer et al., 2009). In the coronal plane during single leg stance, the hip abductors prevent the drop of the pelvis, and consequently body COM, by contracting and pushing the standing leg laterally against the ground. This muscular action lifts the pelvis against the pull of gravity and minimizes the vertical oscillations of the COM (Saunders et al., 1954). The stability of the body COM in the coronal plane is important for both energetic efficiency and mediolateral balance of the body during walking and running (Saunders et al., 1954).

The mechanics dictating torque about the hip joint are based on simple Newtonian principles and can be used to predict hip abductor muscular force required for stabilization of the pelvis during single leg stance. In this model, hip abductor muscle force is a function of the magnitude of the ground reaction force (GRF) and the ratio of the hip abductor moment arm, r, to the GRF moment arm, R, known as the effective mechanical advantage (EMA) of the joint (Biewener, 1989, Figure 1.1). In previous investigations of hip abductor muscle force production, biomechanics about the hip have been modeled in a static single leg stance position where the GRF (or alternately the body weight force vector) is assumed to pass nearly vertically through the body COM (Inman, 1947; Saunders et al., 1953; Merchant, 1965). Under this assumption, one-half biacetabular width (the diameter between the centers of the femoral heads) approximates the length of R during midstance of the support phase of walking (Inman, 1947; Merchant, 1965). All else being equal, under this model greater biacetabular width would be expected to increase hip abductor force production by increasing R and thus the moment exerted by the GRF that must be resisted by the hip abductor muscles.

Increased hip abductor force production due to greater biacetabular width and R may impact both the mechanical loading of the hip joint and the metabolic cost associated with stabilization of the pelvis in the mediolateral plane. However, forces generated in the mediolateral plane have been largely ignored in the biomechanics literature (although see Eng and Winter, 1995 and Pandy et al., 2010), and it is unclear how hip abductor moments may compare to forces developed in the rest of the limb. Additionally, because locomotor cost appears to be closely tied to the amount of muscle volume that must be

activated to support body weight during locomotion (Gottschal et al., 2003; Pontzer et al., 2009), increasing hip abductor force to support the body COM in the coronal plane could potentially increase energetic expenditure during walking and running.

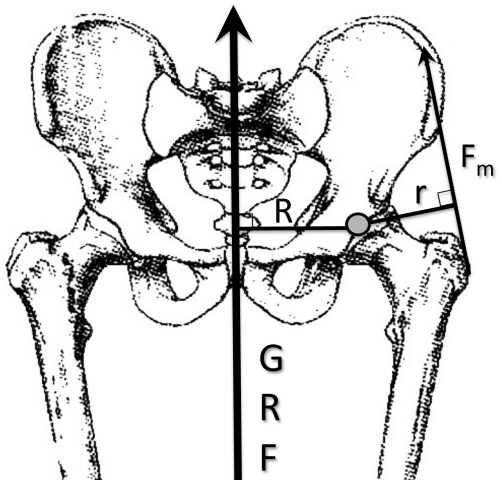

Figure 1.1. Free body diagram of the hip in the mediolateral plane. The multiple of muscle force, F_m and hip abductor muscle moment arm, r, must equal the ground reaction force, GRF, times its moment arm, R. The effective mechanical advantage of the joint is defined as the ratio of r/R.

Accurate prediction of hip abductor force production has important applications in both clinical practice and anthropological investigations of gait mechanics in living humans and extinct hominins. Hip implants and techniques for surgical repair of hip anatomy are designed around the current static single leg stance model described above (Wiesman et al., 1978; Johnston et al., 1979; Hsin et al., 1996; Fetto et al., 2002; Traina et al., 2009). The growing acknowledgement that individual variation in hip anatomy may significantly influence the performance of prosthetic devises and the restoration of

hip function after total hip replacement is driving new prosthetic design (Sariali et al., 2008; Traina et al., 2009). However, if the static single leg stance model does not provide accurate estimates of forces about the hip during locomotion, this error could have serious consequences for patient outcomes.

Additionally, anthropological investigations of gait patterns in extinct hominins have used the same biomechanical model (Lovejoy et al., 1973; McHenry, 1975; Berge, 1994; Ruff, 1998), but interpretations of the calculated hip abductor and joint reaction forces have been diverse. While some research has indicated that wider biacetabular dimensions in some hominins, particularly *Australopithecus*, may have resulted in higher hip abductor forces or otherwise compromised gait performance and energetics (Berge, 1994; Ruff, 1995, 1998), other studies have concluded that hip abductor force production was similar in early hominins compared to modern humans (Lovejoy et al., 1973; McHenry, 1975). In living humans, wider average biacetabular breadth in women is often described as resulting from a natural selection tradeoff between parturition and efficient locomotion. This idea, known as the "obstetrical dilemma" (Washburn, 1960; Rosenberg, 1992), has been used to explain both the difficulty of human childbirth and the perceived locomotor differences between men and women.

While both the clinical and anthropological interpretations of hip abductor function rest on the static single leg stance model that predicts muscle force production from skeletal measures, this model has not been tested during locomotion. Dynamic changes in the mediolateral component of the GRF or other kinematic responses during walking and running may alter the expected relationship between hip morphology and hip

abductor mechanics. Furthermore, while many anthropological investigations of hip biomechanics have concluded that locomotor economy is negatively impacted by greater biacetabular diameter, the direct contribution of the hip abductors to locomotor cost has not been established.

1.2 Research Questions

The purpose of this dissertation is to explicitly test the relationship between dimensions of the pelvis and hip abductor function during walking and running and relate hip abductor mechanics to locomotor cost. Movement profiles, force production and metabolic data were collected on 27 individuals. Additionally, while most previous biomechanical studies have relied on cadaveric specimens to obtain anatomical data, this study utilizes subject-specific skeletal and muscular measurements obtained through Magnetic Resonance Imaging (MRI). Three specific research questions were addressed:

1. ***How do hip abductor effective mechanical advantage (EMA) and muscle force production compare to other muscle groups of the lower limb?***

Muscle force production in the mediolateral plane has largely been ignored in biomechanical studies of human locomotion (Pandy et al., 2010), but Eng and Winter (1998) found external torques about the hip in the coronal plane to be substantial and comparable to those acting at the hip in the sagittal plane. Chapter 5 provides a comparative analysis of EMA and muscle force between the hip abductors, hip and knee extensors and ankle plantarflexors. These comparisons will help to place hip abductor

mechanics and kinetics within the context of lower limb force production during locomotion so that their contribution to overall locomotor mechanics and energetics can begin to be assessed.

2. ***Can R at the hip in the coronal plane and EMA of the hip abductors be predicted from skeletal dimensions of the pelvis and hip (biacetabular width and femoral neck length)?***

During locomotion, greater biacetabular width is expected to increase the moment arm of the ground reaction force vector, R, thereby reducing the EMA of the hip abductors and requiring greater force production to maintain equilibrium about the hip (Fig. 1.1). Conversely, EMA of the hip abductors will increase if the muscle moment arm, r, is increased due to greater femoral neck length. Therefore, the effective mechanical advantage of the hip abductors measured during locomotion, EMA_{loc}, will be positively correlated with the effective mechanical advantage of the hip abductors measured from skeletal dimensions, EMA_{skel} (femoral neck length/0.5 biacetabular width). Chapter 6 tests these predictions and analyzes the additional factors that may influence hip abductor mechanics during locomotion. Additionally, hip abductor EMA, mediolateral force production and pelvic kinematics in men and women are compared.

3. ***What is the relationship between active muscle volume of the hip abductors and locomotor cost? How much do the hip abductors contribute to whole body cost during walking and running?***

While the metabolic cost of locomotion is closely tied to the volume of muscle activated to support body weight (Kram and Taylor, 1990; Roberts et al., 1998; Griffin et al., 2003; Sockol et al., 2007; Pontzer et al., 2009), individual variation in locomotor cost is not entirely explained by muscle activation to produce vertical GRF (Pontzer, 2005, 2007). While muscle force required to swing the contralateral limb (Gottschall and Kram, 2005; Pontzer, 2007) and produce horizontal forces (Pontzer, 2005, 2007) are likely also substantial, the contribution of the hip abductors to total lower limb active muscle volume during locomotion may help explain inter-individual variation in oxygen consumption during locomotion. Chapter 7 quantifies the relationship between active muscle volume of the lower limb and locomotor cost and then extrapolates the metabolic demand of the hip abductors based on their muscle activation. Cost associated with the activation of the abductors and total body cost in men and women is then compared. Additionally, Chapter 8 provides further comparisons of joint moments, EMA and muscle force in men and women.

This research will provide the first empirical data relating pelvic morphology to locomotor cost during walking and running, which will be important for validating investigations of pelvic shape and locomotor mechanics in fossil hominins and modern humans. Additionally, this research increases understanding of locomotor biomechanics in the coronal plane, which has often been ignored (Eng and Winter, 1995), but which is important for the analysis of gait in clinical settings and for prosthetic development (Fetto et al., 2002; Traina et al., 2009).

CHAPTER 2
ANATOMY AND BIOMECHANICS OF THE HIP ABDUCTORS

2.1 Introduction

This chapter presents background on the anatomy and function of the hip joint and the hip abductor muscles specifically as they relate to the dynamics of gait. The mathematical model for determining hip abductor effective mechanical advantage and muscle force production is then presented and linked to locomotor performance and cost.

2.2 The hip joint

The hip joint is a congruous articulation between the femoral head and the acetabulum of the pelvis. The joint is lined by hyaline cartilage on both the surface of the femoral head and most of the acetabular cup. The hip is stabilized by a fibrous membrane and three strong ligaments, which prevent dislocation of the femoral head from within the acetabular ring (Drake et al., 2005). The hip joint has three degrees of freedom allowing flexion and extension, adduction and abduction, and internal and external rotations of femur within the joint. These movements take place about a fixed point located within the femoral head.

The primary function of the hip joint is to support the weight of the body on the lower limb during both static and dynamic movements. In upright posture, the weight of the body is transferred from the fifth lumbar vertebrae, through the sacroiliac joint and ilia, passing onto the head of the femur and down through the lower limb to the floor.

During quiet standing, the body COM is behind the hip joint center of rotation. However the strong iliofemoral ligament on the anterior surface of the hip capsule prevents the collapse of the joint against the backward pull of gravity and permits standing posture without additional muscle contractions (Drake et al., 2005).

During locomotion, the hip joint is mobile in all three planes with the largest movements taking place in the sagittal plane as the thigh flexes and extends during walking and running. Several muscles are particularly important for the movements at the hip during locomotion, gluteus maximus, iliopsoas, the hamstrings (semitendinosus, semimembranosus, biceps femoris), the adductors (adductor magnus, adductor brevis, adductor longus, pectineus, gracilis), tensor fasciae latae and the hip abductors (gluteus medius and mimimus). At the completion of swing phase and the initiation of heel strike during walking and running the hip is in a flexed position primarily due to the action of the iliopsoas muscle, but as the foot contacts the floor gluteus maximus and the hamstrings muscles initiate extension of the thigh which continues through the remainder of stance phase. The adductors are responsible for pulling the body COM over the supporting limb at foot contact and also adducting the limb as it leaves the floor and passes through swing phase of gait (Saunders et al., 1953). The hip abductors and tensor fasciae latae act to stabilize the pelvis during the stance phase of gait and are discussed in more detail in the remainder of this chapter.

2.3 Anatomy and function of the hip abductors

In humans, the hip abductor muscle group is comprised of the gluteus medius, gluteus minimus and tensor fasciae latae. The anterior gluteus maximus also plays a role in hip abduction through fibers that insert into the iliotibial band of the thigh, but it is not traditionally characterized as a primary abductor (Drake et al., 2005). Gluteus medius is the largest of the abductors (Clark and Haynor, 1987) and originates from the lateral surface of the ilium in the area bounded by the iliac crest and the posterior and anterior iliac lines (Drake et al., 2005). Gluteus minimus is a smaller muscle, deep to gluteus medius, which arises from the ilium between the anterior and inferior gluteal lines (Drake et al., 2005). Both muscles end in thick tendinous attachments on the anterosuperior aspect of the greater trochanter, with the gluteus medius more laterally positioned. The tensor fasciae latae is a smaller muscle originating from the anterior superior iliac spine (ASIS), and inserting into the fascia latae of the thigh, which forms the iliotibial band (Drake et al., 2005).

Traditionally, the minor gluteal muscles have been considered primarily as thigh abductors and pelvic stabilizers (Fick, 1910; Pauwels, 1976), though more recent research has indicated they also act to stabilize the head of the femur in the acetabulum and rotate the pelvis during locomotion (Gottschalk et al., 1989; Beck et al., 2000). During walking and running, the gluteus medius produces a phasic contraction, first activating the posterior portions of the muscle during early stance to stabilize the femoral head in the acetabulum, while the middle and anterior portions fire slightly later, initiating abduction and pelvic rotation during midstance (Gottschalk et al., 1989) and the second half of

stance phase (Pandy et al., 2010). The tensor fasciae latae is most active at midstance. Its more vertical orientation and lateral placement on the pelvis gives the tensor a long moment arm relative to the minor gluteals, which enhances its force contribution to pelvic stabilization (Gottschalk et al., 1989). Gluteus minimus appears to function primarily as a stabilizer of the femoral head within the hip socket (Gottschalk et al., 1989; Beck et al., 2000). However, functional MRIs taken just after abduction exercises showed increased signal intensity from the muscle, indicating activity related to these abduction tasks (Kumagai et al., 1997). Taken together, the hip abductor group acts dynamically to both stabilize the femoral head in the acetabulum as well as abduct the thigh during single leg support in walking and running.

The importance of the hip abductor muscles for proper walking and running mechanics is well recognized. During normal bipedal gait in humans, the body center of mass (COM) is displaced both vertically and horizontally as the trunk moves over the supporting limb (Saunders et al., 1953). This displacement is minimized by several stereotyped movements of the pelvis and lower limb, including tilting of the pelvis in the coronal plane by approximately 5 degrees down towards the swing side (Saunders et al., 1953). This movement minimizes the rise of the COM at midstance and adducts the supporting limb, which reduces the horizontal shift required at the step-to-step transition (Saunders et al., 1953). By minimizing these vertical and horizontal shifts, tilting of the pelvis helps to reduce energetic expenditure during locomotion (Saunders et al., 1953).

While normal gait is characterized by some degree of pelvic tilt during single limb support, excessive tilting of the pelvis caused by weakness or paralysis of the hip

abductor muscles results in severe gait abnormalities. Affected individuals are unable to control the medial drop of the pelvis during single leg support, a condition known as Trendelenburg sign (Inman, 1947; Drake et al., 2005). The effect on walking mechanics is dramatic. The impairment results in a lurching gait where the trunk is thrown laterally over the supporting limb in an attempt to balance the body during single leg stance (Inman, 1947). Patients with Trendelenburg gait symptoms related to proximal femoral prosthetic reconstruction were documented to have a 141% increase in locomotor cost compared to normal control subjects (Kawai et al., 2000). Energetic costs were highest in patients with the weakest hip abductors (Kawai et al., 2000).

In addition to muscular contraction, the iliotibial band may contribute significantly to pelvic stabilization during locomotion (Fetto et al., 2002). Because predicted force measurements of the hip abductors were substantially larger than actual forces determined through electromyography, Inman (1947) argued that, through passive tendon strain, the iliotibial band aided the hip abductors in counterbalancing the pelvis during single leg support (although see Merchant (1965) and McLeish and Charnely (1970) for discussion). Passive resistance by the iliotibial band could help explain why above knee amputees are unable to maintain pelvic stability during locomotion, while pelvic stabilization is unaffected in below knee amputees (Fetto et al., 2002). In both groups the minor gluteals remain intact, but the iliotibial band has been transected in above knee amputees, and the resulting impairment suggests that the minor gluteals are not solely responsible for preventing pelvic tilt during locomotion.

2.4 Effective mechanical advantage and muscle force in the hip abductors

In order to maintain equilibrium about a joint, the external force, estimated as the body weight moment arm from the body center of mass or directly measured from the ground reaction force (GRF) and external moment arm, the perpendicular distance from the joint center of rotation (COR) to the GRF line of action, must be equal to the multiple of muscular force and the muscle moment arm, defined as the perpendicular distance from the COR to the muscle's line of action (see Fig. 1.1). Inertial and gravitational forces of the body segments must also be accounted for to obtain mathematically accurate values for moments about a joint (Winter, 2005). This is particularly important at more proximal joints of the body, where these forces will be greatest during movement (Winter, 2005).

At the hip in the mediolateral plane, the external force vector passes medially to the hip joint center and the hip abductors must produce force to prevent the pelvis from dropping away from the supporting limb. The required muscular force is determined by the magnitude of the external force, here described as the GRF, and the lengths of the GRF moment arm and the hip abductor moment arm.

$$GRF \times R = F_m \times r \quad (1)$$

where R is the moment arm of the GRF vector, r is the moment arm of the hip abductor muscles and F_m is the force of the hip abductor muscles, then

$$F_m = GRF \times R/r \quad (2)$$

The effective mechanical advantage, EMA, of the joint is defined as the ratio r/R (Biewener, 1989), so the equation can be rewritten as

$$F_m = GRF \times 1/EMA \quad (3)$$

Larger GRF or poor EMA at a joint will increase the muscle force required to maintain the joint in equilibrium.

Previous investigations of hip abductor force production have measured force during static single leg support, with the assumption that this posture accurately reflects at least the minimum loading of the hip during locomotion (Inman, 1947; Merchant, 1965; McLeish and Charnley, 1970). The experimental techniques have varied from biomechanical analysis of subjects standing on one extremity with the pelvis at different levels of inclination (Inman, 1947; McLeish and Charnley, 1970), to experimental rigs where an articulated pelvis and femur were outfitted with strain gauges to approximate muscle action during loading (Merchant, 1965).

The body center of gravity during single leg support is generally assumed to lie in the median sagittal plane, and therefore the distance from the center of the femoral head to this plane is determined either by calculating one-half biacetabular distance or the distance from the femoral head to the lower lumbar vertebrae (Inman, 1947, Saunders et al., 1953; Merchant, 1965). This estimation implies that, all else being equal, EMA of the hip abductors would decrease as pelvic width increased because the GRF moment arm is linearly related to pelvic width. Conversely, EMA of the hip abductors would improve as femoral neck length increased, providing better mechanical leverage for these muscles. In their study of hip biomechanics, McLeish and Charnley (1970) adjusted their measurements of body weight moment arm in accordance with pelvic inclination, pointing out that single leg stance is not a symmetrical posture. However, the two

subjects in their study produced pelvic tilt in very different manners by altering the position of the spine, which seems unlikely to reflect actual posture during locomotion.

Inman (1947) calculated both a theoretical torque, based on radiographs of the pelves of 35 individuals to obtain a minimum value of the body weight moment arm, and experimental torques determined from electromyography of the hip abductors during single leg stance. The results for experimentally determined torque were significantly lower than the theoretically estimated values (by an average of 9.3% and 8.9% in males and females respectively), which Inman (1947) attributed to the passive role of the iliotibial band in counteracting body weight. Muscle force of the hip abductors was found to be approximately 1.65 times body weight, or 2430N for a 68kg man (see Merchant, 1965). By comparison, McLeish and Charnely (1970) found hip abductor muscle force to be approximately 1.3 times body weight while the pelvis was level but as high as 2.25 times body weight when the pelvis sagged away from the supporting limb. Using an experimental rig, Merchant (1965) found hip abductor muscle force to be 1509N for a pelvis in neutral position, or approximately equal to body weight, with an increase of over 100% as the pelvis was adducted away from the support side by 30 degrees. These findings contradicted those of Inman (1947) who reported the highest torque values at the hip when the pelvis was abducted towards the support limb.

More recent studies have demonstrated that torque about the hip in the mediolateral plane is substantial during locomotion, about 1.3Nm/kg body mass (Eng and Winter, 1995; Perron, 2000). This figure is comparable to the moment about the hip in the sagittal plane during walking (Eng and Winter, 1995; Perron, 2000; Pandy et al.,

2010). However, the assumptions that the body weight moment arm can be determined from skeletal dimensions, and that static single leg stance can approximate the dynamics of locomotor movement have not been fully explored.

A recent analysis of the whole body center of mass movement in the mediolateral plane seems to contradict some of the tenets of the hip abductor model as currently understood. Pandy et al. (2010) described the mechanics of mediolateral balance, not as a problem of creating equilibrium between the hip abductors and gravity pulling the body center of mass medially, but as a dynamic problem where the center of mass is being pulled laterally by muscular contraction (vastus, soleus, gastrocnemius, hip adductors and ankle everters) and gravity. This lateral pull must be opposed by the generation of a medial acceleration of the body center of mass created by the abductors. This means that the hip abductors generate a lateral force on the ground, which keeps the body center of mass medial to the support limb throughout stance phase (Pandy et al. 2010) instead of specifically preventing excessive pelvic tilt as traditionally thought. If confirmed, these results would fundamentally alter the model of hip abductor force production and require reevaluation of the interaction between skeletal architecture and locomotor dynamics in the mediolateral plane.

2.5 Locomotor cost and force production models

Variation in locomotor cost, both within and among species, has been investigated for over a century, (Taylor et al., 1970; Pontzer, 2007), but it is only in the last twenty years that the anatomical and physiological underpinnings determining this variation have

been illuminated (Pontzer, 2007). Locomotor cost derives primarily from the rate of muscular force production required to support the body during the course of ground contact (Kram and Taylor, 1990; Roberts et al., 1998a; Roberts et al., 1998b; Griffin et al., 2003; Pontzer, 2005; Pontzer, 2007). Longer contact times decrease the rate of muscle force production, reducing metabolic cost (Kram and Taylor, 1990; Pontzer, 2005, 2007), which helps to explain why larger animals, with longer limbs, have lower costs per kilogram per meter traveled than smaller animals (Taylor et al., 1970; Taylor et al., 1982). Limb length is also an important determinant of cost in humans particularly at a walking gait (DeJaeger 2001; Pontzer, 2005, 2007). However, external work to accelerate the body center of mass, the production of horizontal GRF and muscle force required to swing the contralateral leg must also be accounted for in within-species comparisons of cost (Pontzer, 2005, 2007).

Limb posture also affects muscle force production during locomotion. More extended limbs in large animals decrease the external moment arm about the joints, increasing muscle EMA, which reduces muscular force and metabolic cost (Biewener, 1989; Biewener et al., 2004). Additionally, muscle fiber length plays a role in determining metabolic cost. Muscles with long fibers will activate more volume per unit force produced, which increases the energetic cost (Roberts et al., 1998a; Roberts et al., 1998b; Pontzer et al., 2009).

While a number of studies have explored the relationship between force generation and locomotor cost in humans (Gottschall and Kram, 2003, Griffin et al., 2003; Pontzer 2005, 2007), they have been focused on movements in the sagittal plane.

The energetic demands of mediolateral control of the body have largely been ignored, although it is often assumed that greater pelvic breadth will decrease locomotor efficiency (Zihlman and Brunker, 1979; Meindl et al., 1985; Rosenberg, 1992; Biewener et al., 2004). Because women, on average have wider pelves than men (Tague, 1989, 1992) numerous investigations have attempted to quantify differences in locomotor cost between males and females. Bunc and Heller (1989), Bourdin et al. (1993) and Hall et al. (2004) all reported no statistical difference in either walking or running economy between the sexes when comparably trained athletes were tested under similar conditions. In contrast, Bhambhani and Singh (1983) found significantly higher running costs in females when controlling for body mass, while walking speeds were not different between men and women. However, when cost was adjusted for stride frequency, the differences between the sexes disappeared. Ariëns et al. (1997) found females to have better economy than males in their sample. The inconsistency of these results derives partly from methodological differences. However the lack of consensus illustrates that the biomechanical relationship between pelvic shape and locomotor cost is more complex than previously thought (Williams, 1987).

Large external torques about the hip in the mediolateral plane during locomotion (Eng and Winter, 1995; Pandy et al, 2010) must be balanced by equal force produced by the hip abductors in proportion to their mechanical advantage. As discussed above, EMA at the hip joint is a ratio of the mechanical moment arms of GRF and the hip abductors measured during locomotion, r/R (Biewener, 1989; Biewener et al., 2004). Low EMA, will increase the amount of muscular force required by the hip abductors to oppose

external torque about the joint, while larger EMA will decrease the force that must be produced by these muscles. This mechanical relationship links body kinematics to locomotor cost. By extension, anatomical variability that decreases EMA, will in turn, increase metabolic demand during locomotion. By specifically linking hip anatomy and pelvic breadth (biacetabular diameter) to the mechanics of hip abductor force production during locomotion, the hypothesis that wider pelvis in women and extinct hominins increases locomotor cost can be addressed with greater accuracy.

CHAPTER 3
ANATOMICAL VARIATION IN THE PELVES OF EXTINCT HOMININS AND MODERN HUMANS

3.1 Introduction

In this chapter variation in pelvic morphology among extinct hominin genera and in living humans is described in detail. Previous biomechanical interpretations of this variation are presented and discussed with particular reference to their application for understanding locomotor energetics and gait kinematics in early hominins. The influence of locomotor demands and parturition on sexual dimorphism in the modern human pelvis, with particular reference to the "obstetrical dilemma," is also discussed.

3.2 Pelvic anatomy related to bipedal locomotion

Selection for bipedal locomotion has dramatically altered the shape of the hominin pelvis from the condition seen in quadrupeds and apes. The ilium has become shorter, broader and oriented more laterally, which places the minor gluteal muscles in a position to abduct the lower limb and stabilize the pelvis during locomotion (Reynolds, 1931; Jordaan, 1976; Stewart, 1984; Lovejoy, 1988; Lovejoy et al. 2005). The ischium has an expanded and posteriorly projecting tubercle that provides the hamstring muscles greater mechanical advantage in an upright posture (Lovejoy et al., 2005). The anterior inferior iliac spine (AIIS) is formed by a secondary ossification center, unlike other primates (Lovejoy, 2005) and is large and anteriorly projecting. The sacrum is also wider

and more cephalically oriented than in other primates with an enlarged sacroiliac articulation (Reynolds, 1931; Jordaan, 1976). These morphological changes alter muscular function in accordance with the demands of bipedalism (i.e. the abductors and hip extensors). Additionally, in bipeds the pelvic viscera must be supported against the downward pull of gravity requiring increased support from the fascial and muscular diaphragms of the pelvis (Wilson, 1973 cited by Jordaan, 1976; sources).

While many of these morphological adaptations are present to some degree in all hominin pelves currently known, variation in pelvic shape throughout the hominin lineage may be related to the shifting requirements of parturition and functional changes in gait during human evolution (Lovejoy et al., 1973; Rak, 1990; Tague and Lovejoy, 1986; Lovejoy, 1988; Tague, 1992; Walker and Ruff, 1993; Berge, 1994; Ruff, 1995, 1998; Bramble and Lieberman, 2004; Lovejoy et al, 2005: Berge and Goularas, 2010). Table 1 gives relevant pelvic dimensions for the most complete fossil specimens. The interpretations of the functional significance of this variability have produced divergent opinions regarding just what locomotion and birth looked like in our ancestry. The following sections discuss the morphology and biomechanical interpretations of the pelvis, particularly related to hip abductor function, in extinct hominins and modern humans.

Table 3.1. Pelvic dimensions in fossil hominins and modern humans of European American descent

	A.L. 288-1[1] *A. afarensis*	**Sts 14**[2] *A. africanus*	**Gona BSN49/P27**[3] *H. erectus*	**KNM-ER 15000**[4] *H. erectus*	**SH Pelvis 1**[5] 'archaic' *Homo*	**Kebara 2**[6] *H. neanderthalensis*	**Male**[6] *H. sapiens*	**Female**[8] *H. sapiens*
Date (Ma)	3.2	2.4	1.8	1.5	0.6	0.5	-	-
False Pelvis (cm)								
Bi-iliac	26.8	25.6	28.8	22.5	34.0	30.5	27.7±1.5	26.9±1.8
Inlet AP	7.7	8.3	9.8	8.8	12.1	11.8	10.2±0.9	11.1±0.8
Inlet ML	12.4	11.6	12.4	10.0	13.8	14.2	13.0±0.8	13.4±0.8
True Pelvis (cm)								
Midplane AP	8.5	7.3	11.1	-	13.3	9.4	11.9±0.7	12.7±0.8
Biacetabular	11.8	10.7	13.1	10.2	13.3	12.9[+]	11.8±0.7	12.6±0.7
Bispinous	9.4	9.3	11.4	10.5	10.8	-	8.6±0.6	10.2±0.4
Outlet AP	8.8	8.5[*]		-	12.6	8.8	11.1±0.8	11.9±0.9
Outlet ML	8.7	10.5	13.3	12.6	13.5	11.4	10.2±1.0	12.0±0.9

[1]Schmid (1984), [2] Berge and Goularas (2010), [3] Simpson et al. supplemental (2008), [4] Walker and Ruff (1993), [5] Arsuaga et al. (2007), [6] Tague (1989) data for white males and females, [7], [*] Häusler and Schmid (1995), [+] Rak and Arensburg (1987).

3.3 Fossil hominin pelvic shape

3.3.1 *Ardipithecus*

The recent description of the relatively complete skeleton of *Ardipithecus ramidus*, from Afar, Ethiopia has been interpreted to indicate that skeletal adaptations for bipedalism evolved in a mosaic nature (Lovejoy et al., 2009). Unfortunately, the pelvis is not well enough preserved to determine transverse diameters accurately, but based on the virtual reconstruction of the very fragmentary remains (Lovejoy et al., 2009) the ilia

appear to be shortened and broad when compared to those of chimpanzees', and they have been reoriented into the sagittal plane as in later hominins (Lovejoy et al., 2009). This pelvic reorganization indicates the recruitment of the minor gluteals as lower limb abductors and pelvic stabilizers during bipedal locomotion. However, other aspects of the pelvis appear to be more ape-like. The hamstrings attachment is inferiorly oriented, which would have been advantageous for climbing, but less effective for extending the lower limb during bipedal locomotion (Lovejoy et al., 2009). Features of the foot associated with climbing, and ape-like limb proportions show that climbing remained a predominant part of the *Ardipithecus* locomotor repertoire, even as pelvic adaptations were taking place to facilitate bipedal locomotion (Lovejoy et al., 2009).

3.3.2 *Australopithecus*

The pelvis of *Australopithecus* is known primarily through two relatively complete specimens: A.L. 288-1, 'Lucy,' assigned to *Australopithecus afarensis* (Johanson et al., 1982) from Hadar, Ethiopia, and Sts14, *Australopithecus africanus* (Lovejoy et al., 1973), from Sterkfontein, South Africa. Both individuals are thought to be females (Häusler and Schmid, 1995). Additionally, newly discovered fragments from Sterkfontein, South Africa have allowed the reconstruction of the previously known Stw 431 *A. africanus* male pelvis (Kibii and Clarke, 2003). Other more fragmentary remains have been found in South Africa from Makapansgat (MLD7 and MLD8) and Swartkrans (SK50, SK3155). Recently, a partial pelvis (portions of right and left ilium and left ischium, MH1) from the newly designated species, *Australopithecus sediba* were found

at Malapa, South Africa, which has been dated between 1.95 and 1.78Ma (Berger et al., 2010). Although taxonomic attribution is not clear for all of these specimens, they share morphological characteristics that allow discussion of overall pelvic morphology in the genus (Kibii and Clarke, 2003).

The australopithecine pelvis is most notable for being exceptionally mediolaterally broad (Tague and Lovejoy, 1986; Häusler and Schmid, 1995; Kibii and Clarke, 2003; Berge and Goularas, 2010), particularly in the false pelvis, but also at the mid and inferior pelvis (Tague and Lovejoy, 1986; Berge and Goularas, 2010). Despite their small stature, the reconstructions of Sts14 by Berge and Goularas (2010) and A.L. 288-1 by Schmid (1984) place these two specimens within one standard deviation of the human means in bi-iliac, biacetabular, bispinous and bi-tuberous diameters (see Berge and Goularas, 2010). The relative width and height proportions of the *Australopithecine* pelvis indicate the overall shape was both broad and short when compared to modern humans. Pelvic indices of bi-iliac and biacetabular diameters to pelvic length are 163-173% and 69-75% respectively across the australopithecine reconstructions, while the human mean ratios are 128% and 55% respectively (Berge and Goularas, 2010). In addition, the australopithecines lack any significant increase in anteroposterior diameter at the pelvic midplane (Tague and Lovejoy, 1986; Berge and Goularas, 2010), a trait that reflects obstetric demands in modern humans (Tague and Lovejoy, 1986; Ruff, 1995).

Few australopithecine specimens preserve muscular and ligamentous attachments with sufficient clarity to allow definitive evaluation of muscle architecture, but several important characteristics can be assessed. The very broad ilium clearly indicates an

expanded area of attachment for the minor gluteals when compared to chimpanzees (Lovejoy et al., 1973), and the presence of a posterior gluteal line indicates that posterior portions of the gluteus maximus arose directly from the ilium (Häeusler, 2001). The orientation of the A.L. 288-1 ilium is slightly different from Sts 14 and Sts 431, with the external surface more posteriorly oriented (Häeusler, 2001; Berge and Goularas, 2010), but whether this affected the function of the hip abductors is uncertain. Berge (1994) concluded that an ape-like arrangement of the hip musculature in A.L. 288-1 would have provided better mechanical advantage for the hip extensors, and facilitated medial rotation and adduction of the thigh during bipedal locomotion. However, other analyses have proposed that a human-like muscular arrangement was more likely in australopithecines (Häeusler, 2001). A.L. 288-1 differs from *A. africanus* in other aspects of the pelvis as well, particularly the lack of a well developed attachment for the iliofemoral and sacroiliac ligaments, which stabilize the femoral head and sacrum during locomotion (Stern and Susman, 1981; Häeusler, 2001). 'Lucy's' pelvis also lacks a defined iliopsoas groove inferior to the anterior inferior iliac spine or iliopectineal eminence, which have been interpreted as compromising bipedal locomotion (Stern and Susman, 1981; Häeusler, 2001).

Controversy over the "effectiveness" and "efficiency" of australopithecine gait could fill an entire manuscript. The problems in determining locomotor behavior related to the function of the hip are numerous, including differing reconstructions of the A.L. 288-1 (Lovejoy, 1979; Häusler and Schmid, 1995) and Sts14 pelves (Robinson, 1972; Abitbol, 1995; Häusler and Schmid, 1995; Berge and Goularas, 2010), and poorly

defined functional parameters for efficient and "effective" bipedalism. While the overwhelming majority of researchers agree that *Australopithecus* was a habitual biped (see Ward, 2002 for a full review), the argument remains over the specific mechanics of bipedal progression in this genus, and whether a shift toward bipedalism reduced arboreal practice and competency (Ward, 2002).

In accordance with the divergent views of locomotor behavior, biomechanical analyses of the hip abductors have produced two very different reconstructions of function and gait in *Australopithecus*. In a detailed biomechanical analysis of the A.L. 288-1 pelvic complex, Ruff (1998) calculated potential hip abductor, joint reaction and mediolateral bending forces of the femur. Joint reaction force was expected to be 12% greater than modern humans, hip abductor muscle force 27% higher and mediolateral bending forces at upper and mid-shaft length to be 36% and 39% greater respectively (Ruff, 1998). Based on these measurements, if A.L. 288-1 walked with a normal human gait, Ruff (1998) hypothesized that she would have greater femoral head diameter, iliac buttressing, and mediolateral reinforcement of the femur relative to body mass, than seen in modern humans. Because these features are absent, Ruff (1998) concluded that this individual walked with a slightly waddling gait, which would have diminished hip joint forces, but been energetically costly. Other researchers have drawn similar conclusions regarding the kinematics and energetics of australopithecine locomotion (Napier, 1964; Stern and Susman, 1983; Berg, 1994; Hunt 1998).

In contrast, Lovejoy et al. (1973), Lovejoy (1988, 2005) and McHenry (1975) have argued that australopithecine pelvic morphology maintained proper mechanical

advantage of the hip abductor muscles, and differed from the modern human form because of parturition requirements in *Homo*, not because of locomotor differences between the taxa. Richmond and Jungers (2008) have recently argued that *Orrorin tugenensis* femoral morphology indicates that the transversely wide pelvic complex seen in *Australopithecus* is the ancestral condition for the hominin clade.

Although A.L. 288-1 and Sts 14 have wide biacetabular dimensions, EMA of the hip abductors may have been similar to modern humans due to the very long femoral necks of this genus (McHenry and Temerin, 1979; Lovejoy, 2005). Therefore the transversely wide pelvis seen in australopithecines would not have increased hip abductor muscle force production during locomotion. Based on this analysis of hip mechanics, Lovejoy et al. (1973) and Lovejoy (2005) argue a fully striding bipedal gait pattern would have characterized australopithecine locomotion (see also Kimble and Delezene, 2009 for a review of the debate). In addition to clear changes in the pelvis associated with habitual bipedalism (Lovejoy et al., 1973; Lovejoy 1988; Lovejoy, 2005; Kimble and Delezene, 2009; Haile-Selassie et al., 2010), *Australopithecus* displays a suite of features, including valgus knee (Ward, 2002; Haile-Selassie et al., 2010), development of transverse and longitudinal arches (Ward et al., 2011), and adduction of the great toe (Kimble and Delezene, 2009) which all suggest a form of bipedal progression similar to later *Homo* (Ward et al., 2011).

While there remains debate regarding the efficiency of australopithecine locomotion (Stern and Susman, 1983; Berge, 1994; Ruff, 1998; also see Ward, 2002 and Kimble and Delezene, 2010), recent research suggests that, even with kinematics that

differed from those of modern humans, bipedalism in australopithecines may have been more efficient than quadrupedalism in a chimpanzee like ancestor (Sockol et al., 2007; Pontzer et al., 2009). Multiple methods have been used to try and estimate walking cost in *Australopithecus*, with varying results. Kramer and Eck (2000) used a work driven mechanical model of locomotion based on A.L. 288-1 skeletal proportions and found that cost would have been lower than in a human female, while forward simulation techniques using the same skeletal anatomy (Nagano et al., 2005) found 'Lucy' to have costs comparable to that of a modern human of her size.

In a recent analysis of inter-species locomotor expenditure predictions based on muscle volume activation, Pontzer et al. (2009) found that varying lower limb effective mechanical advantage and muscle fascicle length produced cost estimates between 0.19 and 0.10 $mlO_2/kg/m$ for A.L. 288-1, with the majority of cost estimates, from a chimpanzee-like muscle arrangement to a human-like configuration, falling under the actual cost of locomotion for a quadrupedal chimpanzee. These results highlight both the relatively high cost of locomotion in chimpanzees (used as a model for LCA) (Sockol et al., 2007) and the substantial effect of small alterations in lower limb mechanics and anatomy on locomotor cost (Sockol et al., 2007; Pontzer et al., 2009).

3.3.3 *Homo erectus*

Pelvic morphology of *Homo erectus* has been primarily described based on the reconstructed pelvis of KNM-WT 15000 (Walker and Ruff, 1993), the os coxae of KNM-ER 3228 (Rose, 1984) from Lake Turkana, Kenya, and the nearly complete pelvis,

BSN49/P27, from Gona, Ethiopia (Simpson et al., 2008). A partial os coxae, OH 28 is also known from Olduvai, Tanzania (Day, 1971).

The *Homo erectus* pelvis is described as having more laterally flared iliac blades than those of modern humans, while the auricular surface is relatively small (Rose, 1984; Ruff, 1995; Simpson et al., 2008). The ischial tuberosity is large and the anterior superior iliac spine is described as being protuberant (Rose, 1984; Ruff, 1995). KNM-ER 3228 has a clear attachment site for the iliofemoral ligament on the superior aspect of the acetabular margin and a shallow groove for the iliopsoas tendon between the anterior inferior iliac spine and the iliopubic eminence (Rose, 1984). The attachments for the sacroiliac ligaments are well developed and can be seen in the Gona pelvis (Simpson et al., 2008) OH 28 (Day, 1971) and KNM-ER 3228 (Rose, 1984). The iliac tubercle and iliac pillar are very robust, while the lateral surface of the ilium shows a deep fossa for the attachment of gluteus medius and minimus muscles (Rose, 1984; Simpson et al., 2008). Some of these features are missing in KNM-WT 15000, but this is readily attributable to the young age of that individual (Ruff, 1993).

There is general agreement that gait and kinematics in *Homo erectus* were very similar to those of modern humans including the function of the mediolateral balance mechanisms of the pelvis (Day, 1971; Rose, 1984; Ruff, 1995; Arsuaga, 1999). The laterally flaring ilia in combination with a long femoral neck (Brown et al., 1983; Ruff, 1995) have been interpreted as increasing hip abductor mechanical advantage in *Homo erectus* (Brown et al., 1985), even though the gluteal musculature appears to be very well

developed (Rose, 1984; Simpson et al., 2008) and hip abductor forces have been estimated to be greater than those of modern humans (Ruff, 1995).

Further information about the shape and mechanical properties of the pelvis in early *Homo* has been deduced from femoral morphology, for which there is a significantly larger fossil collection. Ruff (1995) analyzed the femoral cross-sectional geometry in early *Homo* and argued that, based on the increase in mediolateral bending strength of the proximal femur, the primitive wide pelvic complex seen in australopithecines was maintained until 0.5 Ma, although changes in gait altered the biomechanical loading of the lower limbs. The mediolaterally broad pelvic shape would have limited increases in cranial capacity within the genus until after the advent of rotational birth, which was facilitated by an increase in anteroposterior dimensions of the mid-pelvis (Ruff, 1995). This allowed biacetabular width and femoral neck length to decrease and changed the biomechanical loading of the femur, reducing mediolateral stress (Ruff, 1995).

Ruff (1995) excluded KNM-WT 15000 from his analysis of femoral cross-sectional geometry because, as a juvenile individual, the femoral morphology likely would not follow predicted adult patterns. Yet, while conclusions about its adult morphology are necessarily tentative, the argument that biacetabular width remained wide in early *Homo* is at odds with KNM-WT 15000 pelvic morphology as originally reconstructed. Walker (1993) speculated that the long femoral neck and very narrow biacetabular width of this individual indicated increased hip abductor leverage in *Homo erectus* compared to modern humans. Walker (1993) further argued that with selection

for larger brains in later *Homo,* which necessitated increases in the size of the bony birth canal, long femoral necks were maintained only in populations where cold climates allowed for wider body builds. In equatorial regions, femoral neck length was reduced to minimize body breadth thereby sacrificing abductor function (Walker, 1993). These interpretations may need to be revised in light of the recent recognition that the original reconstruction of the KNM-WT 15000 pelvis likely underestimated the true breadth (Arsuaga et al., 1999; Trinkaus, pers. comm.).

This picture has been further complicated by the discovery of the Gona pelvis, which is relatively complete, though slightly distorted (Simpson et al., 2008). Although the Gona pelvis shares certain diagnostic features with other *Homo erectus* specimens (Simpson et al., 2008), her extremely small estimated femoral head diameter (33.4-36.8 mm, Simpson et al., 2008) and inferred body size, make her the smallest individual of the known Early or Middle Pleistocene *Homo* specimens (Ruff, 2010). The pelvis is also unique in being extremely mediolaterally broad. In bi-iliac, and transverse pelvic midplane and outlet diameters, Gona is larger than the modern female means from Simpson et alia's (2008) comparative sample (Table 3.1).

The curious combination of very small stature and body mass with very great mediolateral dimensions of the pelvis have prompted some to question the assignment of the Gona pelvic specimen to *H. erectus* (Ruff, 2010). However, Simpson et al. (2008) note the presence of a well-developed sacral tuberosity demonstrating the presence of strong sacroiliac ligaments, a feature absent in australopithecines. Additionally, the enigmatic nature of the *Homo erectus* remains from Dmanisi, Georgia, and the recently

discovered calvarium from Ileret, Kenya (KNM-ER 42700) are expanding the known variability of this species both cranially and postcranially (Gabunia et al., 2000; Spoor et al., 2007). Regardless of taxonomic categorization, the known pelves from Early and Middle Pleistocene *Homo* (except for KNM-WT 15000) share the ancestral mediolaterally wide pelvis and long femoral neck of *Australopithecus* (Arsuaga et al., 1999), which has implications for the interpretation of hip abductor function through the early evolution of our genus.

3.3.4 *Archaic Homo*

The most complete fossil pelves representing 'archaic' *Homo* are those from Jinniushan, China (Rosenberg, 1998; Rosenberg et al., 2007) and SH Pelvis 1 from Sima de los Huesos, Spain (Arsuaga et al., 1999). The pelves of Kebara 2 from Mt. Carmel, Israel (Rak and Arensburg, 1987) and the recently virtually reconstructed pelvis of Tabun C1 (Ponce de León et al., 2008; Weaver and Hublin, 2009) provide important insights into derived Neandertal pelvic morphology. Fragmentary remains from Shanidar, Tabun, Krapina and La Ferrassie also highlight differences in Neandertal pubic morphology compared to modern humans (see Arensburg and Belfer-Cohen, 1998 and Rosenberg, 1998).

Recently, the Sima de los Huesos hominin-bearing locality has been re-dated. Originally thought to be around 200 thousand years old (ka) (Arsuaga et al., 1999), new mass-spectrometer analysis has shown the hominin deposit to be approximately 600ka (Bischoff et al., 2007), which places the Sima de los Huesos hominins at the very

beginning of the Neandertal ancestral lineage (Bischoff et al., 2007). The Jinniushan pelvis is estimated to be approximately 260ka (Chen et al., 1994; Rosenberg et al., 2007). The more recent Neandertal pelves from Kebara and Tabun date to 65ka and 110ka respectively (Grün and Stringer, 1991). Jinniushan (Rosenberg, 1998; Rosenberg et al., 2007) and Tabun C1 (Weaver and Hublin, 2009) are both considered to be females, while Kebara 2 (Rak and Arensburg, 1987) and Pelvis 1 (Arsuaga et al., 1999) are males.

Morphologically, these pelves share many similarities with those of Early and Middle Pleistocene *Homo*, including a mediolaterally broad false pelvis with flaring ilia, a general platypelloid shape, developed iliac buttress and tubercle, and prominent anterior superior iliac spines (Rosenberg, 1998; Arsuaga et al., 1999; Rosenberg et al., 2007). The extremely long and thin pubic ramus of the Neandertal specimens (Trinkaus, 1976; Rak, 1990) has historically been interpreted as part of a suite of obstetric and fetal developmental features thought to be unique to this group (see Rosenberg, 1998). However, Neandertal males have longer pubic rami than females, which is at odds with an obstetrical interpretation of this trait (Rosenberg, 1998). Additionally, both Pelvis 1 and Jinniushan share this pubic elongation, which is probably an ancestral characteristic that has been lost in modern humans (Rosenberg, 1998; Arsuaga et al., 1999). In cross-section the pubic rami of these earlier specimens is intermediate between the reduced cross-sectional area seen in Neandertals and the broader area characteristic of modern humans (Rosenberg et al., 1998; Arsuaga et al., 1999). The functional significance of this difference between the earlier and later 'archaic' groups is unclear (Rosenberg, 1998).

While differences in pelvic shape between Neandertals and modern humans have focused primarily on obstetrics (Trinkaus, 1984; Rosenberg, 1988; Weaver and Hublin, 2009), locomotor biomechanics have also been proposed to explain differences in morphology (Rak and Arensburg, 1987). Functionally, the combination of flared iliac blades, large biacetabular diameter, and long femoral necks would indicate similar hip abductor mechanics in 'archaic' *Homo* and earlier *H. erectus* specimens (Arsuaga et al., 1999). But Rak and Arensburg (1987) argue that the long pubic bones seen in Kebara 2, place the acetabula more laterally. This would have the effect of increasing the body weight moment arm, which would require greater hip abduction forces.

3.4 The modern human pelvis

The sexually dimorphic morphology of the modern human pelvis has often been interpreted as reflecting a natural selection 'trade-off' scenario, where the female pelvis must adapt to the demands of both bipedalism and childbirth, while the male pelvis reflects only the demands of locomotion (Meindl et al., 1985; Abitbol, 1996). While the pelves of males and females are generally easily distinguished based on both metric and shape characteristics (Jordaan, 1976; Meindl et al., 1985; Tague, 1992), the obstetrical and locomotor implications of these differences are not as clearly understood. It is generally assumed that efficient bipedalism requires a narrow pelvis (Zihlman and Brunker, 1979; Rosenberg, 1992; Bramble and Lieberman, 2004), whereas a wider pelvis is more advantageous for childbirth (Rosenberg, 1992; Abitbol, 1996). Pelvic shape is also variable among males and females because of genetic (Sharma, 2002) and nutritional

factors (Stewart, 1984; Tague, 1989; Konje and Ladipo, 2000; Merchant et al., 2001: Neilson et al., 2003) as well as climatic adaptation (Ruff, 1994). Populations living in higher latitudes tend to have broader pelves, particularly the false pelvis, which is associated with increased body mass related to thermoregulation in cold environments (Ruff, 1994). Previous sections have highlighted the assumed locomotor and energetic consequences of female pelvic shape. This review will discuss the anatomical variation in pelvic shape between men and women and the obstetric demands placed on the female pelvis.

3.4.1 Anatomical variation between female and male pelves

On average, the female pelvis is significantly larger than that of males in dimensions of the true pelvis, which include both transvers diameters and the posterior pelvic space (Tague, 1992). In the transverse plane, females are significantly larger in biacetabular, bispinous and pelvic outlet diameters (Tague, 1992). In the anteroposterior plane, females are larger than males at the pelvic outlet, as well as showing greater angulation of the sacrum (Tague, 1992). The subpubic angle is wider in females and the linea terminalis is longer (Tague, 1992). These differences hold true across a wide diversity of groups analyzed by Tague (1992), which included the Indian Knoll, Pecos Pueblo, Libben, Haida and American blacks and whites. Pelvic inlet diameters have been found to be dimorphic in some studies (Correia et a., 2005) but not in others (Tague, 1992). However, these measures are heavily influenced by nutritional status during

development and are therefore more plastic than those of the pelvic midplane and outlet (Stewart, 1984; Tague, 1989).

Males are generally absolutely larger in bi-iliac width and pelvic depth (Tague, 1992). Acetabular diameter and corresponding femoral head dimensions are also larger in males compared to females (Tague, 1992). Male pelves are visually distinguished by having a more 'heart shaped' inlet, thicker bones, a more 'funneled' shape from the superior to inferior planes of the pelvis, and a narrow greater sciatic notch (Abitbol, 1996).

3.4.2 Obstetrical constraints on female pelvic shape

The constellation of features described above are the established criteria by which male and female pelves can be distinguished osteologically and has shaped the attempts of obstetricians to divide the female pelvis into architectural sub-types that have obstetric implications: gynecoid, android, anthropoid and platypelloid (Caldwell et al., 1934: Caldwell et al., 1939; Tague, 1994). As obstetrician Maurice Abitbol (1996) has written, during childbirth "the parturient woman with a gynecoid pelvis will have an easier time and the one with an android pelvis will have a harder time". Evidence from prehistoric populations suggests that pelvic shape may have played an important role in womens' differential ability to survive under difficult obstetric conditions (Sibley et al., 1992; Wall, 2006).

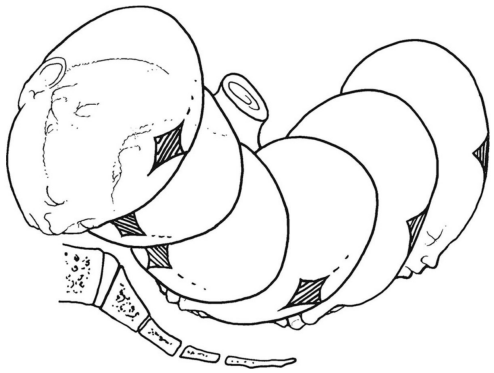

Figure 3.1. Rotational birth mechanics in humans, showing the progressive re-orientation of the fetal head with respect to the maternal pelvis during labor. Copyright Worldwide Fistula Fund, used by permission.

While adaptations to the true pelvis are likely a response to parturition, additional important changes in the birth process have occurred, which ease labor and delivery of the neonate. The most important of these is the rotational mechanism of labor (Fig. 3.1), where the largest dimensions of the fetal head must align with the largest dimensions of the maternal pelvis as the head passes through each pelvic plane during labor. The fetal head generally engages with its sagittal length transversely or obliquely oriented to the maternal pelvis as labor begins. Descending through the midpelvis, the head must rotate to align with the sagittal plane of the pelvis. Once the head emerges, another rotation occurs to face the fetal body laterally so that the shoulders can be delivered under the pubis (Rosenberg, 1992). This elaborate mechanism of labor, which may vary somewhat depending on the shape of the pelvis in question (Caldwell et al., 1934; Caldwell et al., 1939; Trevathan, 1996), is completely different from the obstetrical mechanics of the

other primates whose infants generally drop through the pelvis without any rotation or realignment (Rosenberg, 1992; Abitbol, 1996).

In humans, the fit between the fetal head and the mother's pelvis is extremely tight (Fig. 3.2). Even with such elaborate birth mechanics, the fetal cranium generally undergoes extensive molding, allowed by large fontanelles, to fit though the birth canal. Additionally, mothers almost universally (Rosenberg and Trevathan, 2002) receive assistance during childbirth because the mechanics of rotational birth cause the fetus to emerge facing posterior to the mother's body, preventing her from clearing her baby's airway or helping ease its head out of her body (Berge, 1984; Rosenberg and Trevathan, 2002).

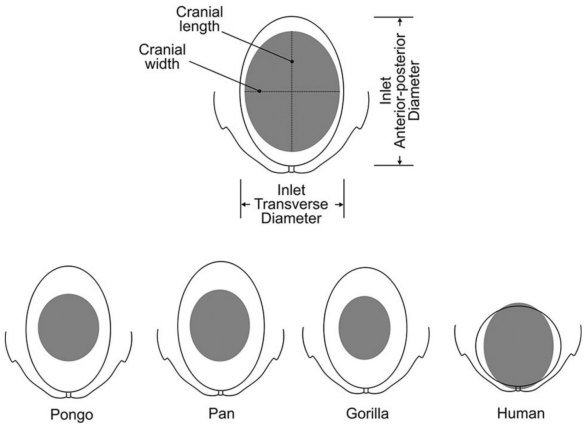

Figure 3.2. Relationships between the fetal head and maternal pelvis in higher primates: Pongo (orangutan), Pan (chimpanzee), Gorilla (gorilla), and humans. Redrawn from Schultz (1969) and Leutenegger (1982). Copyright Worldwide Fistula Fund, used by permission.

3.4.3 The 'obstetrical dilemma"'

The human birth experience has often been thought of as uniquely difficult, traumatic and complicated (Rosenberg, 1992), so much so that it was described by Krogman (1951) as one of the "scars of human evolution." The idea that bipedalism and childbirth were competing selective demands on the female pelvis was formalized in the phrase the "obstetrical dilemma" coined by Washburn (1960). As originally described by Washburn (1960), the adoption of bipedalism required a decrease in the size of the bony birth canal, while selection for larger brains in the Middle Pleistocene demanded that neonates be born with much larger cranial dimensions. Washburn (1960) argued that the human mother, burdened by the need to carry a neonate who was physically and neurologically underdeveloped at birth, would be "slow moving" and unable to participate in hunting or travelling long distances. These new maternal demands created a fundamentally different type of social organization in the human species (Washburn, 1960).

While Washburn (1960) did not argue that the narrowness of the female pelvis itself affects locomotor performance, subsequent interpretations of the "obstetrical dilemma" have interpreted female pelvic morphology as a compromise formed by the competing demands of natural selection for childbirth and efficient locomotion. The pelvis must be large enough to pass an encephalized infant, but these obstetrical demands prevent the pelvis from being sufficiently narrow for the most efficient locomotion (Rosenberg, 1998). Although pelvic shape can be linked to birth outcome (Abitbol, 1996), even though obstetricians still have difficulty identifying the exact pelvic-fetal

relationships that result in cephalopelvic disproportion and dystocia (Abitbol et al., 1991; Liselele et al., 2000), the effect of sexual dimorphism of the human pelvis on locomotion is less well established (see Chapter 2).

3.4.4 The birth process through hominin evolution

What does the fossil record tell us about the evolutionary timing of changes in childbirth throughout the hominin lineage and the development of sexual dimorphism in the human pelvis? Only a few fossil pelves are complete enough to measure the dimensions of the birth canal, and, until recently (see Ponce de León et al., 2008), fetal head diameters had to be estimated from allometric scaling relationships of body-brain-size known for living primates (Leutenegger, 1982). Despite these limitations, several authors have attempted to describe birth mechanics in extinct hominins (Leutenegger, 1972, 1974; Berge et al., 1984; Tague and Lovejoy, 1986; Walker and Ruff, 1993; Häusler and Schmid, 1995; Ruff, 1995; Ponce de León et al., 2008; Weaver, 2009).

The transversely wide pelvic dimensions seen in australopithecines (A.L. 288-1 and Sts 14), erectus and 'archaic' *Homo* (Pelvis 1, Sima de los Huesos and the Gona pelvis) and Neandertals (Tabun C1) have generally been interpreted as most compatible with non-rotational birth mechanics until at least the Middle Pleisotcene (Ruff, 1995; Weaver, 2009), although not all authors agree with this interpretation (Berge et al., 1984; Tague and Lovejoy, 1986; Häusler and Schmid, 1995). However, interpreting birth mechanics in extinct hominins is particularly difficult because no female *Homo* pelves have preserved pelvic outlets, a dimension which is critical for determining the

relationship between the pelvic planes through which the fetus must rotate. Additionally, the poor state of preservation of the Tabun C1 pelvis, and lack of a sacrum, make the measurements of all the pelvic diameters suspect.

3.5 Discussion

This discussion has provided the background for anthropological interpretations of hip abductor function in extinct hominins and living humans. Because these analyses of hip abductor force production have been based on the static model of hip mechanics described in previous sections, it is unclear whether the energetic and gait consequences hypothesized for both early hominins and modern human females will also be supported when the model is evaluated in the dynamic situation of walking and running. If hip abductor function cannot be predicted by skeletal dimensions of the pelvis and thigh, then the broader pelves of *Australopithecus* and other early hominins may not have sacrificed locomotor performance or altered gait kinematics. Additionally, a primary tenant of the "obstetrical dilemma," that parturition requirements in females negative impact locomotor performance, may need to be reevaluated.

CHAPTER 4
MATERIALS AND METHODS

4.1 Experimental design

4.1.1 Participants

Twenty-seven individuals, 14 males and 13 females (Appendix, Table A1-A5) participated in this study, which was approved by the Human Research Protection Office, Washington University in St. Louis (IRB: E07-04). Subjects were physically fit recreational runners and non-smokers, who were recruited from the Washington University main campus and medical school. Subjects reported weekly running distances between 4km and 48km. Recreational runners were chosen for this study because research indicates that elite runners, particularly females, show reduced variation in aspects of lower limb morphology and pelvic shape compared with the general population (Williams et al., 1987). This reduced variability could mask the influence of anatomical variation on locomotor energetics, the ultimate goal of this study.

Before participating, subjects read and signed a consent form and filled out an MRI screening form to ensure they were able to complete all aspects of the study. Participants received $75 reimbursement for their time, which was distributed at each of two or three trial sessions. Sessions included either one or two visits to the Human Evolutionary Biomechanics Laboratory, Washington University in St. Louis, where kinematics, force plate and oxygen consumption trials were performed at the first visit, and a subgroup of 7 subjects also returned for a second session to repeat the oxygen

consumption trials. These second trials were analyzed to determine the repeatability of the O_2 data obtained at individual trials. VO_2 differed by an average of 5.2% between sessions for all trial speeds. Each subject also underwent a full lower body MRI performed at the Center for Clinical Imaging Research, Washington University in St. Louis.

4.1.2 Kinematics and Kinetics

For all biomechanics trials, subjects were given tight fitting spandex shorts and were allowed to wear their own shirt, which was secured up above the hips for the duration of the trials. Individuals were shod for all trials performed on the treadmill (kinematics and oxygen consumption) and unshod during force plate trials. This was done to maximize the comfort of the participants, none of who habitually ran barefoot, on the treadmill.

Kinematics data were obtained simultaneously during force plate trials and again on a series of treadmill trials. Infrared reflective markers were adhered to the skin above palpable bony landmarks on the pelvis (right and left anterior superior iliac spines, and left greater tubercle of the iliac crest), left thigh (greater trochanter and lateral femoral epicondyle), leg (fibular malleolus) and foot (calcaneal tuberosity, first and fifth proximal inter-phalangeal joints). The movement of these markers during walking and running was recorded in three dimensional space using the Vicon motion capture system with four high-speed infrared cameras recording at 200Hz. For treadmill trials, subjects walked at 1.0m/s, 1.5m/s and 2.0m/s and ran at 2.0m/s, 2.5m/s and 3.0m/s. As the treadmill was started at each successive speed, the subject was allowed to walk for several seconds to

transition their gait before data collection began. Once the subject was comfortable at the given speed eight second trials were collected. These data were used to calculate step length and contact time to be matched with data obtained in the other portions of the session (Appendix, Table B2).

In order to determine force production during walking and running, subjects were asked to walk and run at self-selected slow, preferred and fast speeds (Appendix, Table B1) over an AMTI (model-OR) force plate collecting at 1000Hz. The force plate was embedded halfway down a 7.8m long raised track-way made of wood. Three infrared cameras were placed on tripods at a distance away from the end of the trackway, and one camera was positioned facing side on to the force plate to capture the subjects' left side in sagittal profile as they moved down the trackway. Subjects were given time to familiarize themselves with the equipment setup and take "practice walks" at each speed as many times as they needed to feel comfortable moving down the walkway with a normal stride and gait. Once trial collection began, a series of at least three successful trials at each speed and gait were collected. At this stage of collection, trials were considered acceptable when the subject's entire left foot was within the borders of the force plate, only one foot touched the plate, and they proceeded with two steps prior to and two steps after the force plate with no noticeable change in gait or speed.

4.1.3 Metabolic Data

Metabolic data during quiet standing, walking (1.0 and 1.5 m/s) and running (2.5 and 3.0m/s) were obtained using an open-flow oxygen consumption approached described by Fedak et al. (1981). A loose fitting mask, allowing the free flow of ambient

air, was placed over the subject's nose and mouth. Air was pulled through a tubing system into the circuit by a mass flow pump (Sable Systems) collecting at 500L/min. The gas volume was then subsampled at 250ml/s, scrubbed of H_2O and CO_2 and then passed through an O_2 Analyzer at 100ml/s. First, deflection was measured during quiet standing followed by two walking trials and two running trials. For each trial, the subjects were asked to walk or run at the designated speed for two minutes prior to data collection. Oxygen deflection from the ambient room air was monitored during the trial, and exercise was continued until a two-minute plateau of O_2 consumption had been reached (Fig. 4.1). After each subject, a nitrogen calibration bleed was performed where the deflection caused by the known flow rate of N_2 through the system could be determined for future calibrations (Fedak et al., 1981).

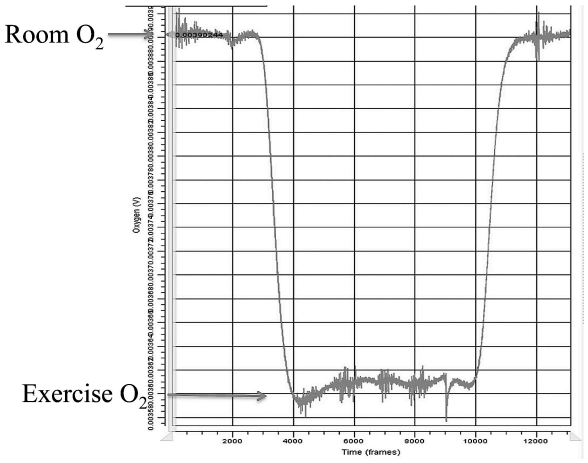

Figure 4.1. Deflection graph from oxygen consumption trial.

4.2 Magnetic resonance imaging

4.2.1 Scanning Protocol

Magnetic resonance imaging to obtain anatomical data was carried out on an Avanto 1.5T scanner at the Center for Clinical Imaging Research, Mallinckrodt Institute of Radiology, Washington University School of Medicine, St. Louis. Each subject's entire lower body was scanned from the fourth lumbar vertebrae to the mid-metatarsals. Four overlapping sections from the pelvis to the feet were scanned isotropically at 1.7mm resolution. Subjects' lower limbs were supported in anatomical orientation with a leg board and dividers, and their feet were placed in a dorsiflexed position secured against a footboard.

4.2.3 MRI Analysis

Analyze 10.0 software (Biomedical Imaging Resource, Mayo Clinic, Rochester, MN, USA) was used to reconstruct and visually inspect the images. For each subject, the four overlapping scanning sections were cropped and the images were then appended and inspected to insure proper fit between body sections. Using the appended image, the subject's entire lower body could be viewed simultaneously in coronal, transvers and sagittal cross-section (Fig. 4.2). In this 3D view, x,y,z coordinates of skeletal and muscle landmarks could be obtained. These coordinates were then used in subsequent calculations to determine planar and 3D dimensional anatomical measurements of the lower extremity (detailed descriptions below). Additional tools including object masks and linear measurement calipers were also used to find muscle cross-sections and linear dimensions of some muscles in the thigh.

Figure 4.2. Multi-planar view of appended MRI image of the lower body

4.3 Anthropometrics

Prior to biomechanics trials, body mass, height, lower extremity and segment lengths were measured on each subject using a standard bathroom scale and flexible seamstress's tape measure. All further anatomical variables were determined from MRI.

4.3.1 Skeletal Dimensions

Skeletal dimensions of the pelvis and lower limb were measured in 3D, with the exception of femoral neck length, using the coordinate tool in the multi-planar view of Analyze 10.0. Anatomical landmarks were used to define the end points of a line where

$$a = x_1 - x_2 \quad (4)$$

$$b = y_1 - y_2 \quad (5)$$

$$c = z_1 - z_2 \quad (6)$$

where x is the mediolateral coordinate, y is the anteroposterior coordinate and z is the vertical coordinate of the point. Therefore the distance (h) between the two anatomical landmarks is

$$h = \sqrt{(a^2 + b^2 + c^2)} \times 1.7 \quad (7)$$

where the constant 1.7mm is the voxel size of the scans.

Variables measured at the hip included bi-iliac, bi-anterior superior iliac spine (bi-ASIS), true biacetabular, biacetabular, femoral neck length, bi-trochanter, inlet transverse, inlet anteroposterior, bi-spinous, midplane anteroposterior, outlet anteroposterior, bi-tuberous and femoral head diameter (Appendix, Table A1).

Measurements followed Lovejoy et al. (1973), Tague (1989,2005) and Ruff (1995). Table 4.1 lists detailed descriptions of each measurement taken.

Table 4.1. Skeletal variable measurement definitions

Variable	Measurement	Reference
Bi-iliac	Distance between the most lateral points of the right and left iliac tubercles	Tague 1989
Bi-anterior superior iliac spine (bi-ASIS)	Distance between the most anterior projections of the ilium in the coronal plane	
True biacetabular	Distance between the center of the acetabulum marked by the ligamentum teres femoris	Adapted from Tague 1989
Biacetabular	Distance between the center of the femoral heads	Ruff 1995
Femoral neck length	Measured as the mediolateral distance from the most superior aspect of the femoral head to the most lateral projection of the greater trochanter	Adapted from Lovejoy 1973
Bi-trochanter	Distance between the most lateral points on the right and left greater trochanter	
Pelvic inlet (transverse)	Maximum distance between the linea terminals visualized in the transverse plane	Adapted from Tague 1989
Pelvic inlet (anteroposterior)	Distance from the sacral promontory to the dorsomedial aspect of the superior border of the pubic symphysis	Tague (2005)
Bi-spinous	Distance between the ischial spines	Tague 1989
Midplane (anteroposterior)	Distance from the sacral promontory to the dorsomedial aspect of the inferior border of the pubic symphysis	Tague 1989
Pelvic outlet (anteroposterior)	Distance from the inferior coccyx to the dorsomedial aspect of the inferior border of the pubic symphysis	Adapted from Tague 1989
Bi-tuberous	Distance between the inferiomedial aspect of the right and left ischial tuberosities	Tague 1989
Femoral head diameter	Measured through the center of the femoral head, the most superior to the most inferior points on the circumference of the head	

4.3.2 Muscle Moment Arms and Joint Center of Rotation

In order to assess the relative importance of the hip abductors to both force production and locomotor cost, it was necessary to quantify the activity of the other major muscle groups of the lower limb active during locomotion. Previous work has demonstrated that a major component of locomotor cost is the production of force required to resist the vertical gravitational force acting on the body center of mass (Kram and Taylor, 1990; Roberts et al., 1998a; Roberts et al., 1998b; Griffin et al., 2003; Pontzer, 2005, 2007). Because of this, the hip and knee extensors and ankle plantarflexors, which act to extend the lower limb against the vertical component of the ground reaction force, were included in the analysis. The thigh adductors were excluded because analysis of joint moments showed these muscles generated only small moments during walking and running trials. Table 4.2 shows the individual muscles included in the hip abductor, hip and knee extensor and ankle plantarflexor groups.

Muscle moment arms are an important anatomical variable in analysis of muscle function because, all else being equal, they are inversely related to the magnitude of force the muscle must produce to oppose external force (Biewener, 1989). The composite moment arm for each lower limb muscle group was defined based on the contribution of each individual muscle's moment arm in relation to that muscle's ability to generate force about the joint (Biewener et al., 2004). These composite moment arms were then used in all further analysis. To do this, the moment arm of each individual muscle in each lower limb group was measured as the perpendicular distance from the joint center of rotation to the line of action of that muscle and weighted by that muscle's cross-sectional area.

$$r_m = r_1 \times A_1/A_{tot} + r_2 \times A_2/A_{tot} + \ldots r_i \times A_i/A_{tot} \quad (8)$$

where r_m is the composite muscle moment arm for each muscle group, $r_{1\ldots I}$ is each individuals muscle's moment arm, $A_{1\ldots i}$ is each muscle's maximum cross sectional area and $A_{tot} = A_1 + A_2 + \ldots A_i$ (Biewener et al., 2004. Appendix, Table A3). Defining individual muscle moment arms required both the accurate and repeatable definition of a joint center at the hip, knee and ankle, and origin and insertion sites to be located for each muscle included in the analysis to define its line of pull. The moments of each muscle were defined in the plane for which its action was to be analyzed using the inverse dynamics routine (described below). All extensor muscle moment arms are in the sagittal plane, while the hip abductor group was defined in the coronal plane.

Table 4.2. Muscle groups of the lower limb

Group	Muscle
Hip Abductors	Gluteus medius Gluteus minimus Tensor fasciae latae
Hip Extensors	Gluteus maximus Semitendinosus Semimembranosus Biceps femoris long head Biceps femoris short head
Knee Extensors	Rectus femoris Vastus lateralis Vastus intermedius Vastus medialis
Ankle Plantarflexors	Gastrocnemius (medialis) Gastrocnemius (lateralis) Soleus Flexor hallicus longus Flexor digitorum longus Tibialis posterior

The center of rotation of a joint is the axis about which a body segment moves. This axis, or point in two-dimensional analysis, is easily definable in joints that are highly congruent, such as the ball and socket hip joint where the center of the femoral head is the fixed point about which movement occurs. However, for joints where the articular surfaces are incongruent, their geometry may not be wholly dictated by the rotation of the two skeletal elements (van den Bogert et al., 2008).

Knee: The knee has often been modeled as a joint with a finite helical center axis that incorporates multi-planar movements about a single axis and undergoes translation during the course of knee flexion (Krevolin et al., 2004; Sheehan, 2007; van den Bogert et al., 2008). Alternately, knee kinematics can be viewed as occurring about two fixed axes (Chruchill et al., 1998; Asano et al., 2005) that allow flexion/extension about the axis located within the posterior femoral condyles (transepicondylar axis) and a superioinferiorly oriented axis (tibial axis) allowing tibial rotation at the knee joint (Chruchill et al., 1998; Asano et al., 2005). This latter model is appropriate between approximately 5 and 90 degrees of flexion, excluding the screw-home mechanism occurring before final extension and deep flexion which requires posterior translation of the femoral condyles (Churchill et al., 1998). While both models are frequently cited (see Bull and Amis, 1998 for a review), the transepicondylar model is generally replacing the finite helical model in many biomedical applications, particularly knee arthroplasty (Asano et al., 2005).

For this study, several methodological considerations dictated the use of the dual axis model of knee kinematics. First, muscle action at the knee was characterized solely in flexion and extension, which meant that incorporating additional degrees of freedom when measuring knee joint kinematics was unnecessary. Second, the physical constraints of the MRI chamber precluded lower limb scans being conducted with the knee in flexed conditions, which is necessary for locating an instantaneous joint axis. In vitro and in vivo studies have shown the transepicondylar axis of knee passes through the origins of the collateral ligaments (Churchill et al., 1998; Asano et al., 2005) providing reliable anatomical landmarks for determining the center of rotation axis.

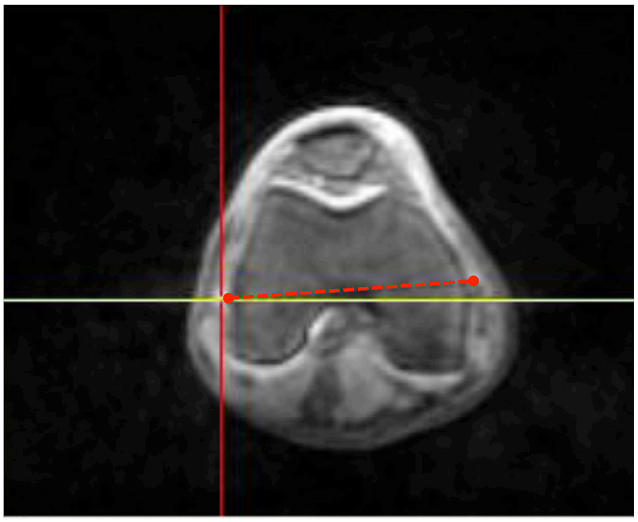

Figure 4.3. Axis of rotation of the knee defined by the origins of the medial and lateral collateral ligaments. In practice the point of origin was confirmed in the sagittal plane

The origins of the lateral and medial collateral ligaments were visualized in the transverse plane on each subject's MRI. With the cursor marking each site in the 3D view, the images were scrolled through the sagittal plane to the approximate center of the lateral and medial condyles to confirm that the site marked passed through the center of the condyle in mid cross-section (Fig. 4.3) (Churchill et al,.1998; Asano et al., 2005). Once the location had been confirmed, the x,y,z coordinates of each ligament origin were recorded as the endpoints of the transepicondylar axis, and the midpoint of this axis then defined the joint center of rotation in all subsequent calculations (Appendix, Table A2).

For each muscle crossing the knee, the moment arm was defined as the perpendicular distance from the muscle's line of action to the midpoint of the

transepicondylar axis in the sagittal plane. Muscles included the semitendinosus, semimembranosus, biceps femoris, and the medial and lateral heads of the gastrocnemius muscle, as well as the patellar tendon, which translates quadriceps force for the rotation of the tibia in extension (Appendix, Table A3). The patellar tendon line of action was measured as the line passing through the center of the tendon from its origin at the distal patella to its insertion on the tibial tuberosity.

The hamstring muscles' origin was defined from a common point on the midpoint of the ischial tuberosity where the long head of the biceps femoris and semimembranosus emerge. The insertion point of the semimembranosus and semitendinosus was defined as a point perpendicular to the insertion on the medial tibial surface, but passing through the midpoint of the muscles as they crossed the knee joint. This ensured that the line of action as it passed the joint center of rotation, was within the muscle, did not cross through bony structures, or truncate the length of the moment arm. Similarly, the insertion of the common tendon of the biceps femoris long and short heads was determined perpendicular to their insertion on the fibular head at the midsection of the muscle as it passed the knee joint. The moment arms of the medial and lateral heads of the gastrocnemius were defined from a line passing through each head of the muscle perpendicular to the insertion point on the posterior distal femur and terminating at the insertion of the Achilles tendon on the calcaneal tuberosiry.

Ankle: The axis of rotation at the talocrural joint, about which flexion and extension predominate, has been noted to shift its orientation when the foot changes from dorsiflexed to plantarflexion (see Lundberg et al., 1989). Despite this potential

reorientation, in vivo experiments have shown that the axes of movement in the coronal, transverse and sagittal planes meet at a common point when superimposed (Lundberg et al., 1989). This point is at, or slightly lateral to the midpoint of a line connecting the distal tibial and fibular malleoli (Lundberg et al., 1989). Additionally, the effect of using fixed versus instantaneous centers of rotation on muscle moments arms appears to be minimal. Analysis of the Achilles tendon moment arm using both fixed and moving centers of rotation showed average moment arm values change by only 1.6mm through 50 degrees of ankle rotation (Rugg et al., 1990).

Based on the conclusions of Lundberg et al. (1989), the ankle joint center of rotation was defined as the midpoint of an axis that passes through the most distal points of the medial and lateral malleoli (Fig. 4.4). Moment arms of the Achilles tendon, flexor hallicus longus, flexor digitorum longus and tibialis posterior where measured in the sagittal plane as the perpendicular distance from this center of rotation to the muscles' lines of action (Appendix, Table A3). The line of action of the Achilles tendon was the line passing through the origin of the tendon from the soleus and gastrocnemius muscles to the insertion on the calcaneal tuberosity. The deep flexor muscles' lines of action were modeled as a pulley with a via point at the posterior margin of the sustentaculum tali where the tendons of all three muscles converge before inserting onto the plantar surface of the foot. The x,y,z coordinates of the origin of flexor hallicus longus, flexor digitorum longus and tibialis posterior were determined from the proximal posterior surface of the fibula, tibia and interossious membrane of the two bones respectively. For the flexor hallucis longus, its line of action terminated at the first metatarsal proximal phalanx. The

flexor digitorum longus line of action was measured to the plantar surface of the medial cuneiform and tibialis posterior was measured to the plantar surface of the cuboid. Again, all origin and insertion sites were determined perpendicular to the bony marker at the center of the muscle or tendon.

Figure 4.4. The axis of rotation of the ankle defined by the line passing through the most distal points of the medial and lateral malleoli.

Hip: The center of rotation in the hip joint was defined as the center of the femoral head, visualized in the 3D perspective in Analyze 10.0 (Fig. 4.5). This meant that the midpoint of the femoral head in sagittal, coronal and transverse cross sections could be simultaneously assessed to ensure accurate determination of the joint center (Appendix, Table A2).

Muscle moment arms for gluteus medius, gluteus minimus and tensor fasciae latae were determined in the coronal plane while gluteus maximus, semitendinosus,

semimembranosus and biceps femoris were measured only in the sagittal plane (Appendix, Table A3). The flexor muscle moment arm of rectus femoris was also determined in the sagittal plane. The line of action of the tensor fasciae latae was from the anterior superior iliac spine to the insertion of the muscle into the ilio-tibial tract. Because the gluteal muscles have broad origins over the surface of the ilia, an origin point for each muscle was chosen that best represented the line of action at the muscle's midline, and was repeatable across subjects. For both gluteus medius and gluteus minimus, the origins were located at the midsection of each muscle respectively in the coronal cross-section that passed through the center of the femoral head. The line of action terminated for both muscles at a single point where they insert onto the lateral surface of the greater trochanter. The gluteus maximus line of action was defined from the most posterior origination point, at the level of the fourth sacral vertebrae within the center of the muscle mass, to a point perpendicular and within the muscle mass of the

termination point on the inferior linea aspera. The moment arms at the hip of the semitendinosus, semimembranosus and biceps femoris long head were measured from the hip joint center to the line of action of each muscle previously described.

4.3.4 Muscle Cross-sectional area

In order to calculate a composite muscle moment arm for each muscle group examined during locomotion, it was necessary to weight the contribution of each muscle to the total force produced by the group as a whole. Physiological cross-sectional area (PCSA), which is determined by dividing muscle volume by fiber length accounting for pennation angle, is accepted as an appropriate measure of a muscle's ability to generate force (Friederich and Brand, 1990; Albracht et al., 2008). However, obtaining these variables in living humans requires the use of multiple imaging procedures which makes assessment of subject specific PCSA extremely difficult, particularly when multiple muscles must be analyzed (Albracht et al., 2008; Folland and Williams, 2007). Because

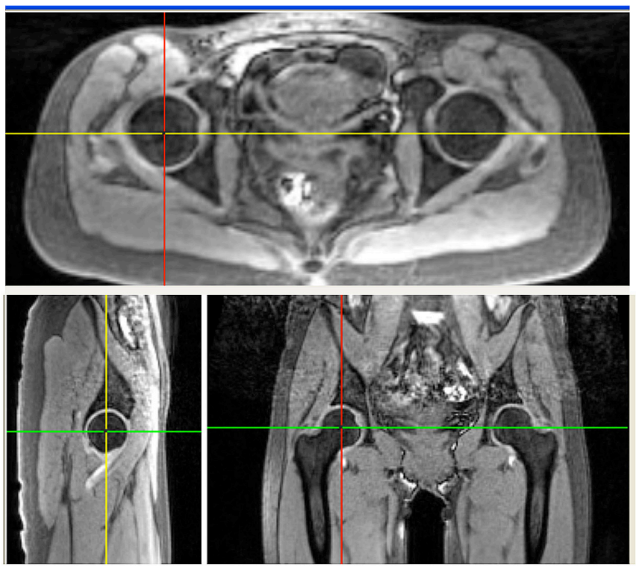

Figure 4.5. Center of rotation of the hip joint visualized in 3D

of these difficulties, measurements are often performed on cadaveric specimens and then scaled by subject specific length and mass parameters (Albracht et al., 2008).

An alternative method for estimating the force generating capacity of a muscle is by determining it's maximum cross-sectional area ($ACSA_{max}$). One of the primary effects of muscle strength training is the hypertrophy of myofibrils causing increase in overall muscle size (Folland and Williams, 2007), although preferential hypertrophy of specific muscle types (slow and fast twitch fibers) has been observed in athletes with differential training regimes (see Folland and Williams, 2007). Additionally, changes in neuromuscular control, pennation angle, and muscle tensile properties affect the maximum force a muscle can produce (see Folland and Williams, 2007). Despite the effects of these factors on muscle strength, studies have documented strong correlations between $ACSA_{max}$ and force production as well as PCSA (Albracht et al., 2008).

$ACSA_{max}$ was used to estimate the force generating capacity of the 18 muscles of the lower limb that made up each muscular group analyzed (Appendix. Table A4). In the transverse plane, an object mask was created which outlined a muscle's boarder in that slice which appeared to have the largest area on visual inspection. The area of this section was noted, and the object mask was then copied to slices both superiorly and inferiorly, and altered to the changing contours of the muscle. This procedure was repeated for successive slices and the area was checked in each slice until the largest ACSA was found. This was repeated for each muscle and total ACSA (A_{tot}) for the hip abductor, hip and knee extensor and ankle plantarflexor groups were calculated.

4.3.5 Muscle Fascicle Lengths

In order to calculate active muscle volume during locomotion, muscle fascicle length is required. Fascicle length and muscle fiber length are assumed to be the same (see below for equation). Muscle fascicles are not viewable on MRI at the resolution used for subject scans, so fascicle lengths from cadaveric specimens were used. Friederich and Brand (1990) noted a consistent ratio of total muscle length to fiber length between individuals in two comparison studies. Therefore, muscle lengths measured on participants from MRI were multiplied by a ratio of fiber to muscle length from dissected specimens to obtain individual measurements for each subject (Appendix, Table A5).

One lower limb from each of four embalmed cadavers (male n = 2, female n = 2; average age = 81.75 years) were dissected in the gross anatomy laboratory at Washington University School of Medicine. For each specimen, muscles were excised at their origin and insertion points. The total length of the muscle and tendons were measured, using a flexible seamstresses tape to the nearest millimeter. Muscles with broad origins, such as the gluteals, were measured along the approximate center of the muscle. The muscles were then cut longitudinally, parallel to the direction of the fascicles. Their length was then measured to the nearest millimeter from the superficial to the deep aponeurosis. Because fascicle lengths change throughout the length of the muscle (Kellis et al., 2010), two or three measurements, depending on the shape of the muscle, were taken along its length. These values were averaged and divided by the total length of the muscle-tendon unit to obtain a ratio.

Fascicle length measurements for each muscle were repeated at least once on one of the four cadavers, so that a second set of measurements constituting a composite total lower limb were available for reliability measures. Average error in determining muscle fascicle length was -2.4±12.7%. However, measurement error of the flexor digitorum longus was extremely high (42.3%) which may be attributable to the atrophied condition of this small muscle in elderly individuals. Without this muscle, average error was -0.1±8.2%.

Average difference in fascicle lengths measured in this study were generally similar to those published by Friederich and Brand (1990) and Wickiewicz et al. (1983) (data provided in Friederich and Brand, 1990). Average differences in fascicle length for all muscles of the lower limb used in this study were 5.3±12.9% when compared to Friederich and Brand (1990) and 8.7±31.4% compared to Wickiewicz et al. (1983) for all muscles except the gluteals and tensor fasciae latae which they did not report. The largest difference between this study and those presented above was in the tibialis posterior. There was a 29.2% and 40.4% difference from Friederich and Brand (1990) and Wickiewicz et al. (1983) respectively.

Composite muscle fiber lengths for the hip abductors, hip and knee extensors and ankle plantarflexors were calculated in a similar manner to composite muscle moment arms. Fascicle length of each individual muscle in the group was weighted by that muscle's $ACSA_{max}$ and averaged to obtain a single value for use in further computations.

4.4 Data Processing

4.4.1 Force Plate and Kinematics Trials

Each force plate trial from the biomechanics testing underwent initial processing using Vicon Nexus 1.3 software. First, the infrared reflective markers adhered to the skin were identified and labeled, foot position on the force plate was verified and cross referenced with notes taken at the time of collection, and the force graphs were inspected for abnormalities. When markers were inconsistent during the time of foot contact with the force plate, a spline tool available in the Vicon software was used to recreate the marker during missing gaps. The spline fill is a polynomial function which uses the coordinates before the marker disappears and at the time of reappearance to predict the trajectory of the point during the missing section. This technique is useful for relatively small gaps, less than 60 frames. Within this data, gaps were small, less than 14 frames, accounting for 0.07s of missing data. When a gap could not be successfully filled using the spline fill, no more aggressive filtering options were used and the trial was discarded.

Once the trials were cleaned and gaps were filled, force, center of pressure (COP) and kinematics coordinates were exported and converted to Excel files. These files were then split into a force/COP file and a kinematics file for later analysis. Within the kinematics files, hip, knee and ankle centers of rotation were calculated based on the position of the kinematics markers and a new set of coordinates for these points were added into the kinematics data set. The hip COR was determined as a set distance from the left ASIS by subtracting the mediolateral, horizontal and vertical distance of the femoral head from the ASIS marker coordinates. Similarly, the knee and ankle centers of

rotation were recalculated in the kinematics data by subtracting the know distance of the joint center in all three planes from the knee and ankle markers in the kinematics data. For each joint center, 1.5cm was subtracted from the mediolateral potions (knee and ankle) and horizontal position (hip) to account for the thickness of the marker in the plane of analysis. The new kinematics Excel files containing the COR coordinates for each joint, along with the force and COP file were then used for further calculations.

Kinematics data obtained from treadmill trials was used to determine step length and stride frequency for comparison of force plate and oxygen consumption data. For each trial, the kinematics marker frame was reconstructed in Vicon Nexus 1.3 and the image was aligned so that the virtual floor was parallel to the viewing plane. The time frame of four successive heel-strikes (HS) of the right foot, determined as the point at which the heel marker contacted the floor, were recorded. The difference between two successive frames was taken as the time of one complete stride (right HS to right HS). This was repeated for each interval for a total of three stride periods and the differences were then averaged. Stride length in meters was calculated as the average stride duration (frames) divided by Hertz rate (200) multiplied by speed. Step length, (HS-toe off) calculated as above except the period of calculation was determined as the time of foot contact between HS and toe-off of the right foot.

4.4.2 Oxygen Consumption Trials

Metabolic activity during walking and running was measured as the deflection of oxygen from room air to the subject's oxygen consumption during exercise. For each trial, average room air was determined by averaging pretrial O_2 levels with those

recorded post trial (Fig. 4.1). Exercise consumption was measured as an average of at least 3600 frames of data, at a visual plateau of oxygen consumption during the exercise portion of the trial. The difference between average room air and exercise air was then calculated as the trial deflection. The volume of O_2 used during exercise was then calibrated based on the known flow rate of N_2 passing through the system during the N_2 bleed trials. Volume of O_2 for each trial was calculated from Fedak et al., 1981 as:

$$VO_2 = (0.2094N_{2flow}/0.8) * (\Delta O_2/\Delta N_2) \quad (9)$$

where N_{2flow} is the known flow rate of nitrogen determined during calibration, and ΔO_2 and ΔN_2 are the trial deflection and calibration deflection respectively.

4.5. Joint Moments, Muscle Force and EMA

4.5.1 Inverse Dynamics Approach

Joint moments, muscle force and EMA for each joint of the lower limb in the sagittal and coronal planes were determined using an inverse dynamics approach. The methods described below follow those of Robertson et al., 2004 and Winter, 2005. Inverse dynamics allows for the resolution of unknown forces acting on a body to be resolved from the known resultant force and the kinematic and inertial properties of the body itself. A free body diagram (Fig. 4.6) models the body segments as ridged objects acted upon by external and anatomical forces. By resolving the inverse dynamics equations of motion, the net external forces produced at each joint can be determined and the opposing internal forces quantified. The limitation of inverse dynamics is that it cannot attribute force to a specific muscle or other internal structure, but instead

calculates the force necessary to produce the movement observed by all the anatomical structures acting together (Robertson et al, 2004). While muscle and other structural forces acting on the joint cannot be separated in analysis, the contribution of tendons and ligaments to net force at sub-maximal ranges of activity are likely relatively small (Winter, 2005).

The equations of motion in a 2D analysis resolve the force in the direction of movement (horizontal or mediolateral), vertically and rotationally for each segment in the kinematic chain. These equations are:

$$\sum F_x = ma_x \quad (10)$$

$$\sum F_z = ma_z \quad (11)$$

$$\sum M = I\alpha \quad (12)$$

where a_x is the linear acceleration of the segment center of mass (COM) in the plane of movement, a_z is the linear acceleration of the segment COM in the vertical direction, I is the moment of inertia and α is the angular acceleration of the body segment about its COM. The moment about the COM of the segment is then calculated as:

$$\sum M + [r_d \times F] + [r_p \times F] = I\alpha \quad (13)$$

therefore the joint moment is:

$$\sum M = I\alpha - [r_d \times F] - [r_p \times F] \quad (14)$$

where F is the resolved force vector of F_x and F_z, and r_d and r_p are the distance of the segment's distal and proximal ends to the COM respectively. Beginning distally, the moments about the distal and proximal ends of all the segments in the kinematics chain can be resolved.

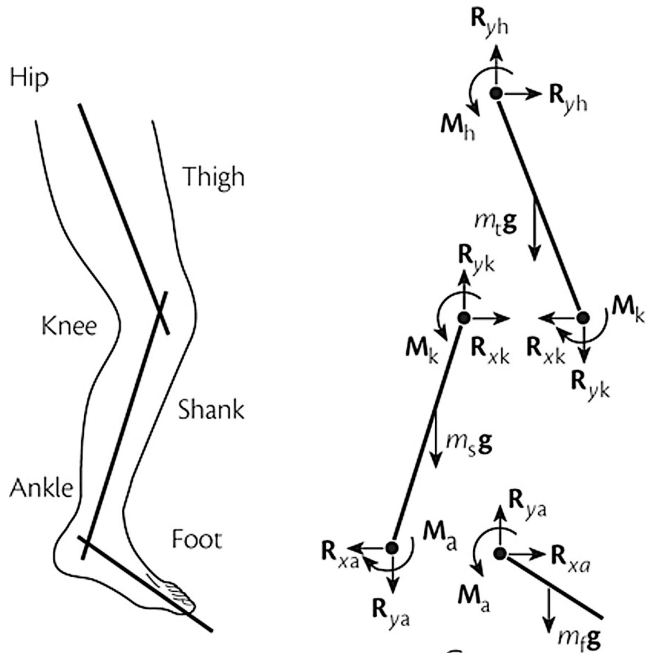

Figure 4.6. Free body diagram depicting forces and moments acting on the segments of the lower limb. M = moment at the joint, m = mass of the segment, R_x = horizontal reaction force, R_y = vertical reaction force.

4.5.2 External Moments

The inverse dynamics equations of motion for each segment of the lower limb (described below) were solved using a custom written MATLAB routine. Kinematics and force Excel files that included subject specific COR coordinates were used as input data for analysis of each subject's force plate trials. Other anthropometric variables were

entered directly into the MATLAB code prior to the processing of each individual's trials. These included body mass, composite muscle moment arms and fascicle lengths for the hip abductors, hip and knee extensors and ankle plantarflexors. Additionally, bi-articulate muscle moment arms and $ACSA_{max}$ for those muscles which act to both extend one joint and flex another were accounted for. These included the rectus femoris at the hip, composite hamstrings (semitendinosus, semimembranosus and biceps femoris long and short) at the knee and gastrocnemius at the knee.

Force data, originally collected at 1000Hz, was looped to match the length of the kinematics time for the trial, creating a new set of force x,y,z and COP x,y,z vectors. Signal noise was smoothed from the kinematics data using a forth order, low pass Butterworth filter (Robertson et al., 2004). The looped force and COP data, and filtered kinematics were then used for all subsequent calculations.

For the time course of foot contact, segment angles for the foot, leg, thigh and pelvis were calculated relative to the horizontal plane (Roberts et al., 2004; Winter 2005). Segment COM vector positions for the foot, leg and thigh were calculated for the duration of stance relative to the position of the kinematics markers at their distal segments. Linear accelerations of the segment COM, and angular accelerations were then computed using the finite difference method (Winter, 2005) where acceleration is calculated based on the linear or angular velocity of a point or segment between sample times. This ensures that the time measurements of the acceleration vector match the time course of the kinematics frames, preventing errors in later computations. Acceleration is given by the equation:

$$Ax_i = \frac{x_{i+1} - 2x_i + x_{i-1}}{\Delta t^2} \quad (15)$$

where x_i is the coordinate position or segment angle in the direction of movement and t is time in seconds.

Beginning with the distal most segment, external joint moments were calculated following the inverse dynamics equations of motion described above for the time course of foot contact with the force plate (touch down to toe off, TD:TO). To determine joint moments at the foot, knee and hip, the initial ground contact forces must be known as well as the anatomical properties of each link in the kinematics chain. Segment mass, COM and radius of gyration scaling values were taken from published statistical tables (de Leva, 1996; Winter, 2005). The moment of inertia of a segment is calculated as the squared multiple of the segment length and scaling factor times the segment mass (Winter, 2005). Beginning at the distal-most segment, the equations of motion for the foot are:

$$\sum F_{x(ankle)} = ma_{x(foot)} - F_{x(GRF)} \quad (16)$$

$$\sum F_{z(ankle)} = ma_{z(foot)} - F_{z(GRF)} + mg \quad (17)$$

$$\sum M_{(ankle)} = I_{foot}\,\alpha_{foot} - [r_{foot(ankle)} \times F_{(ankle)}] - [r_{foot(COP)} \times F_{(GRF)}] \quad (18)$$

where F_{ankle}, M_{ankle}, and $r_{foot(ankle)}$ are the force, moment and r position of the ankle relative to the foot COM respectively; a_{foot}, α_{foot}, I_{foot}, and $r_{foot(COP)}$ are the linear acceleration, angular acceleration, moment of inertia and r position of the foot COP contact point to the foot COM respectively; F_{GRF} is the GRF measured from the force

plate (Fig. 4.8). Because the moment at the proximal end of the ankle is opposed by an equal and opposite moment at the distal segment of the leg, the moment at the knee is:

$$\sum F_{x(knee)} = ma_{x(leg)} + F_{x(ankle)} \quad (19)$$

$$\sum F_{z(knee)} = ma_{z(leg)} + F_{z(ankle)} + mg \quad (20)$$

$$\sum M_{(knee)} = I_{leg}\,\alpha_{leg} - M_{ankle} - [r_{leg(knee)} \times F_{(knee)}] - [r_{leg(ankle)} \times -F_{(ankle)}] \quad (21)$$

where F_{knee}, M_{knee}, $r_{leg(knee)}$, $r_{leg(ankle)}$ are the force, moment, r position of the knee relative to the leg COM, and r position of the ankle relative to the leg COM respectively; a_{leg}, α_{leg}, and I_{leg} are the linear acceleration, angular acceleration, moment of inertia of the leg. Similarly, the moment at the hip is resolved:

$$\sum F_{x(hip)} = ma_{x(thigh)} + F_{x(knee)} \quad (22)$$

$$\sum F_{z(hip)} = ma_{z(thigh)} + F_{z(knee)} + mg \quad (23)$$

$$\sum M_{(hip)} = I_{thigh}\,\alpha_{thigh} - M_{knee} - [r_{thigh(hip)} \times F_{(hip)}] - [r_{thigh(knee)} \times -F_{(knee)}] \quad (24)$$

where F_{hip}, M_{hip}, $r_{thigh(hip)}$, $r_{thigh(knee)}$ are the force, moment, r position of the hip relative to the thigh COM, and r position of the knee relative to the thigh COM respectively; a_{thigh}, α_{thigh}, and I_{thigh} are the linear acceleration, angular acceleration and moment of inertia of the thigh. The equations for each segment of the lower limb were solved separately in the sagittal and coronal planes by substituting the anteroposterior and mediolateral coordinate markers, accelerations and inertial properties. This resulted in six resolved joint moments, two about each plane at the hip, knee and ankle.

4.5.3 Muscle force

Muscle force during stance phase was determined for the composite hip abductors, hip extensors, knee extensors and ankle plantarflexors by solving a series of

equations following Biewener et al., (2004). The force produced to counter the external moments is equal to that moment divided by the agonist muscle moment arm (M/r). Bi-articulate muscles, which produce extension at one joint and flexion at another during contraction, must be partitioned based on their presumed contribution to the moment of a particular joint. At the knee, both the gastrocnemius and the composite hamstrings contribute to the flexion moment of the joint while extending the ankle and hip respectively. At the hip, the rectus femoris both extends the knee and flexes the hip. Therefore the contribution to muscular force of the lower limb was considered on the basis of the primary function of each muscle during ground contact, gastrocnemius an ankle plantarflexor, hamstrings a hip extensor and rectus femoris a leg extensor. Muscle force could then be calculated as:

$$\sum F_{Plantflex} = M_{ankle}/r_{Plantflex} \quad (25)$$

$$\sum F_{Quad} = M_{knee}/r_{Quad} - M_{knee}/(r_{GastFlex} * ACSA_{Gast}) - M_{knee}/(r_{HamFlex} * ACSA_{HamFlex}) \quad (26)$$

$$\sum F_{HipExt} = M_{hip}/r_{HipExt} - M_{hip}/(r_{RecFem} * ACSA_{RecFem}) \quad (27)$$

$$\sum F_{Abd} = M_{Abd}/r_{Abd} \quad (28)$$

where $F_{Plantflex,}$ $F_{Quad,}$ $F_{HipExt,}$ F_{Abd} are the muscle force in the ankle plantarflexors, knee extensors, hip extensors and hip abductors respectively, $r_{Plantflex,}$ r_{Quad}, $r_{GastFlex}$, $r_{HamFlex}$, r_{HipExt}, r_{RecFem}, r_{Abd} are the muscle moment arms of the ankle plantarflexors, quadriceps, gastrocnemius at the knee, hamstrings at the knee, hip extensors, rectus femoris at the hip and hip abductors respectively, and $ACSA_{Gast}$ $ACSA_{HamFlex}$ and $ACSA_{RecFem}$ are the

maximum cross sectional areas of the gastrocnemius, hamstrings and rectus femoris respectively. Peak muscle forces were calculated for further analysis.

4.5.4 EMA

Effective mechanical advantage of each muscle group considered here was determined as the ratio of the composite muscle moment arm divided by the perpendicular distance from the joint center to the resolved force vector determined from the distal articulation of the limb segment being considered. This approach avoids the incorrect determination of the force moment arm, R, based solely on the resolved GRF vector, which ignores the inertial and gravitational moments of distal segments as external moments are determined at more proximal body joints (Winter, 2005). For each joint, the moment at the proximal articulation of the segment was divided by the cross product of the F_x (either sagittal or coronal orientation) and F_z force vectors resolved at the distal segment to solve for R.

$$R_{ank} = M_{ank}/F_{GRF} \quad (29)$$

$$R_{knee} = M_{knee}/F_{ank} \quad (30)$$

$$R_{hip} = M_{hip}/F_{knee} \quad (31)$$

where R_{ank}, R_{knee}, and R_{hip} are the force moment arms about each joint. EMA was then determined by dividing, each segment R by the composite muscle moment arm acting about that joint in the plane of analysis, weighted by the vertical component of the GRF vector. This meant that EMA during mid-stance, where GRF is highest and requires the greatest muscle force production by the abductors, was more influential in the calculation than EMA at the beginning and end of ground contact

4.6 Metabolic Cost of Locomotion

Hip abductor mechanics were directly linked to locomotor cost by determining the contribution of active muscle volume in each muscle group of the lower limb to metabolic demand during walking and running. The link between muscle volume activation and metabolic cost is explained by the force production model (Kram and Taylor, Griffin et al, 2003; Pontzer et al, 2009), which demonstrates that locomotor cost is closely linked to the magnitude and rate of GRF development during the course of stance phase.

The energetic demands of locomotion result primarily from the activation of muscle to support and propel the body, requiring the utilization of ATP to fuel muscle contraction. Previous research has demonstrated that locomotor cost is best predicted by the magnitude and rate of force production required to lift and accelerate the body COM (Kram and Taylor, 1990; Griffin et al., 2003), although swinging the contralateral limb and producing horizontal ground forces also contributes to overall cost (Gottschall and Kram, 2003, 2005; Pontzer, 2005, 2007).

Averaged over the course of a single stride, the acceleration of the body upward must be equivalent to the downward pull of gravity on the body's mass. These upward forces are generated at the time of foot contact. As foot contact time decreases, the muscles of the lower limb must generate force equivalent to the multiple of bodyweight and vertical acceleration in a shorter time interval, thereby increasing both the rate and magnitude of force production (Kram and Taylor, 1990; Biewener, 2003; Pontzer et al.,

2009). This increase in force has been directly linked to an increase in locomotor cost (Kram and Taylor, Griffin et al., 2003; Pontzer 2005, 2007). The force production model is advantageous because it incorporates not only forces that act to move body segments and therefore produce work, but also isometric muscle contractions (Roberts et al., 1998b; Pontzer et al., 2009).

Muscle architecture also plays a key role in the determination of metabolic cost during locomotion. The contraction of skeletal muscle results from the inter-digitation of myosin and actin filaments within the muscle fiber sarcomeres produced by the cross-bridge cycling of myosin heads attaching and pulling the two filaments together (Biewener, 2003). Each time a myosin head releases the actin filament one molecule of ATP is split (Biewener, 2003). Because the entire length of a muscle fiber is activated in contraction, muscles with long fibers require more cross-bridge cycles to shorten and produce a contraction. This requires the use of more ATP molecules (Biewener, 2003). While both a long and short muscle will activate the same cross-sectional area for a given amount of force production, the active volume in a long fibered muscle will be greater and therefore more metabolically expensive.

4.6.1 Active muscle volume

Active muscle volume of the hip abductors, hip and knee extensors and ankle plantarflexors was calculated during the course of stance phase from force plate trials. Active muscle volume (cm^3) of a muscle group is given by the equation:

$$V_{muscle} = L_{fasc} * F_m / \sigma \quad (32)$$

where L_{fasc} is the composite muscle fascicle length for the muscle group, F_m is muscle force and σ is a constant of muscle stress (20 N/cm^2; Biewener et al., 2004). Active muscle volume per meter traveled was calculated by dividing by step length. Both whole body and mass-specific comparisons were used in subsequent analyses (cm^3/m, and, cm^3/kg/m) (Pontzer et al., 2009). Total active muscle volume of the lower limb was calculated as the sum of all four groups of muscles combined.

4.6.2 Cost of transport

The cost of transport (COT) is the rate of oxygen consumption per meter traveled (mlO2/m). COT was calculated for each walking and running speed of the treadmill metabolic trials as exercise VO_2 minus standing metabolic rate. Because force plate trials were collected at variable speeds, comparisons of force plate and oxygen consumption data were made based on the closest speed matched values between the two testing conditions.

4.7 Statistical Analysis

Because calculations of muscle force and EMA at each joint are dependent on accurate joint moment data, the moments generated by the hip abductors, hip and knee extensors and ankle plantarflexors were evaluated at each speed (slow, preferred and fast walking and running) to detect outliers. Boxplots were constructed and subjects who's moment values were two standard deviations away from the mean at a given gait were investigated further to establish the validity of their value at that particular speed. Subject specific scatterplots of joint moments by speed allowed assessment of deviations from

expected patterns of joint magnitude across speed and gait. Data points were only eliminated if they were beyond two standard deviations from the group mean and that joint moment deviated from the individual subject's pattern by speed.

Once data had been verified for each subject's trials, the values of each trial at a given walking or running speed were averaged to obtain a single trail for each walking and running speed. In some instances, no trials at a given speed were available for a subject. This was most common at faster running speeds where it is more difficult to for the high-speed cameras to visualize body marker placement. For the final analyses, data was available for 27 subjects at slow and preferred walking speeds, 26 at a fast walk, 23 at a slow run, 22 at a preferred run and 21 at a fast run.

Least squared regression was used to determine the proportion of variance in EMA, GRF moment arm, R, and hip abductor moment arm, r, explained by skeletal dimensions of the pelvis and hip. Differences in means of EMA, muscle force and active muscle volume between speeds and between males and females were tested using two-factorial ANOVA. Significant results for gait comparisons were further assessed using Tukey's HSD in order to determine which speeds reached significance. Additionally, effect size (d statistic) was calculated to assess the strength of the relationship between comparisons. Un-paired T-tests were performed to compare variable values in men and women at specific speeds as well as to assess significant differences in anthropometric measurements. Results were considered significant at $P < 0.05$. All statistical analysis was performed using PASW Statistics 18 software.

CHAPTER 5
THE HIP ABDUCTORS IN CONTEXT
JOINT MOMENTS AND MUSCLE FORCE OF THE LOWER LIMB

5.1 Introduction

The gait abnormalities that result from a deficit in hip abductor force production demonstrate the mechanical importance of these muscles. Multiple studies have analyzed hip abductor kinematics and kinetics, but these studies have all relied on static models of single leg stance (Inman, 1947; Merchant, 1965; McLeish and Charnley, 1970). Dynamic biomechanical analyses of locomotion often neglect moments generated in the coronal plane altogether (but see Eng and Winter, 1995), even though researchers recognize that these forces are likely substantial (Biewener et al., 2004).

In order to place hip abductor mechanics within the context of lower limb locomotor dynamics joint moments, effective mechanical advantage and muscle force were determined for the hip, knee and ankle in the sagittal plane as well as the hip abductors in the coronal plane. Moment magnitudes could then be directly compared across these joints and the effects of GRF and joint mechanics in determining muscle force production were evaluated. The inclusion of the hip abductors brings important information to reconstructions of gait dynamics. Additionally, by determining the contribution of the hip abductors to overall force production, we can begin to assess their influence on locomotor cost. Because the focus of this section is to place the hip abductors in context during locomotion, all 27 subjects were included in the data

analysis, and no distinctions were made based on sex. Differences between males and females, where present, will be discussed in following sections.

5.2 Joint Moments

Typical internal moments at the foot, shank and thigh in the sagittal plane and the thigh in the coronal plane during stance phase are shown in Figures 5.1.1 and 5.1.2 These moments are produced to oppose the external moments on the body developed by GRF. For clarity, the moments will be described based on the muscular groups that produce them.

At the hip in the coronal plane, walking is characterized by a brief and variable adduction moment as the body center of mass is pulled over the supporting limb. This moment quickly changes to an abduction moment where the lower limb is producing lateral force on the ground, resulting in a medial GRF throughout the course of stance phase (Fig. 5.1.1). The pattern is similar during running (Fig. 5.1.2). At the hip in the sagittal plane, moments are variable during both walking and running, but both are generally characterized by an extension moment for the first 40 percent of stance phase followed by a flexion moment for the remainder of stance (Figs. 5.1.1 and 5.1.2).

Knee moments are more stereotyped during both gaits, with walking extensor moments being relatively small because the knee remains extended throughout the course of stance (Fig. 5.1.1) (Biewener et al., 2004; Eng and Winter, 1995). When gait changes to a run, knee moments are much larger producing a single peak extensor moment approximately at midstance (Figure 5.1.2). At the ankle, plantarflexor moments are large

and peak in the last half of stance phase during a walk, and at approximately midstance during a run (Figs 5.1.1 and 5.1.2).

The largest moments at all speeds during both gaits are generated at the ankle, followed by the hip abductors and extensors, while knee extensor moments are equal to or smaller than those at the hip during walking and running (Table 5.1). When preferred walking and running speeds are compared, the ankle accounts for 41.7±1.2% of the total torque developed in the lower limb during a walk, while hip abductor and extensor moments are 22.4±0.7% and 21.9±1.4% of the total respectively. The knee extensor moment during a walk is 13.8±1.0%. During a run, the ankle is 33.8±0.8% of total lower limb moments, while the other three joints each accounts for approximately 20% (Table 5.1).

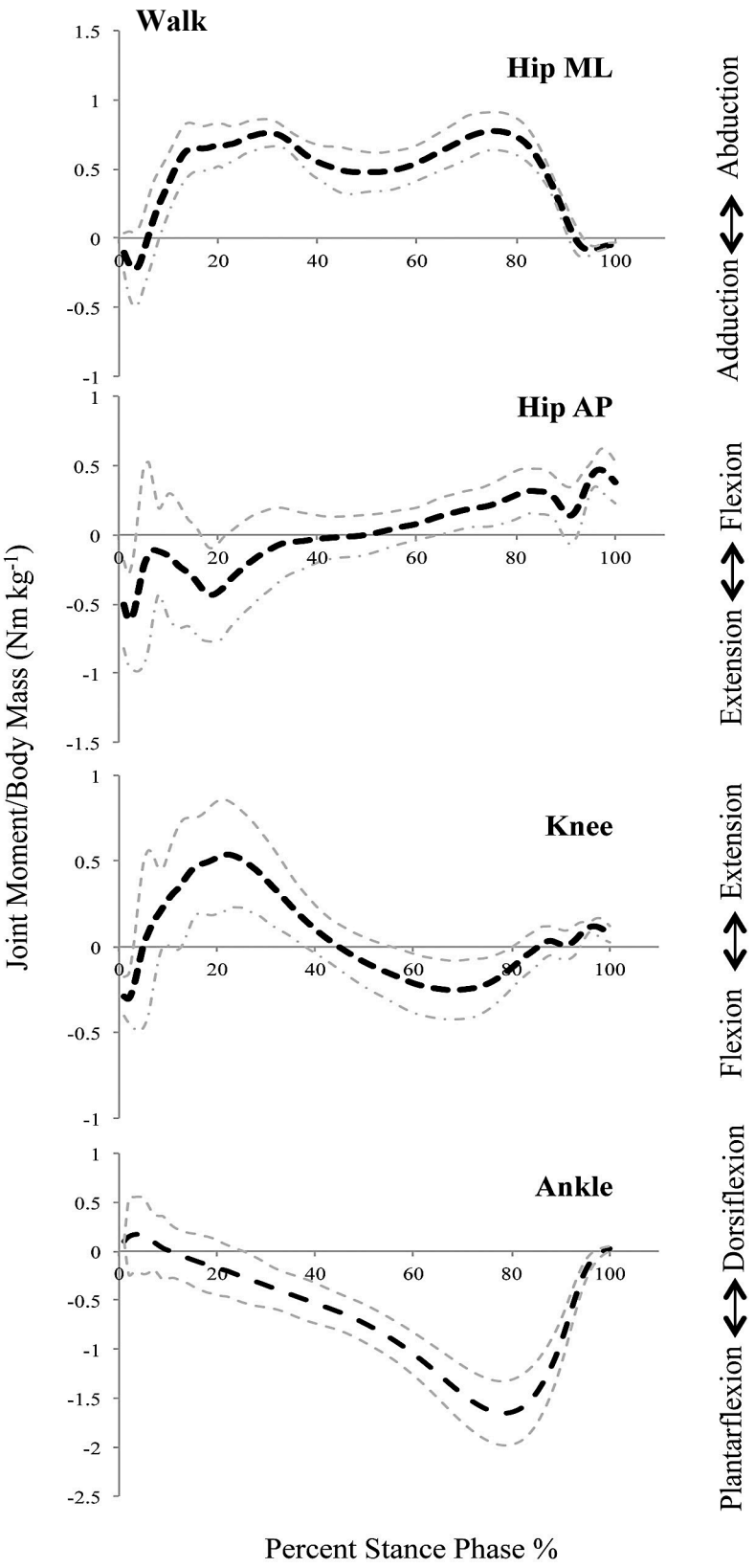

Figure 5.1.1. Moments during a walk at the hip in the coronal (ML) and sagittal (AP) planes, and the knee and ankle in the sagittal plane. Data is from five representative individuals at a preferred walking speed. Black dotted line indicates mean moment magnitude. Grey dotted lines indicate plus and minus one standard deviation.

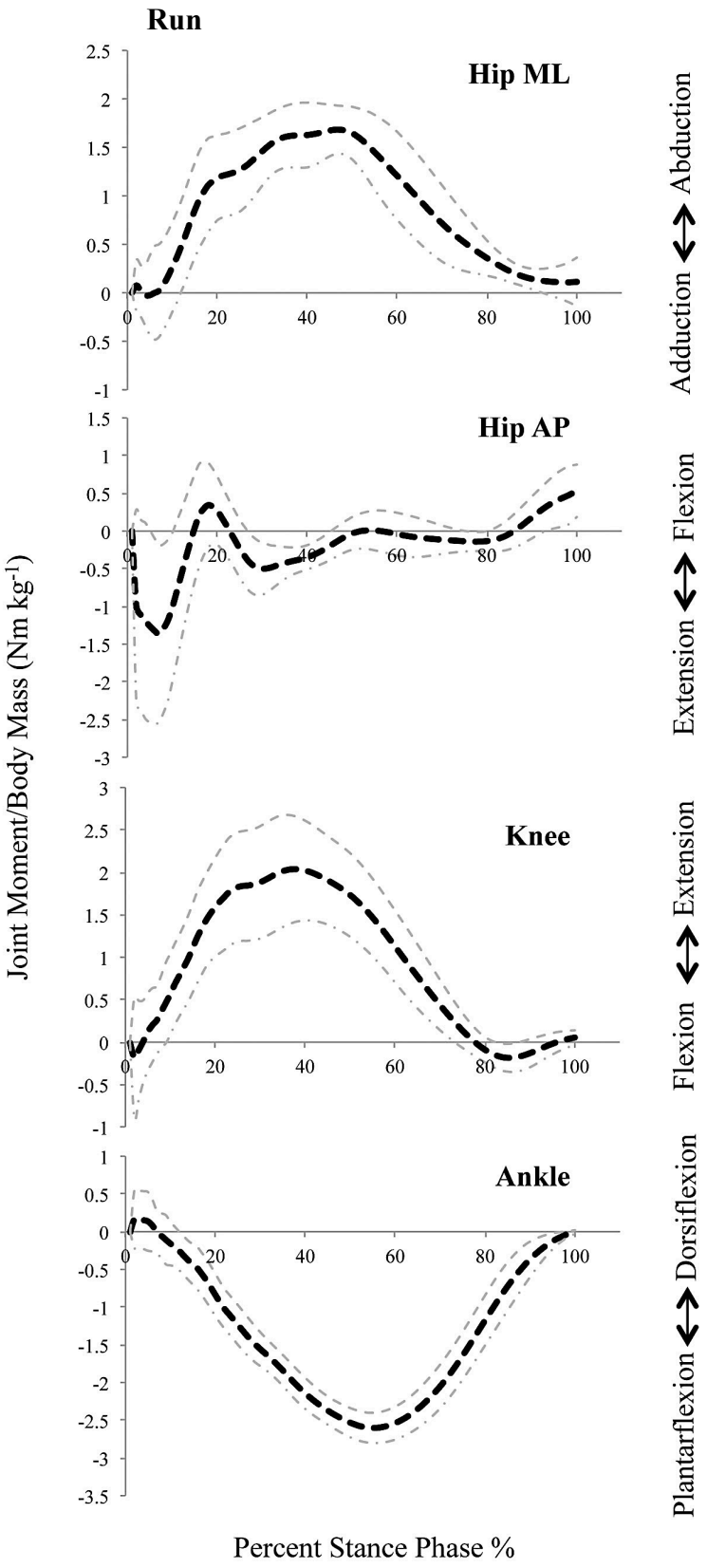

Figure 5.1.2. Moments during a run at the hip in the coronal (ML) and sagittal (AP) planes, and the knee and ankle in the sagittal plane. Data is from five representative individuals at a preferred running speed. Black line indicates mean moment magnitude. Grey dotted lines indicate plus and minus one standard deviation.

Table 5.1. *Joint moments, effective mechanical advantage, R and muscle force*

Joint	**SW**	**PW**	**FW**	**SR**	**PR**	**FR**
N	27	27	26	23	22	21
Peak Moment/Body Mass (Nm kg^{-1})						
Hip ML*	0.86±0.14	0.89±0.15	0.98±0.16	1.71±0.35	1.85±0.34	1.93±0.32
Hip AP^{+}	0.67±0.25	0.91±0.39	1.3±0.46	1.31±0.53	1.60±0.66	1.92±0.53
Knee*	0.37±0.20	0.57±0.26	0.86±0.31	1.54±0.35	1.64±0.35	1.74±0.45
Ankle*	1.50±0.14	1.65±0.15	1.72±0.18	2.34±0.42	2.60±0.34	2.70±0.36
EMA (r/R)						
Hip ML	0.70±0.18	0.71±0.17	0.70±0.18	0.71±0.18	0.68±0.17	0.71±0.19
Hip AP	2.41±1.09	1.77±1.00	1.10±0.38	1.58±0.78	1.51±1.10	1.23±0.73
Knee^{+}	1.00±0.62	0.78±0.34	0.70±0.25	0.47±0.16	0.43±0.14	0.47±0.16
Ankle	0.37±0.05	0.36±0.04	0.37±0.05	0.33±0.03	0.34±0.03	0.33±0.04
R, GRF Moment Arm (cm)						
Hip ML	8.8±1.4	8.2±1.2	8.4±1.4	8.3±1.5	8.5±1.4	8.3±1.5
Hip AP	3.4±1.4	4.6±1.9	6.8±3.1	4.9±2.0	5.9±3.4	6.3±2.6
Knee*	5.1±1.7	6.3±2.0	6.6±1.6	10.1±2.4	10.8±3.3	10.0±3.3
Ankle	10.6±1.4	10.9±1.3	10.6±1.3	11.9±1.3	10.9±1.3	12.1±1.6
Muscle Force/Body Mass (N kg^{-1})						
Hip ML*	15.5±3.7	16.2±4.1	17.9±4.7	30.7±8.5	33.7±8.8	34.8±8.5
Hip AP*	11.0±4.6	14.8±6.9	21.7±7.8	21.3±9.5	26.2±11.9	30.7±7.9
Knee*	8.9±4.7	13.6±6.8	20.6±7.6	36.5±9.8	39.5±10.3	41.8±12.0
Ankle*	38.2±4.3	41.9±4.5	43.8±4.9	58.7±11.5	65.6±9.1	68.6±9.2
Total*	73.7±10.5	86.6±14.6	104.1±13.7	147.4±24.1	165.1±20.0	176.1±21.3

Means± 1 SD for all subjects at each walking and running speed. Hip ML, hip abductors; Hip AP, hip extensors; Knee, knee extensors; Ankle, ankle plantarflexors; Total, summed lower limb force. Walking speeds; SW = slow walk, PW = preferred walk, FW = fast walk. Running speeds; SR = slow run, PR = preferred run, FR = fast run. $^{+}$ differences are significant at the $P < 0.01$ level. * difference between preferred walking and preferred running speeds are significant at $P < 0.001$.

At all three joints, moments increase significantly when gait changes from a preferred walk to a preferred run (all joints $P < 0.001$; hip coronal, $d = 3.65$; hip sagittal, $d = 1.27$; knee, $d = 3.47$; ankle, $d = 3.61$,). Within a walking gait, hip, knee and ankle sagittal moments also increase significantly with speed (slow walk versus fast walk; hip, $P < 0.001$, $d = 1.8$; knee $P < 0.001$, $d = 1.87$; ankle, $P = 0.04$, $d = 1.36$) (Table 5.1, Fig.5.2). Moments generated by the hip extensors and ankle plantarflexors during running also increase significantly from slow to fast speeds (hip, $P < 0.001$, $d = 1.16$; ankle, $P < 0.001$, $d = 1.02$). A clear grade shift in moment magnitude is evident at the ankle, knee and hip in the coronal plane when gait changes from a walk to a run, while hip moments in the sagittal plane increase more linearly across speeds (Fig. 5.2). Comparisons between preferred walking and preferred running speeds show that the largest shift between gaits occurs at the knee with moments increasing 187% between gaits. Hip abductor moments increase by 107%, while ankle and hip extensor moments are 57% and 75% larger respectively. Increases in the magnitude of the GRF are partly responsible for the increases in joint moments when gait transitions. Peak vertical GRF increases 85% from a preferred walk to a preferred run (742.5±95.5N to 1411.0±216.4N, $P < 0.001$, $d = 8.72$). The increases in anteroposterior (45%) and mediolateral (56%) force when gait changes from a preferred walk to a preferred run are not as large but are still statistically significant (anteroposterior PW = 128.4±26.8N, PR = 195.2±42.4N, $P < 0.001$, $d = 1.9$; mediolateral PW = 31.3±8.0N, PR = 50.1±22.6N, $P < 0.001$, $d = 1.18$).

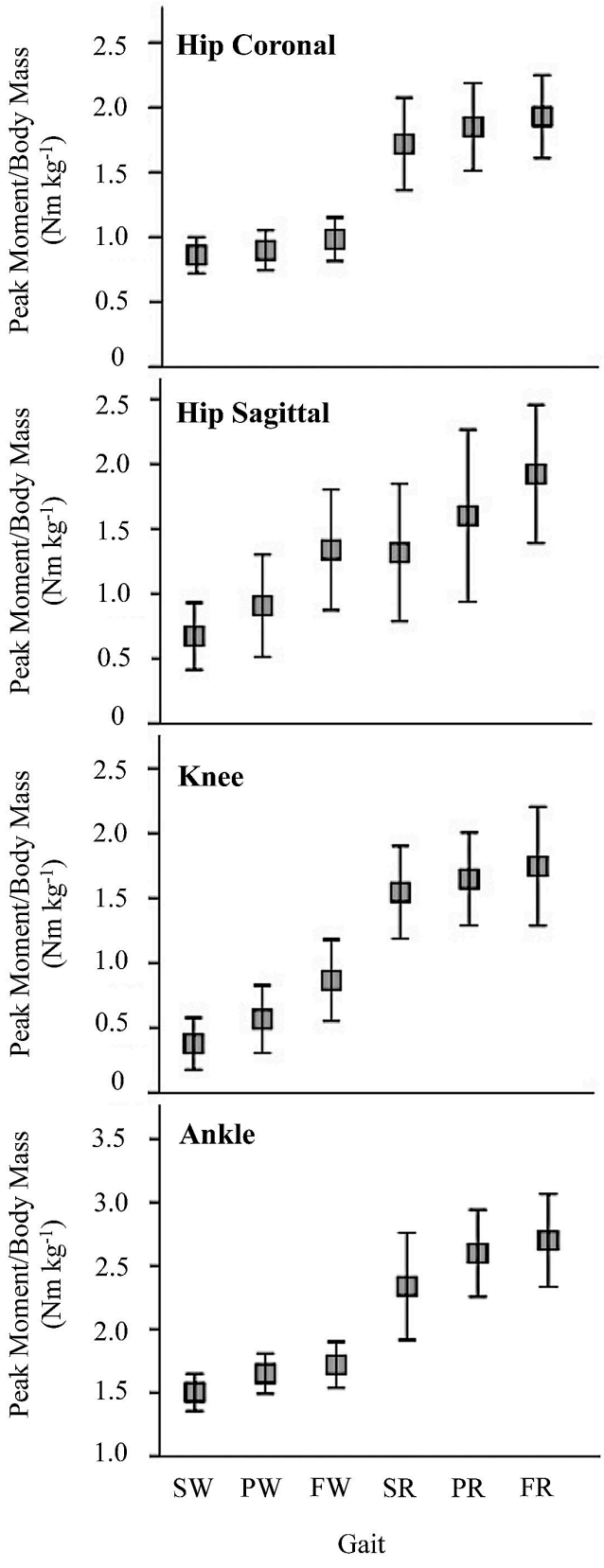

Figure 5.2. Mean mass-specific peak joint moments versus gait (SW, slow walk n = 27; PW preferred walk, n = 27; FW, fast walk, n = 26; SR, slow run, n = 23; PR, preferred run, n = 22, FR, fast run, n = 21). Error bars are one standard deviation from the mean. When preferred walking and running speeds are compared, peak joint moments increase significantly at all joints ($P < 0.001$). Speed also affects moments in all three joints in the sagittal plane, but not at the hip in the coronal plane (see text).

5.3 Effective Mechanical Advantage

While the moment at the hip in the coronal plane increases significantly from a walk to a run, EMA of the hip abductors does not change at any gait or speed condition (Table 5.1, Fig. 5.3). EMA of the abductors averages 0.71±0.17 and 0.68±0.17 at preferred walking and running speeds respectively. This consistency is in contrast to EMA at the hip, knee and ankle in the sagittal plane. Average hip extensor EMA decreases gradually with increasing speed (preferred walk = 1.77±1.0; preferred run = 1.51±1.1), but only the slowest walking speed is statistically distinguishable from fast walking and running speeds ($P < 0.01$, Tukey HSD). EMA of the knee extensors decreases by 39% from a preferred walk to a preferred run ($P < 0.01$, $d = 1.34$) in part because of a 1.7-fold increase in the GRF moment arm, R, about the knee ($P < 0.001$. $d = 1.64$) (Table 5.1). However, speed also affects knee EMA, with fast walking overlapping both running and normal walking speeds, while being significantly lower than slow walking speeds ($P < 0.05$, $d = 0.63$). At the ankle, EMA decreases slightly from a preferred walk to a preferred run (5.5%). There appears to be a slight grade shift in ankle EMA when gait transitions from a walk to a run (Figure 5.3), and while differences between preferred speeds are not statistically significant, all other comparisons between gaits at slow and fast speeds are significant (slow walk versus slow run, $P < 0.01$, $d = 0.97$; fast walk versus fast run, $P < 0.01$, $d = 0.88$). There are no significant differences within a gait.

Across the joints, EMA is highest at the hip in the sagittal and coronal planes, even as speed increases. This is the result of a smaller R at this joint in both planes

compared to the ankle and knee (Table 5.1), while composite muscle moment arms for the hip abductors (5.6±0.8cm) and extensors (6.2±0.5cm) are longer than those of the other two joints (knee r = 4.3±0.7cm, ankle r = 3.9±0.3cm).

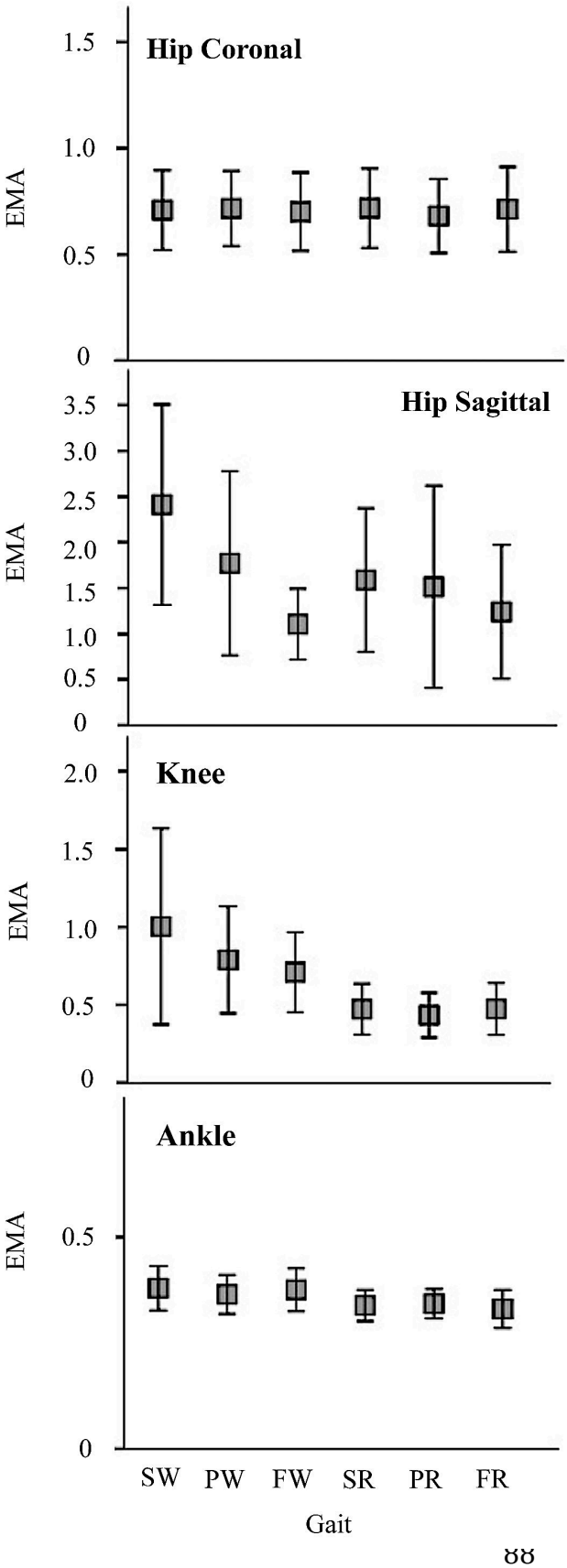

Figure 5.3. Effective mechanical advantage, EMA of the hip abductors, hip and knee extensors and ankle plantarflexors versus gait (SW, slow walk, n = 27; PW, preferred walk, n = 27; FW, fast walk, n = 26; SR, slow run, n = 23; PR, preferred run, n = 22; FR, fast run, n = 21). Error bars are one standard deviation. When preferred walking and running speeds are compared, EMA decreases significantly at the knee and the ankle when gait changes to a run ($P < 0.001$) but not in the hip abductors or extensors.

5.4 Muscle Force

At a preferred walk and a preferred run, summed muscle force for all four muscle groups of the lower limb is 86.6±14.6N kg^{-1} body mass during a walk, and 165.1±20.0N kg^{-1} body mass during a run. The ankle plantarflexors generate the largest portion of this force, 49.9±7.4% during a preferred walk and 39.9±5.1% at a preferred run (Table 5.1). The hip abductors account for 18.6±3.4% and 20.3±4.1% of total muscle force, while the hip extensors are 16.6±5.8% and 15.7±6.3% of the total at preferred walking and running speeds respectively. The knee extensors contribute 15.3±6.5% to overall force production during walking and increase to 23.9±5.9% during a run (Table 5.1).

The changes in force production between gaits are significant in all four groups of muscles (preferred walk versus preferred run; all muscle groups $P < 0.001$, hip abductors $d = 2.5$, hip extensors $d = 1.1$, knee $d = 2.9$, ankle $d = 3.3$), but within a gait, speed also affects the amount of muscle force produced in the hip and knee extensors and ankle plantarflexors (Table 5.1, Figure 5.4). From a slow walk to a fast walk, both hip and knee extensor force increases significantly ($P < 0.001$, hip $d = 1.6$, knee $d = 1.8$). Ankle plantarflexor force also increases as walking speed goes up, and although this change does not reach statistical significance, the effect size is large indicating an important increase in plantarflexor force as speed increases within a walking gait ($P = 0.06$, $d = 1.2$). During running, hip extensor and ankle plantarflexor force also increases significantly between the slowest and fastest speeds ($P < 0.01$, hip extensors $d = 1.0$, ankle $d = 0.9$). The hip abductors remain constant within a gait, increasing by less than 15% between the slowest and fastest speeds within each gait (Table 5.1).

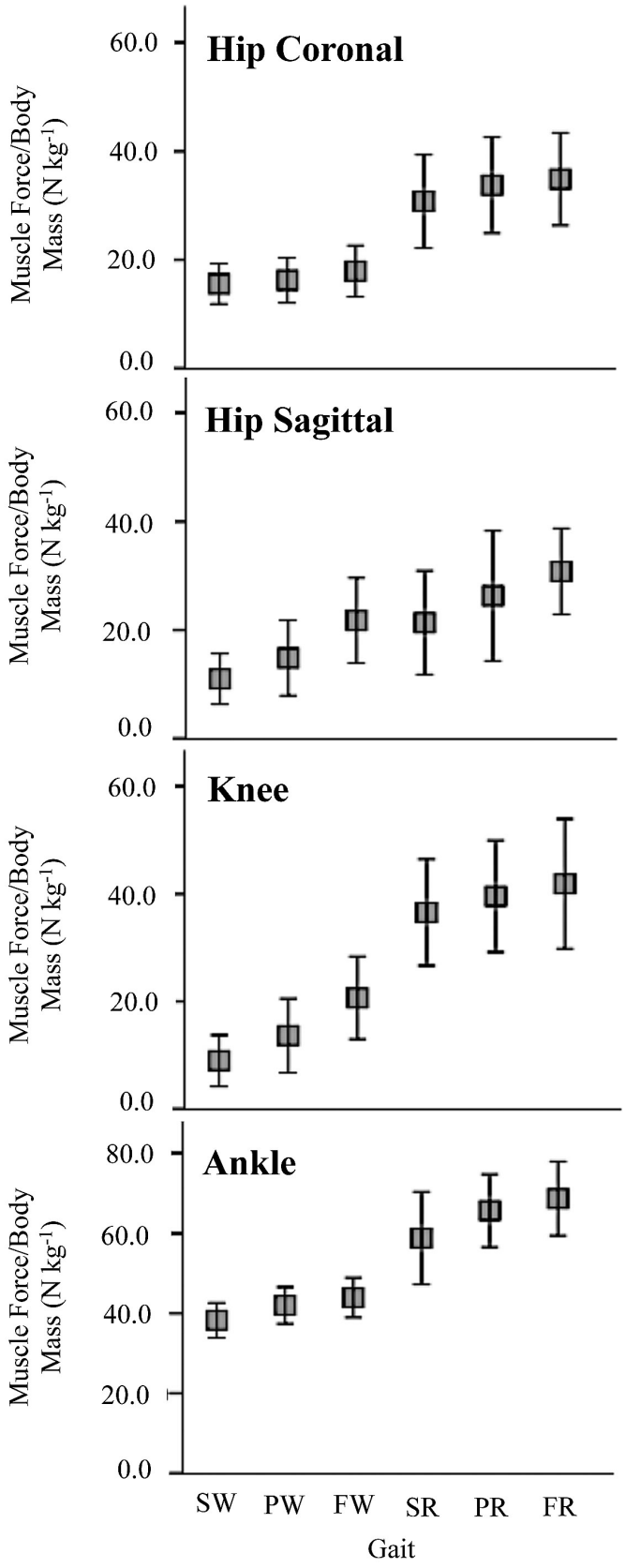

Figure 5.4. Mass-specific muscle force versus gait (SW, slow walk, n = 27; PW, preferred walk, n = 27; FW, fast walk, n = 26; SR, slow run, n = 23; PR, preferred run, n = 22; FR, fast run, n = 21). Error bars are one standard deviation. Mass-specific muscle force increases significantly in all groups when gait changes from a preferred walk to a preferred run ($P < 0.001$). Hip and knee extensor force also increases significantly with speed within a walking gait ($P < 0.001$), and hip and ankle force increase with speed during running ($P < 0.01$).

5.5 Discussion

Results of this analysis demonstrate that hip abductor moments are substantial when compared to other joints of the lower limb, being equal to or greater than those at the hip and knee in the sagittal plane. The hip abductors account for up to 20% of the total lower limb force produced during locomotion, indicating that they likely contribute substantially to locomotor cost.

Like the other joints of the lower limb, hip abductor moments increase significantly when gait transitions from a walk to a run, but unlike at the knee, and to a lesser extent the ankle, EMA of the hip abductors remains remarkably constant across speeds (Fig. 5.3). The consistency of the GRF moment arm, R, about the hip in the coronal plane is explained by the relatively small change in the magnitude of the mediolateral component of GRF, which increases by 18.8±8.2N from preferred walking to a preferred running speed ($P < 0.05$, $d = 1.1$). In contrast, vertical GRF increases by 668.4±72.5N between preferred walking and running speeds ($P < 0.001$, $d = 3.9$), which explains the significant increase in hip abductor moment even though hip abductor kinematics are stable.

Previous studies of abductor muscle force while standing reported values between 1 and 2.25 times body weight (Merchant, 1965; McLeish and Charnley, 1970). By comparison, this study shows hip abductor force is 1.65±0.42 times body weight during a preferred walk and 3.44±0.9 body weight during a preferred run. Walking and running values are higher primarily because static models use body weight as a proxy for vertical

force production and ignore mediolateral forces altogether when calculating the resisting hip abductor force. Peak vertical force is more than two times body weight during a run in this study, while only during slow walking is vertical GRF nearly equal to body weight (see McLeish and Charnley, 1970). The effect of estimating R from pelvic dimensions on hip abductor force production will be discussed further in the next section.

Results for moments, EMA and muscle force about joints in the sagittal plane are generally similar to those reported in other studies with some exceptions. Ankle moments were greater than those of the hip and knee in both walking and running in this analysis, and all three joints showed significant increases when gait changed from a walk to a run. Biewener et al. (2004) and Griffin et al. (2003) also report that ankle moments and muscle force were largest during a walk, but Biewener et al. (2004) found knee moments to be the greatest during running. Additionally, while hip extensor and knee moments increased with gait, there was no significant change in ankle moments between walking and running in their study.

The differences between these studies seem to derive primarily from measurements of EMA. While ankle EMA measured across all three studies is fairly similar, there are significant differences in reported knee and hip extensor EMA (Table 5.2). The discrepancies appear to lie in the calculation of GRF moment arms about the hip and knee in the sagittal plane, as average muscle moment arm values are quite similar between studies. Variation in R may be due to marker placement, the period of stance phase over which the value is calculated or differences in sample size that may impact the

amount of inter-individual variability in locomotor patterns (Biewener et al., 2004 N = 4, Griffin et al., 2003 N = 8).

Table 5.2. *Effective mechanical advantage compared across studies*

Joint EMA	Gait	Biewener et al. (2004)[+]	Griffin et al. (2003)	This Study
Hip AP	Walk	0.6	2.49±0.79	1.77±1.03
	Run	0.7	-	1.45±0.88
Knee	Walk	1.4	3.42±1.26	0.83±0.43
	Run	0.4	-	0.46±0.15
Ankle	Walk	0.3	0.28±0.03	0.37±0.049
	Run	0.4	-	0.33±0.038

Values are averages for walking and running trials ± one standard deviation, when available. [+] EMA from Biewener et al. (2004) are based on estimates from graphic representation. They do not report the actual values in text.

Despite differences, these studies make clear that ankle plantarflexor force is predominant during a walk and large during a run. Knee extensor force increases dramatically at running gaits because of greater flexion of the joint which moves the COR farther from the GRF force vector (Biewener et al., 2004). Hip extensor force increases gradually with increasing speed (Giffin et al., 2003; Biewener et al., 2004) due to larger GRF and inertial forces as speed increases (Biewener et al., 2004). In addition, it is now clear that hip moments in the coronal plane are equally large compared to moments generated in the sagittal plane. Hip abductor moments are remarkably consistent between individuals and across speeds within a gait. This analysis demonstrates the necessity of including coronal plane moments in future biomechanical analyses of gait (also see Eng and Winter, 1995).

CHAPTER 6
PELVIC SHAPE AND HIP ABDUCTOR MECHANICS DURING LOCOMOTION

6.1 Introduction

The assumption that pelvic width influences locomotor dynamics and cost by altering hip abductor mechanics is central to many arguments concerning the nature of bipedalism in extinct hominins (Napier, 1964; Lovejoy et al., 1973; McHenry, 1975; McHenry and Temerin, 1979; Stern and Susman, 1983; Lovejoy, 1988, 2005; Rak, 1991; Berge, 1994; Ruff, 1995; MacLatchy, 1996; Hunt, 1998; Rosenberg, 1998; Ruff, 1998; Arsuaga et al., 1999; Kramer, 2000; Haeusler, 2002; Bramble and Lieberman, 2004; Lovejoy et al., 2009) and differences in locomotor performance between men and women (Burr et al., 1970; Zihlman and Brunker, 1979; Bhambhani and Singh, 1984; Smith et al., 2002; Cho et al., 2004; Ferber et al., 2003; Chumanov et al., 2008). This assumption is based on a static model of hip abductor mechanics where the GRF moment arm, R, passes approximately vertically through the body center of mass during single leg stance (Inman, 1947, Saunders et al., 1953; Merchant, 1965) (see Fig. 1.1 reproduced below). In this static model, pelvic width, specifically biacetabular width, will affect mediolateral moments at the hip by increasing the distance from the joint COR to the GRF vector. All else being equal, as pelvic width increases hip abductor forces must also increase to maintain the pelvis in equilibrium and prevent excessive pelvic tilting away from the support limb. Conversely, increased femoral neck length decreases hip abductor force by

lengthening the moment arm of the abductor muscles, r. The ratio of these two variables, r/R is the effective mechanical advantage of the hip abductors, EMA.

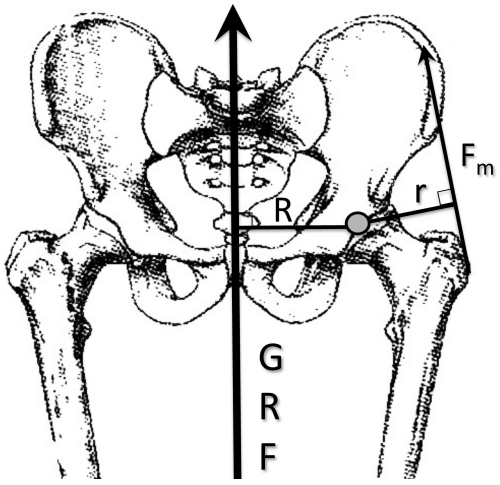

Figure 1.1. Free body diagram of the hip in the mediolateral plane. The multiple of muscle force, F_m and hip abductor muscle moment arm, r, must equal the ground reaction force, GRF, times its moment arm, R. The effective mechanical advantage of the joint is defined as the ratio of r/R.

Based on this static model, skeletal dimensions have been used to calculate hip abductor EMA in fossil hominins, producing varying conclusions regarding hip abductor mechanics. In *Australopithecus*, several analyses concluded that wide pelvic dimensions increased hip abductor force production or altered gait dynamics (Berge, 1994; Ruff, 1998). Conversely, Lovejoy et al. (1973), Lovejoy (2005) and McHenry (1975) argued that wide biacetabular breadth in australopithecines was offset by longer femoral necks and therefore would not have increased mass-specific hip abductor force or altered gait kinematics relative to modern humans. The model has also been applied to early and archaic *Homo* (Arsuaga et al., 1999; Ruff, 1995; Rosenberg, 1998) although no authors

have argued that gait dynamics differed substantially in these groups compared to modern humans, even if pelvic morphology altered hip abductor force production.

In modern humans, the 'obstetrical dilemma' hypothesis, first proposed by Washburn (1960), posits that female pelvic dimensions represent a compromise between obstetrical demands and efficient locomotion (Zihlman and Brunker, 1979; Meindl et al., 1985; Rosenberg, 1992). Analysis of locomotor cost across multiple studies has failed to demonstrate decreased efficiency in women compared to men (Bhambhani and Singh, 1983; Bunc and Heller, 1989; Bourdin et al., 1993; Ariëns et al., 1997; Hall et al., 2004), and while pelvic inclination and rotation have been shown to be greater in women in some locomotor conditions (Cho et al., 2004; Ferber et al., 2003; Chumanov et al., 2008), these differences in kinematics have not been conclusively tied to pelvic shape or locomotor performance.

While the underlying lever mechanics of hip abductor function are not in question, the correlation between biacetabular width and R has never been demonstrated during locomotion. This section will use skeletal dimensions obtained through MRI to test the prediction that biacetabular width and femoral neck length can be used to determine EMA of the hip abductors during walking and running, and hip abductor mechanics will be discussed in relation to pelvic kinematics and mediolateral GRF production during locomotion.

6.2 Predicting EMA during locomotion from skeletal dimensions of the hip

To determine the relationship between skeletal dimensions of the hip and pelvis and EMA of the hip abductors during locomotion, two variables were defined, EMA_{skel} (femoral neck length/ 0.5 biacetabular width) (see Table 4.1 for measurement definitions) and EMA_{loc} (r/ R) (Fig. 1.1) measured during each locomotor trial. Because the slope, y-intercept and coefficient of determination are very similar within a gait (Fig. 6.1), the results presented here will focus on preferred walking and running speeds.

During walking, EMA_{skel} explains a significant amount of variation in EMA_{loc} ($r^2 = 0.49$, $P < 0.001$) while at a run EMA_{skel} is less predictive but still significantly correlated with EMA_{loc} ($r^2 = 0.30$, $P < 0.05$, Fig. 6.1). While observed and predicted EMA_{loc} deviate for many subjects, a single individual (139) has the highest positive deviation in EMA_{loc} at every speed and every gait, except a preferred walking speed (Fig. 6.1). EMA_{loc} for this subject is more than two standard deviations above the mean at each locomotor condition (EMA_{loc} PW = 1.0, PR = 1.2). However, removing this subject from the regression does not dramatically improve the relationship between the EMA_{skel} and EMA_{loc} (PW, $r^2 = 0.52$, $P < 0.001$; PR, $r^2 = 0.34$, $P < 0.01$) because the datum point exerts little leverage on the regression line (centered leverage value, walk = 0.077, run = 0.015).

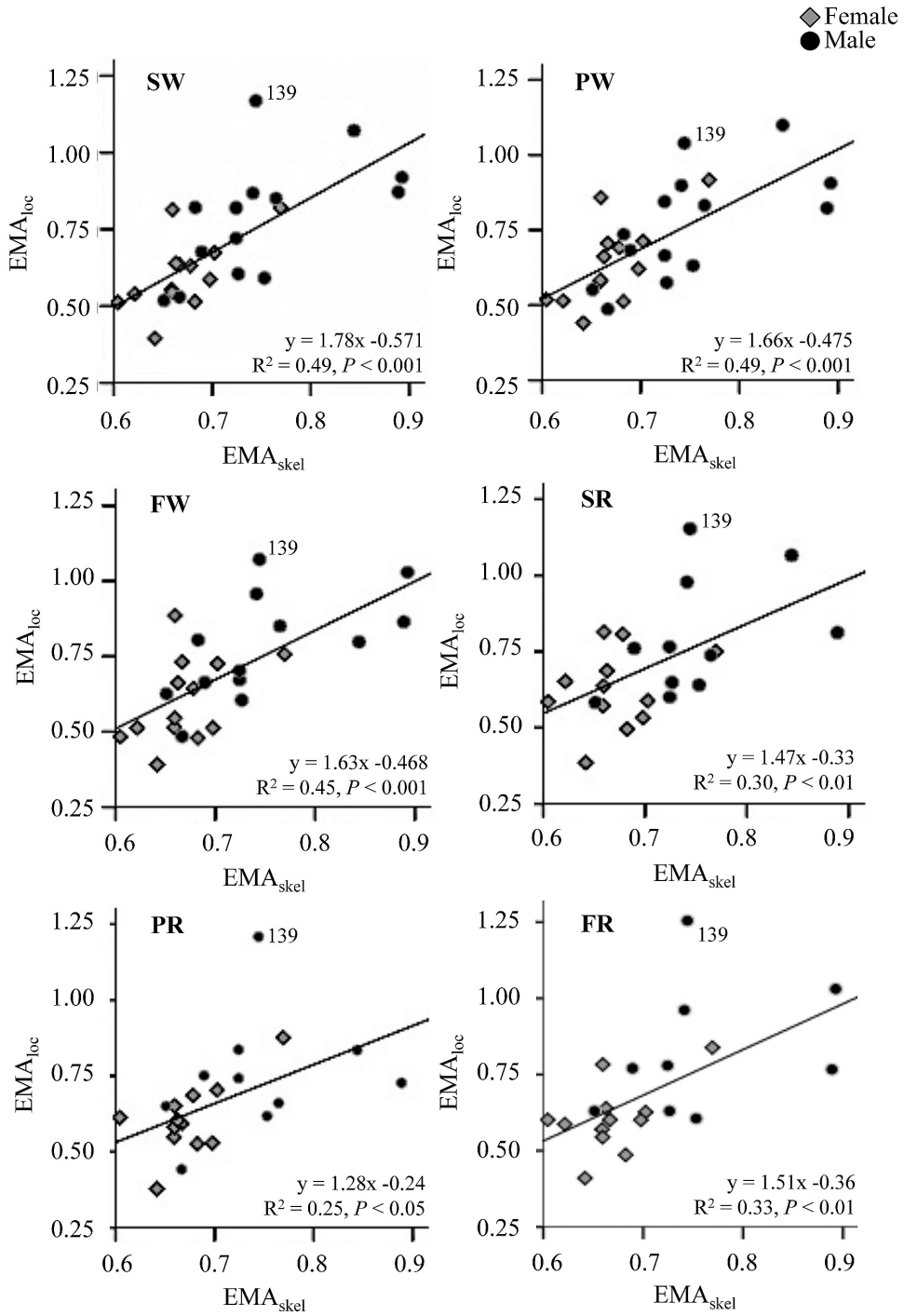

Figure 6.1. EMA_{skel} versus EMA_{loc} at each walking and running speed (SW, slow walk n = 27; PW preferred walk, n = 27; FW, fast walk, n = 26; SR, slow run, n = 23; PR, preferred run, n = 22, FR, fast run, n = 21). Regression line is based on LSR. EMA_{skel} predicts a significant amount of variation in EMA_{loc} at each gait and speed. Subject 139 has the highest EMA_{loc} at each speed except a preferred walk.

The relationship between EMA_{skel} and EMA_{loc} appears to be primarily driven by the correlation between femoral neck length and hip abductor moment arm, r ($r^2 = 0.62$, $P < 0.001$, Fig. 6.2). The slope of the regression line relating these anatomical variables is near identity ($\beta = 1.02 \pm 0.32$) indicating isometric changes in r as femoral neck length increases. Femoral neck length alone predicts 43% of the variation in EMA_{loc} at a preferred walking speed ($P < 0.001$), and 23% during a preferred run ($P < 0.05$, Fig. 6.3).

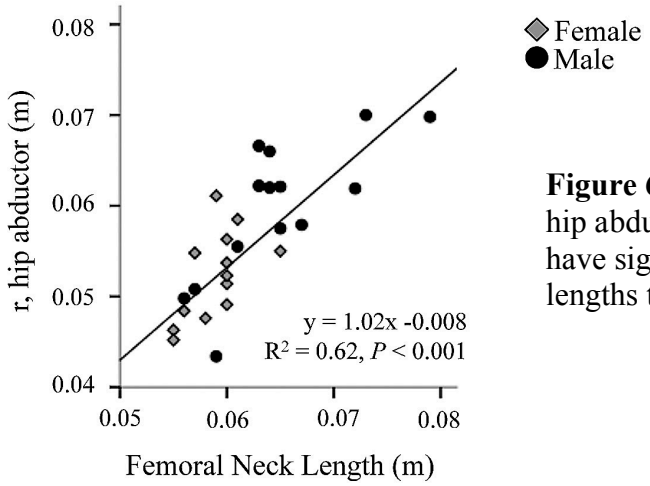

Figure 6.2. Femoral neck length versus hip abductor moment arm, r. Females have significantly shorter femoral neck lengths than males ($P < 0.01$).

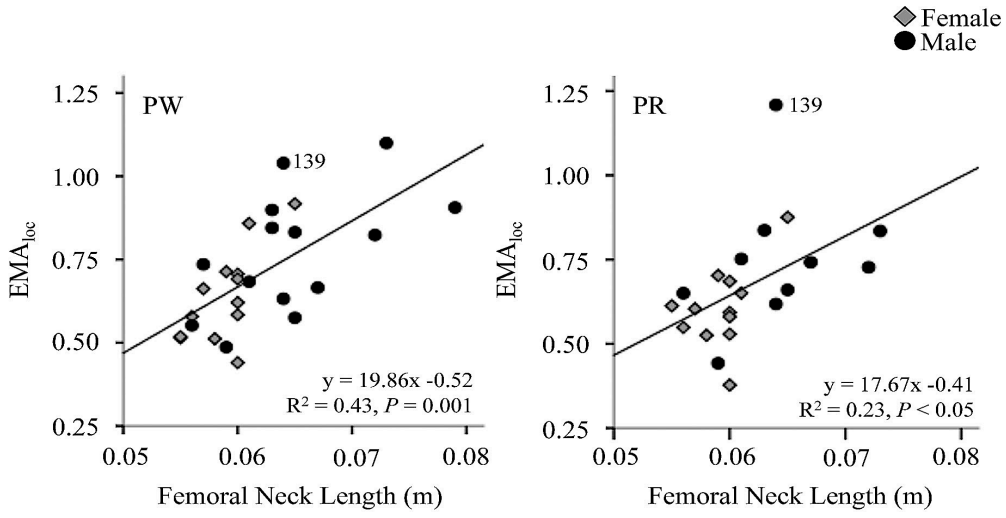

Figure 6.3. Biomechanical femoral neck length versus EMA_{loc} at a preferred walk (n = 27) and run (n = 22).

In contrast, 0.5 biacetabular width explains only 14% of the variation in R during a walk ($P < 0.05$) and is not significantly correlated with R during a run ($r^2 = 0.07$, $P = 0.21$, Fig. 6.4). However, the relationship between biacetabular width and R during walking completely disappears when subject 137 (see Fig. 6.4) is removed ($r^2 < 0.07$). This individual has measurements of R at each speed that are three standard deviations above the subject mean and has substantial influence on the slope and coefficient of determination (centered leverage value, PW = 0.154, PR = 0.169).

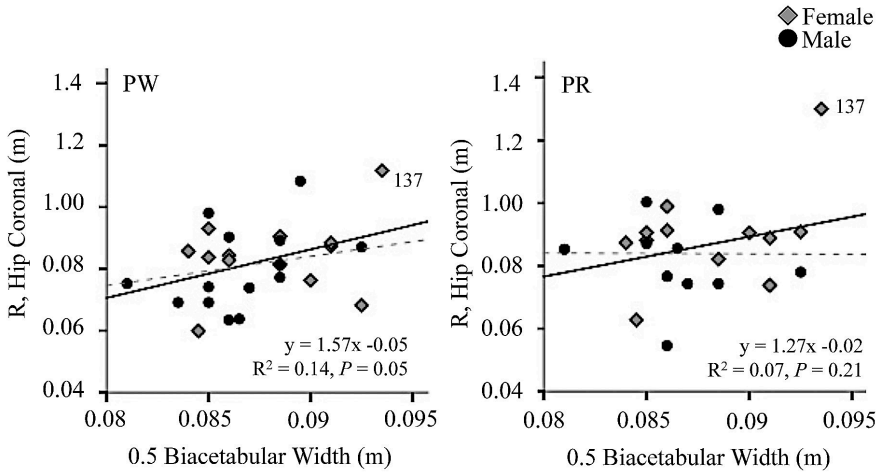

Figure 6.4. Half biacetabular width versus R at the hip in the coronal plane for a preferred walk (n = 27) and run (n=22). Solid line is the LSR including all subjects. Dotted line is the LSR with subject 137 removed.

Because of the low correlation between one half biacetabular width and R, EMA_{loc} is also not well predicted by this pelvic measure (Fig. 6.5). During a walk 0.5 biacetabular width explains 10% of the variation in EMA_{loc} and 8% during a run. However, just as the slope of the regression of 0.5 biacetabular width and R is heavily influenced by subject 137, removal of this individual from the LSR of 0.5 biacetabular

width and EMA_{loc} decreases the slope of the regression line at a walk and especially at a run (Fig. 6.5), although this slope is still within the 95% confidence interval of the original estimate (PW β±95%CI = -18.33±21.87, PR β±95%CI = -15.2±23.7). This difference in slope when subject 137 is excluded from the regression analysis results in an increase in hip abductor EMA_{loc} to 3.44 for an individual with 0.5 biacetabular width of 8.5cm compared to an estimated EMA_{loc} of 0.74 at a preferred walk when subject 137 is included.

While 0.5 biacetabular width is not significantly correlated with either R or EMA_{loc}, the slopes of the regression lines trend in the expected directions. R about the hip in the coronal plane increases with greater biacetabular width and EMA_{loc} decreases as biacetabular width increases. Although EMA_{loc} decreases with increasing biacetabular width, the explanatory power of 0.5 biacetabular width seems to be limited. While this data set is not large, which helps explain the wide confidence intervals of the slope estimate for this regression, measures of true biacetabular width across the study participants incorporate measures between two standard deviations below and three standard deviations above the average modern human mean reported by Tague (1989) for Euroamerican males and females (Table 3.1, Table 6.2). Biacetabular width measured from the centers of the femoral heads is less variable (see below), but the large amount of variation in true biacetabular width provides some confidence that limited subject variability is not limiting the interpretation of the relationship between biacetabular width and EMA_{loc}. However, larger sample sizes will be important to establish the true slope and variability of this relationship.

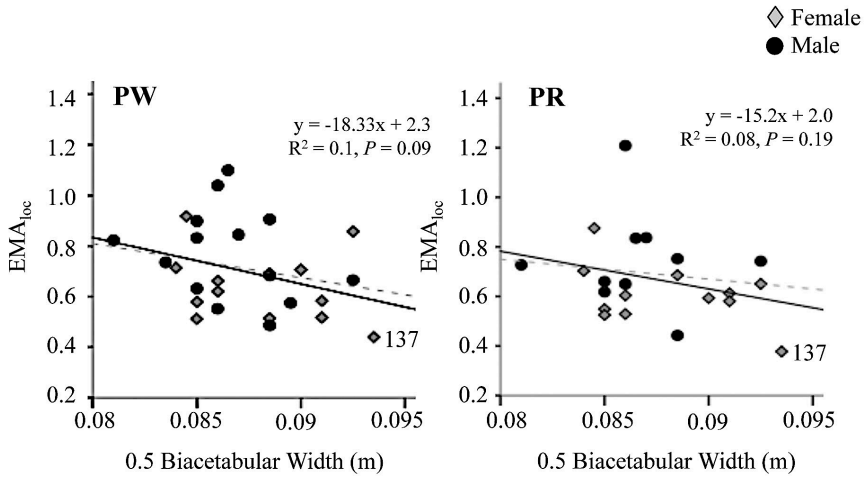

Figure 6.5. Half biacetabular width versus EMA_{loc} at a preferred walk (n = 27) and a preferred run (n = 22). Solid line is LSR. Dotted grey line shows the slope of the LSR with subject 137 removed.

6.3 Pelvic dimensions and EMA in men and women

Although R in the coronal plane is not correlated with biacetabular breadth, females do have significantly lower EMA_{loc} than males at all walking and running speeds (Fig. 6.1, Table 6.1). This difference results from shorter hip abductor r in women compared to men (t =2.87, P <0.01, Table 6.2), which appears to be primarily because femoral neck length is shorter in women (t = 3.11, P < 0.01). Because femoral neck length scales isometrically with femoral length (Wolpoff, 1978; Corruccini, 1980; Ruff, 1995), the reduced hip abductor r in women, and consequently EMA_{loc} is best explained as a correlate of overall size not pelvic dimensions (Fig. 6.6). R in the coronal plane is larger in women than men at each walking and running speed, but none of these

differences are statistically significant (PW, t = 0.83, $P = 0.41$; PR, t = 1.30, $P = 0.20$, Table 6.1).

Men and women in this sample are sexually dimorphic in other aspects of the pelvis, particularly those most closely linked to obstetrics. Women have greater bispinous (t = 5.55, $P < 0.001$) and mediolateral pelvic outlet dimensions (t = 3.68; $P < 0.01$), and, on average, greater true biacetabular width (measured as the distance from the innermost aspect of the right and left acetabula) although this measure does not reach statistical significance ($P = 0.145$). However, when biacetabular distance (diameters between the centers of the femoral heads) is compared, males and females do not differ primarily because the larger femoral heads in males (t = 5.55, $P < 0.001$) increase the mediolateral distance of the hip COR from the body midline (Fig. 6.7, Table 6.2). The result is reduced variation in biacetabular width (CV = 0.035) in comparison to true biacetabular width (CV = 0.079), which is influenced by overall sexual dimorphism of the pelvis (Tague, 1989, 1992; LaVelle, 1995). Regardless, the lack of correlation between R and biomechanical biacetabular width means that hip abductor EMA measured during locomotion does not appear to be affected by sexual dimorphism of the pelvis.

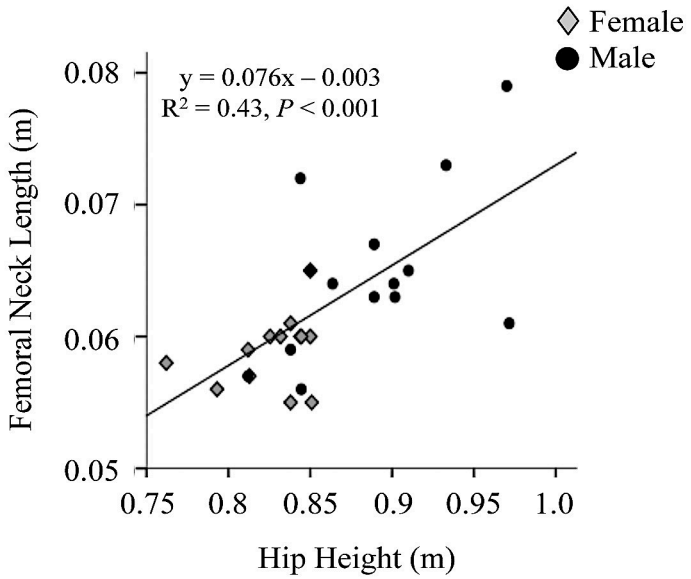

Figure 6.6. Femoral neck length versus hip height measured from the floor to the greater trochanter. Black line indicates LSR.

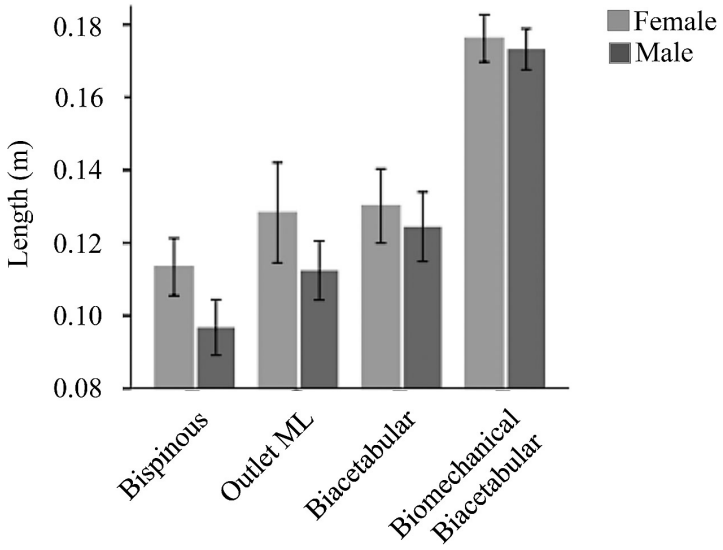

Figure 6.7. Mediolateral dimensions of the pelvis measured from MRI (female N = 13, male N = 14). Females have significantly larger bispinous and mediolateral outlet diameters ($P < 0.01$). True biacetabular width, measured as the distance from the innermost aspect of the acetabula, and biacetabular width are not significantly different between the sexes.

Table 6.1. *Male and female mechanical and force variables during locomotion*

		SW	PW	FW	SR	PR	FR
EMA_{loc} *	N	27	27	26	23	22	21
	Female	0.62±0.14	0.65±0.15	0.62±0.16	0.64±0.15	0.62±0.13	0.62±0.13
	Male	0.78±0.19	0.76±0.18	0.77±0.17	0.79±0.19	0.74±0.19	0.82±0.21
R (m)	N	27	27	26	23	22	21
	Female	0.088±0.013	0.084±0.012	0.089±0.015	0.086±0.017	0.089±0.015	0.087±0.014
	Male	0.078±.0145	0.080±0.013	0.078±0.012	0.079±0.013	0.081±0.013	0.077±0.015
Pelvic Angle°	N	24	26	25	19	19	17
	Female	1.4±1.9	1.8±2.0	1.8±2.0	2.8±3.0	3.0±2.9	2.8±3.3
	Male	0.3±1.4	0.3±1.4	0.4±1.5	2.7±1.6	2.4±2.0	2.1±1.9
ML GRF/Body Mass ($N\ kg^{-1}$)	N	27	27	26	23	22	21
	Female	0.43±0.11	0.48±0.10	0.61±0.19	0.74±0.37	0.82±0.42	1.0±0.42
	Male	0.45±0.10	0.47±0.11	0.56±0.16	0.60±0.28	0.69±0.20	0.81±0.41

Effective mechanical advantage of the hip abductors measured during locomotion (EMa_{loc}), GRF moment arm, R, at the hip in the coronal plane, pelvic angle measured from the horizontal, and peak mediolateral component of GRF per kilogram body mass at each walking and running speed (SW, slow walk; PW preferred walk; FW, fast walk; SR, slow run; PR, preferred run; FR, fast run).

* indicates females are significantly smaller than males at the $P < 0.01$ level when preferred walking and running speeds are compared

Table 6.2. *Pelvic and hip anthropometrics*

	Sex	Mean±1 SD
r, hip abductors (m)*	Female	0.052±0.004
	Male	0.059±0.007
Femoral neck length (m)*	Female	0.058±0.002
	Male	0.064±0.006
True biacetabular diameter (m)	Female	0.130±0.010
	Male	0.124±0.009
Biacetabular diameter (m)	Female	0.176±0.006
	Male	0.173±0.005
Bispinous diameter (m)+	Female	0.113±0.007
	Male	0.096±0.007
ML outlet diameter (m)+	Female	0.128±0.013
	Male	0.112±0.008
Femoral head diameter (m)*	Female	0.041±0.001
	Male	0.045±0.002

* males larger than females at $P < 0.01$
+ females larger than males at $P < 0.01$

6.4. Influence of kinematics and mediolateral GRF on hip abductor EMA

6.4.1 Pelvic tilt during locomotion

Controlling the inclination of the pelvis during locomotion is one of the primary functions of the hip abductor muscles (Inman, 1947; Merchant, 1965; McLeish and Charnley, 1970). Increased pelvic inclination may also influence hip abductor EMA_{loc} by altering the distance of the body center of mass from the hip COR (McLeish and Charnley, 1970). Average pelvic angle was measured from the horizontal plane and weighted by the vertical component of GRF. Positive values indicate tilting of the pelvis away from the supporting limb, and negative values indicate elevation of the pelvis towards the standing leg.

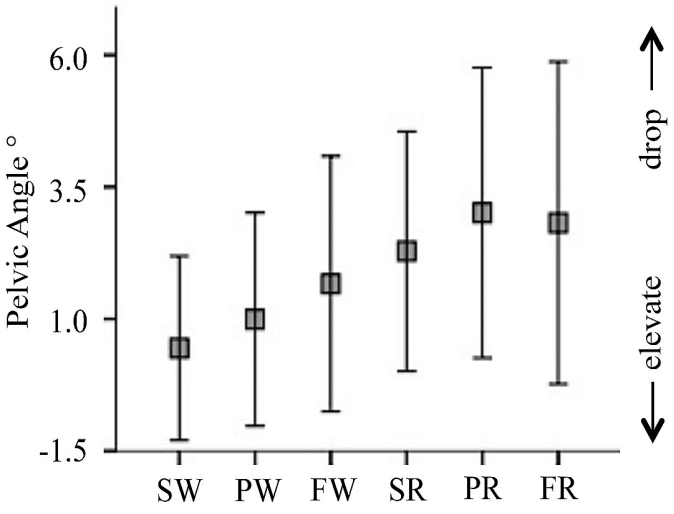

Figure 6.8. Pelvic angle measured from the horizontal plane at each walking and running speed (SW, slow walk n = 24; PW preferred walk, n = 26; FW, fast walk, n = 25; SR, slow run, n = 19; PR, preferred run, n = 19, FR, fast run, n = 17). Positive values indicate tiltling of the pelvis away from the supporting side. Negative values indicate elevation of the pelvis towards the support limb. Error bars are one standard deviation from the mean. There are no significant differences between speeds within a gait or between preferred walking and running speeds.

When viewed across gaits, pelvic angle tends to increase with speed, but there is significant overlap between speeds and gaits (Figure 6.8). When preferred walking and running speeds are compared, pelvic inclination during walking averages 1.09±1.91 degrees and 2.76±2.48 degrees during running ($P = 0.1$). Pelvic angle is extremely variable between subjects in both the magnitude and pattern of pelvic inclination during locomotion. At a walk, pelvic tilt ranges from 5.29 degrees inclination away from the supporting side to -2.01 degrees, indicating elevation of the contralateral side towards the standing leg. At a running gait, maximum pelvic tilt is 8.36 degrees (same subject as maximum walking) and the minimum is -0.99 degrees. Intra-subject variability in pelvic inclination within a particular speed seems to be limited. The maximum range across trials for any subject at a preferred walk is 5.1 degrees and 4.1 degrees at a preferred run. Between individuals, no consistent effect of gait on pelvic inclination is discernible. Some subjects maintain very similar angles when gait transitions from a walk to a run, while in others, angles increase by several degrees during running (Fig. 6.9).

There are no significant differences in pelvic inclination between males and females in this sample during walking or running (Table 6.1). These findings are in contrast to observations from other studies that have shown greater pelvic movement in the coronal plane in females compared to males (Cho et al., 2004; Chumanov et al., 2008) and which have been attribute to aspects of body breadth variation between the sexes (Cho et al., 2004; Chumanov et al., 2008). When pelvic angle is plotted against biacetabular width, there is no meaningful relationship between the degree of pelvic tilt and biacetabular width among these subjects (PW, $r^2 = 0.07$, $P = 0.184$; PR $r^2 = 0.03$, $P =$

0.41, Fig. 6.10). Pelvic inclination is also not correlated with mediolateral R at the hip (PW and PR, $\beta = 0$), suggesting that either pelvic tilt is not large enough to cause major deviations of the body COM, which would affect mediolateral GRF, or that another kinematic process is responsible for the magnitude of R during locomotion.

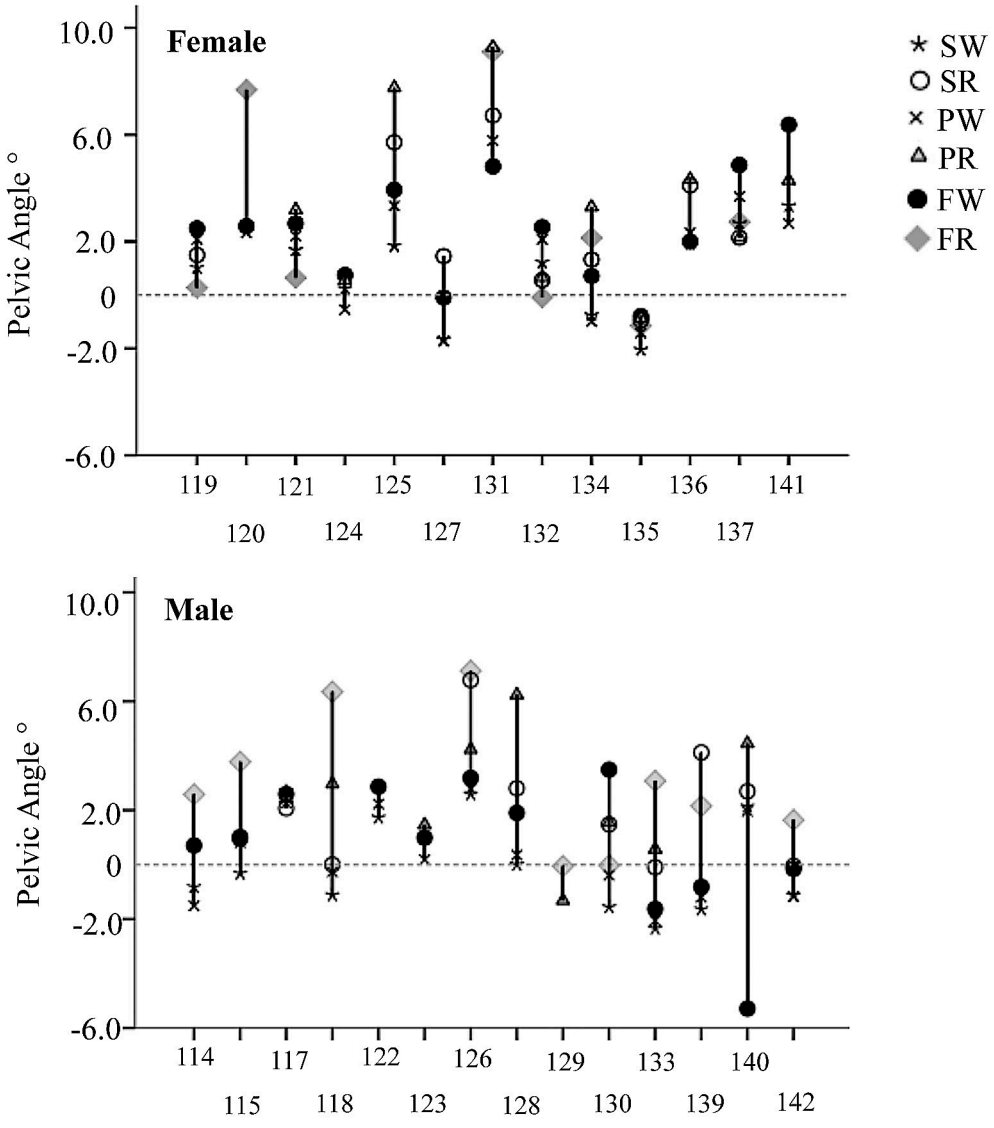

Figure 6.9. Pelvic Angle for each subject at walking and running speeds (SW, slow walk n = 24; PW, preferred walk n = 26; FW, fast walk n = 25; SR, slow run n = 19; PR, preferred run n = 19; FR, fast run n = 17).

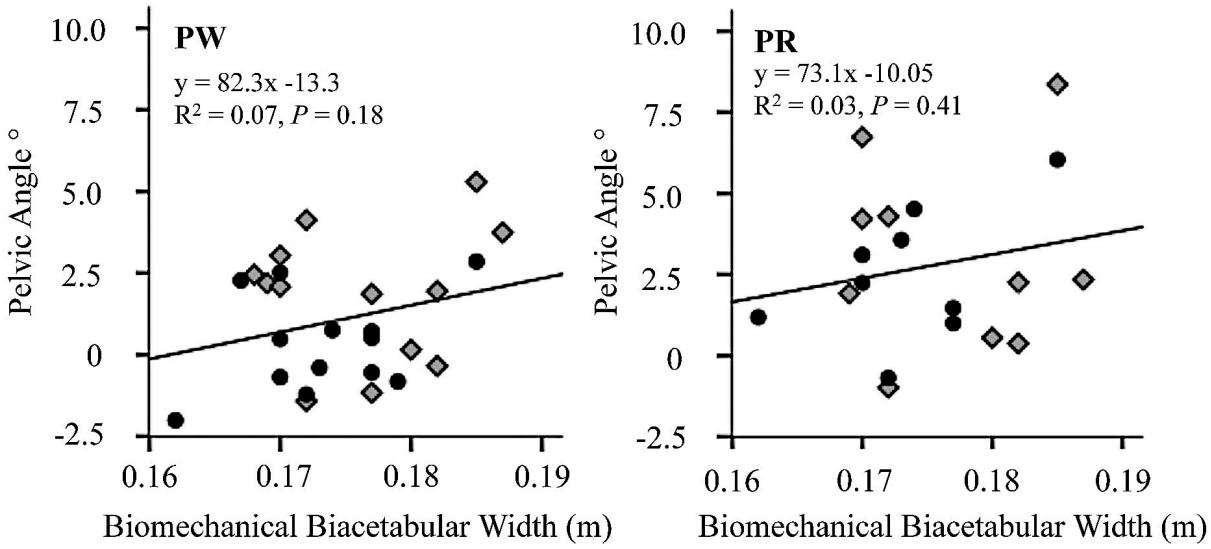

Figure 6.10. Biacetabular width versus pelvic angle.

6.4.2 Mediolateral GRF

The mediolateral component of GRF causes the resolved force vector to deviate medially away from the supporting side during single leg stance. Therefore, changes in magnitude with gait, and inter-subject variation in this measure could influence EMA_{loc} of the hip abductors. Mass-specific mediolateral GRF increases gradually with speed across gait, but similar to pelvic inclination, there is substantial overlap between speeds (Fig. 6.10). When preferred walking and running speed are compared, a significant increase in force per kilogram body mass is evident when gait changes from a walk to a run (PW = 0.47±0.1N kg^{-1}, PR =0.76±0.33N kg^{-1}; $P < 0.01$). Males and females do not statistically differ in mass-specific mediolateral GRF at any speed, but women tend to have slightly higher mass-specific mediolateral GRF at the highest walking speed and during running (Table 6.1), but inter-subject variation is high (Fig. 6.12).

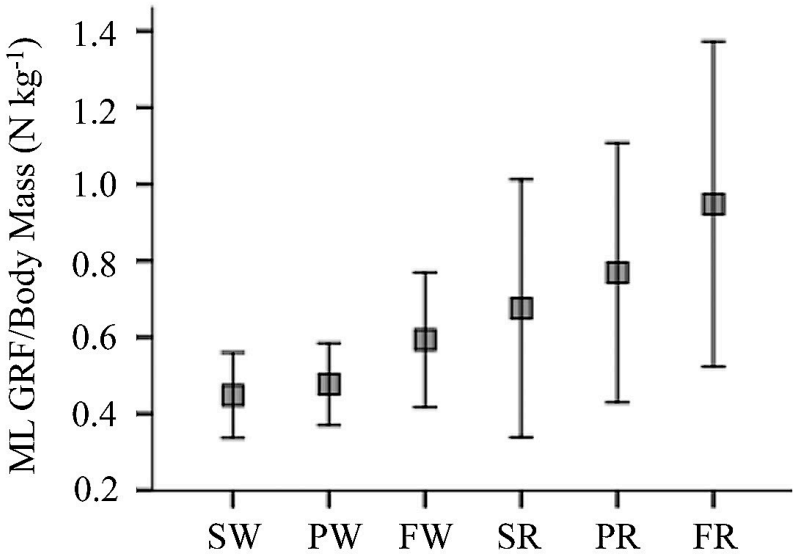

Figure 6.11. Mass-specific mediolateral GRF per kilogram body mass (N kg^{-1}) at each walking and running speed (SW, slow walk n = 27; PW preferred walk, n = 27; FW, fast walk, n = 26; SR, slow run, n = 23; PR, preferred run, n = 22, FR, fast run, n = 21). When preferred walking and running speeds are compared, mass-specific mediolateral GRF increases significantly from a walk to a run ($P < 0.01$)

Although the mediolateral component of GRF causes the GRF vector to move away from the hip COR, the magnitude of this force does not explain subject variability in mediolateral R at the hip (Fig. 6.13). There are two possible explanations for this result. First, comparing peak mediolateral GRF with a weighted average of R may not accurately match the time course of force production and the oscillations of R during the course of stance phase. Alternatively, R may be determined by individual kinematic profiles during locomotion that are not represented in these data, but which would have the effect of moving the hip COR farther from the GRF vector.

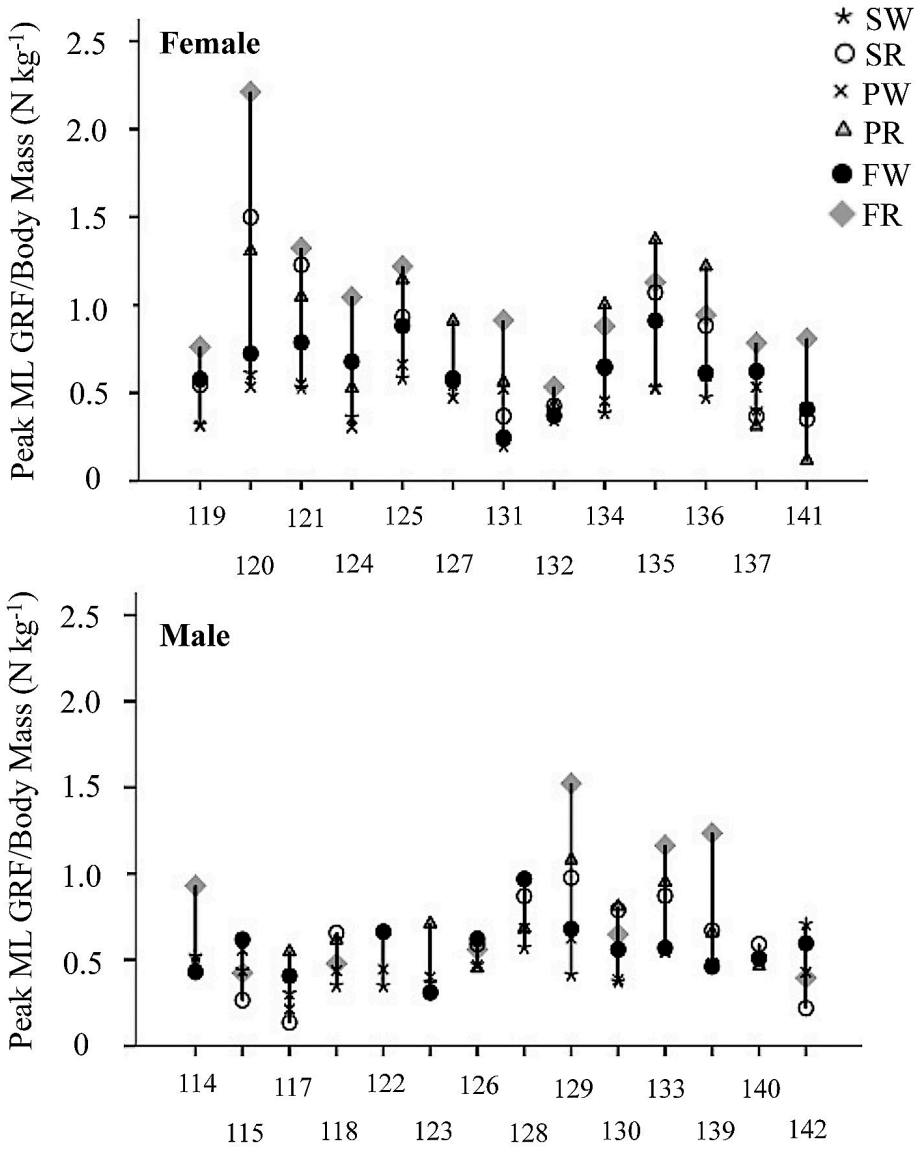

Figure 6.12. Mass-specific mediolateral GRF (N kg^{-1}) for each subject at walking and running speeds (SW, slow walk n = 27; PW, preferred walk n = 27; FW, fast walk n = 26; SR, slow run n = 23; PR, preferred run n = 22; FR, fast run n = 21).

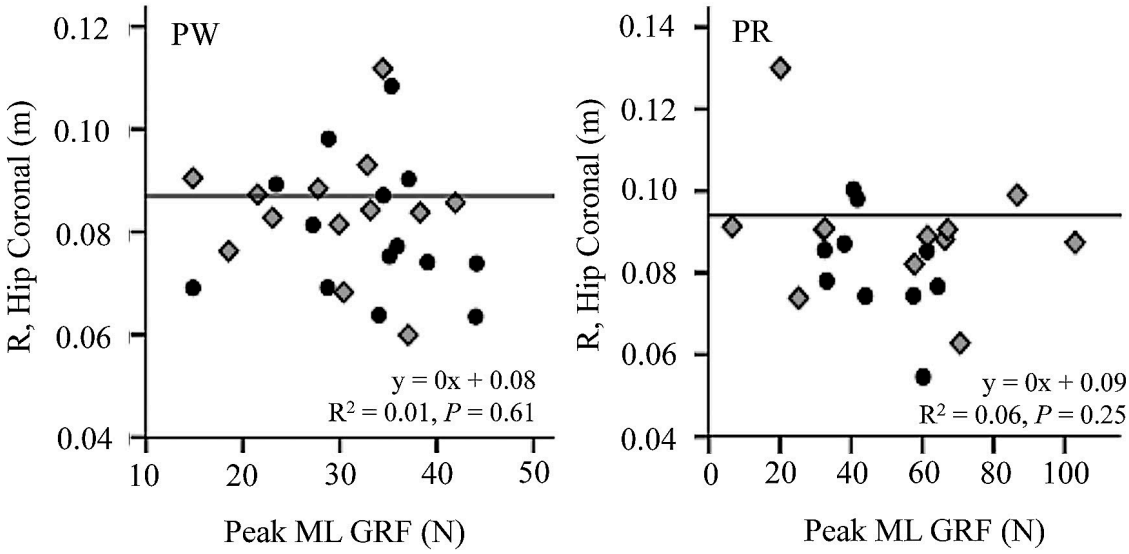

Figure 6.13. Peak mediolateral GRF versus GRF R at the hip in the coronal plane (PW, preferred walk; PR, preferred run).

6.5 Discussion

The results presented above suggest that the relationship between pelvic shape and hip abductor mechanics as currently understood must be re-evaluated. Dynamic changes in coronal R over the course of stance phase cannot be accurately described by the static measure of the distance between the body midline and the hip center of rotation assessed from biacetabular breadth. These findings have important implications for assessment of hip abductor function and gait in extinct hominins and require a re-assessment of a primary tenet of the 'obstetrical dilemma,' that female pelvic shape is a compromise between effective locomotion and parturition. Additionally, the analysis of kinetics and mediolateral force presented above indicates that predicting hip abductor

function requires a more comprehensive approach to understand the dynamic movement of the body center of mass during stance phase and the influence of anatomy.

6.5.1 Biomechanical femoral neck length and fossil hominin EMA

The lack of correlation between biacetabular width and GRF R at the hip limits functional interpretations of hominin pelvic morphology as it relates to hip abductor force production and gait dynamics. While the partial correlation between femoral neck length and EMA_{loc} allows general statements regarding the influence of skeletal morphology on hip abductor mechanics, the functional relevance of this relationship is uncertain.

Biomechanical femoral neck length scales isometrically with femoral length across modern human populations (Wolpoff, 1978; Corruccini, 1980; Ruff, 1995), but is also affected by ecogeographic variation in body shape. Cold adapted populations have longer relative biomechanical femoral neck lengths scaled to femur length than equatorial groups (Ruff, 1995). Isometric scaling likely also applied in early *Homo* (Wolpoff, 1978), though relative biomechanical femoral neck length appears to have been greater through the Middle Pleistocene (Wolpoff, 1978; Ruff, 1995). This is certainly the case in australopithecines where estimated values for the biomechanical femoral neck length of Sts 14 are near the modern human distribution sampled here (range = 0.055-0.079m), and within the values given by Wolpoff (1978) and Ruff (1995), yet femoral length is estimated at only 0.28m compared to a minimum femoral length of 0.33m in this study (also see Ruff, 1995).

Even though relative biomechanical femoral neck length is greater in australopithecines and early *Homo*, it is important to highlight that the lever model of hip abductor mechanics is not scaled to femur or body length. Absolute hip abductor force would have been less in small-bodied hominins because of smaller GRF at comparable speeds (McHenry, 1975), but the effective mechanical advantage of the hip joint is unaffected by stature or limb length. The fact that biomechanical femoral neck length in relation to femoral length appears to have decreased since the Middle Pleistocene is a more interesting question, perhaps, than whether hip abductor function was sacrificed in early hominins. However, the weak correlation between femoral neck length and EMA_{loc} indicates that there are substantial aspects of hip abductor mechanics that cannot be explained by skeletal dimensions alone.

6.5.2 Implications of hip abductor mechanics for the 'obstetrical dilemma'

Sexual dimorphism of the human pelvis is most often characterized as the result of competing selective pressures on the female pelvis acting to enlarge the female birth canal to allow the passage of a large brained infant and minimize the breadth of the pelvis for efficient locomotion (Washburn, 1960; Napier, 1964; Meindl et al., 1985; Rosenberg, 1992). While sexual dimorphism is well documented in several measures of pelvic breadth, particularly at the pelvic midplane and outlet (Tague 1989, 1992; LaVelle, 1995) that are most significant in determining obstetric success (Abitbol, 1996), the link between pelvic morphology and locomotor function has gone unquestioned.

This analysis does not support the assumption that wider biacetabular dimensions in women result in less effective hip abductor mechanics, and thus locomotor inefficiency. While EMA_{loc} is significantly lower in women compared to men, it is because biomechanical femoral neck length is generally shorter resulting from overall smaller limb length and body size (Wolpoff, 1978; Corruccini, 1980), not because biacetabular width increases the distance between the hip joint and the GRF force vector. Additionally, when sexual dimorphism in femoral head diameter is considered, biacetabular width does not differ between males and females, even though females are, on average, larger in true biacetabular dimensions (this sample, and see Tague 1989, 1992; LaVelle, 1995).

While no statistical differences in pelvic inclination or mass-specific mediolateral GRF production between men and women were found in this analysis, females, on average, had greater pelvic angulation, R and mass-specific mediolateral GRF at certain speeds (Table 6.1). While some of these differences can be attributed to the high values of one female subject (137), particularly R, the distinctions between men and women may become more apparent with larger sample sizes. However, the extreme amount of variability in all these measures found in both men and women suggests that other factors are important in determining mediolateral balance of the body during locomotion. The possibility remains that aspects of pelvic shape influence hip abductor function or other aspects of gait, but based on the analysis presented here, sexual dimorphism of the pelvis is best viewed solely as a response to obstetrical demands arising from birthing large brained infants without compromising locomotor performance.

6.5.3 Body center of mass and mediolateral balance in the coronal plane: a broader model of hip abductor mechanics is needed

The lack of correlation between hip abductor mechanics, pelvic inclination and mediolateral GRF presented above suggests that additional factors are influencing moments generated at the hip in the coronal plane. Recent research on the control of mediolateral balance may help explain some of these discrepancies. Pandy et al. (2010) present a double-pendulum model of center of mass balance in the mediolateral plane (reproduced below as Fig. 6.14). In this model the angle formed between the stance leg and the floor dictates the pull of gravity on the body. When the angle is greater than 90°, the body center of mass is pulled medially, away from the supporting limb. When the angle is less than 90°, the body accelerates laterally towards the standing side. In addition to the pull of gravity, Pandy et al. (2010) found muscles that act in the sagittal plane to support and propel the body center of mass also push the center of mass laterally during support phase of locomotion. To counter the lateral acceleration of the center of mass produced by muscular activity and gravity, the hip abductors must produce force causing a medially directed GRF. This has the effect of pushing the body center of mass away from the supporting side and maintaining body equilibrium through the course of stance phase (Pandy et al., 2010).

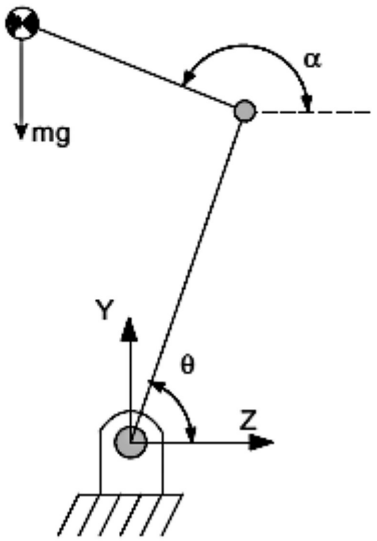

Figure 6.14. Reproduced from Pandy et al., 2010, showing the double pendulum model of mediolateral force production during the stance phase of walking. Body mass is applied at the end of the pelvic segment, and the direction of the pull of gravity on the body is determined by the angle of the stance limb to the floor. Angles of greater than 90° will pull the body center of mass medially, while angles of less than 90° will pull the body laterally requiring hip abductor force to maintain the body in equilibrium (see Pandy et al., 2010).

Because the angle of the stance leg is a function of step width, Pandy et al. (2010) predict that wider step widths will decrease hip abductor activation by creating a medial orientation of the pull of gravity. Because step width is a function of leg length (Donelan et al., 2001), this may be a crucial variable in predicting hip abductor mechanics and force production. Additionally, while Pandy et al. (2010) argue that the angle of the

stance leg dictates the lateral pull of gravity acting on the body center of mass, the orientation of the leg with respect to the ground will also be influence by the femoral bicondylar angle. These complications argue for a more comprehensive model of hip abductor mechanics that incorporates the dynamic movement of the body center of mass and the orientation of the leg and thigh during the course of stance phase, along with lower limb length and step width into the model.

CHAPTER 7
RELATING HIP ABDUCTOR FUNCTION TO LOCOMOTOR COST

7.1 Introduction

Traditionally, wide pelves in both early hominins and in women have been thought to negatively impact locomotor performance by increasing the force required to stabilize the pelvis and therefore increasing the cost of locomotion (Napier, 1964; Zihlman and Brunker, 1979; Stern and Susman, 1983; Meindl et al., 1985; Rosenberg, 1992; Berg, 1994; Hunt 1998; Arsuaga, 1999). Although this analysis has demonstrated a lack of correlation between biacetabular width and hip abductor mechanics, moments and muscle force at the hip in the coronal plane have been shown to be substantial and comparable to those required for support and forward propulsion of the body during walking and running. Therefore the metabolic demand of producing force in the hip abductors may be an important component of energetic cost during locomotion.

Previous research has demonstrated that locomotor cost is closely linked to the vertical ground force impulse required to support body weight and redirect the body center of mass during foot-ground contact (Kram and Taylor, 1990; Roberts et al., 1998a; Roberts et al., 1998b; Donelan et al., 2002; Pontzer, 2005, 2007). Longer contact times decrease the rate and magnitude of ground force produced per step, as well as step frequency, which lowers the rate of oxygen consumption ($mlO_2\ s^{-1}$) during locomotion (Kram and Taylor, 1990; Pontzer, 2005, 2007; Pontzer et al., 2009). This model helps explain the negative allometric scaling of the cost of transport, COT ($mlO_2\ kg^{-1}\ m^{-1}$),

versus body mass across a wide range of species (Taylor et al., 1970; Taylor et al., 1982), where animals with longer limbs use less oxygen per kilogram body mass to travel one unit distance compared to smaller animals who have shorter contact times and take more frequent steps.

However, intra-species comparisons of cost have shown that, while vertical ground force production is still a major determinant of cost (Pontzer, 2005), other aspects of gait and anatomy are important at this scale of analysis (Pontzer, 2005, 2007). In humans, the cost of swinging the contralateral limb is substantial, particularly during running where the swing leg can account for as much as 30% of total cost (Gottschall and Kram, 2005; Pontzer, 2007). Additionally, muscle architecture is important. Muscles with longer fibers must activate a greater volume per unit force produced, which increases their metabolic demand (Roberts et al., 1998a; Roberts et al., 1998b; Pontzer et al., 2009). Finally, the energy demand of different muscle types under different contractile conditions may also affect inter-species comparisons of locomotor cost (Alexander, 2005).

While several studies have examined how vertical and horizontal force production, as well as leg swing and muscle architecture affect the energetics of walking and running (Roberts et al., 1998a; Roberts et al., 1998b; Gottschall and Kram, 2003, 2005; Griffin et al., 2003; Doke et al., 2005; Pontzer 2005, 2007), the cost of mediolateral balance of the body through the action of the hip abductors has not been explored. In order to determine the contribution of the abductors to overall locomotor cost, active muscle volume in the hip abductors, as well as the extensor muscle groups of the lower

limb, was calculated across walking and running speeds. COT ($mlO_2\ m^{-1}$) determined from oxygen consumption trials (see methods) was then plotted against the sum of active muscle volume to determine the relationship between the variables (see methods). Using the slope of the regression line, the contribution of the hip abductors to whole body locomotor cost could then be calculated. Finally, the independent effect of hip abductor EMA_{loc} on locomotor cost was determined using a multiple regression model, controlling for body size and speed.

This muscle volume model explicitly incorporates force production in the vertical, horizontal and mediolateral planes and includes subject specific muscle fascicle lengths (see methods) as potential contributors to variation in locomotor cost. The model does not attempt to account for variation in cost related to swinging the contralateral limb, and the rate of energy use by the muscles is considered to be constant regardless of type and contractile state (Biewener et al., 2004). While these shortcomings will lower the correlation coefficients in the muscle volume cost regressions, the focus of the analysis is on the direct role of the hip abductors as a contributor to cost, which should be well represented by the slope of the muscle volume cost relationship.

7.2 Active muscle volume of the lower limb during locomotion

When preferred walking and running speeds are compared, mass-specific active muscle volume of the hip abductors was 15.4±3.0% of total active muscle volume in the lower limb during a walk and 16.4±3.0% at a run (Fig. 7.1). The ankle plantarflexors made up the largest proportion of active muscle volume of the lower limb at both gaits,

accounting for between 41.9±7.1% and 33.3±5.0% at a walk and run respectively. The hip extensors were 25.6±8.0% at walking gait and 23.8±8.1% at a run, while the knee made up 16.9±7.0% at a walk but increased to 26.3±6.8% of the total when gait changed to a run (Fig. 7.1).

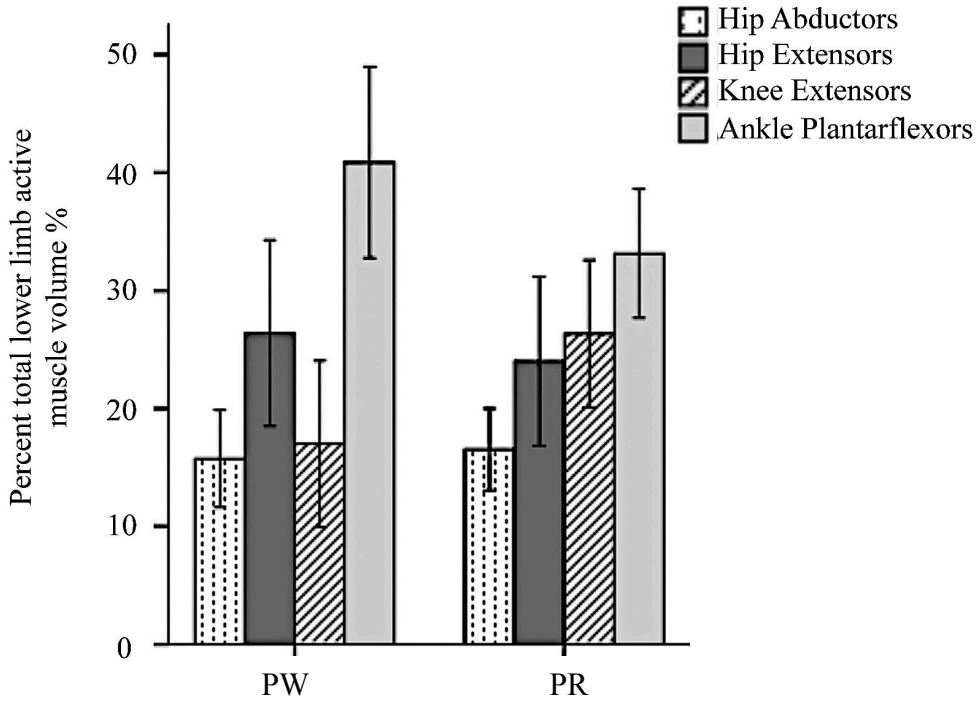

Figure 7.1. Active muscle volume of four muscle groups of the lower limb as a percentage of total active muscle volume of the lower limb during a walk (n = 27) and run (n = 21). Data is for preferred walking and running speeds. Error bars indicate one standard deviation.

When all four muscle groups are summed, total active muscle volume of the lower limb increases significantly at each change in speed within a gait and between gaits ($P < 0.001$) except from a preferred run to a fast run, and from a slow walk to a preferred walk (Table 7.1). In the hip abductors and knee extensors, active muscle volume

increased significantly when gait changed from a walk to a run ($P < 0.001$), but was independent of speed changes within a gait. However, increasing speed within a gait did affect hip extensor and ankle plantarflexor active muscle volume. Hip extensor active muscle volume increased significantly at both a walking and running gait from the slowest to fastest speeds ($P < 0.05$), while active muscle volume at the ankle was significantly greater at the fastest walking speed compared to a slow walk ($P < 0.001$).

Table 7.1. Active muscle volume of each muscle group in the lower limb at slow, preferred and fast walking and running speeds

Gait	N	Hip Abductors ($cm^3\ kg^{-1}$)	Hip Extensors ($cm^3\ kg^{-1}$)	Knee Extensors ($cm^3\ kg^{-1}$)	Ankle Plantarflexors ($cm^3\ kg^{-1}$)	Total Lower Limb ($cm^3\ kg^{-1}$)
SW	27	4.3±0.9	5.8±2.3	3.3±1.6	11.1±1.5	24.7±3.7
PW	27	4.5±1.0	7.8±3.5	5.1±2.3	12.2±1.7	29.7±5.2
FW	26	5.0±1.1	11.6±4.2	7.7±2.7	12.8±1.9	37.3±5.6
SR	23	8.6±2.1	11.4±5.1	13.8±3.6	17.1±3.6	51.1±8.3
PR	22	9.4±2.0	14.0±6.2	14.9±3.6	19.0±3.1	57.4±7.2
FR	21	9.7±2.0	16.5±4.7	15.8±4.4	19.8±3.1	62.0±8.7

7.3 Relating locomotor cost to active muscle volume

In order to assess the relationship between locomotor cost and active muscle volume of the lower limb, whole body COT ($mlO_2\ m^{-1}$) was plotted against total lower limb active muscle volume ($cm^3\ m^{-1}$). When walking and running gaits were pooled, active muscle volume ($cm^3\ m^{-1}$) explained a significant portion of variation in COT ($mlO_2\ m^{-1}$) ($r^2 = 0.77$, $P < 0.001$, Fig. 7.2). When COT was plotted against active muscle volume during walking or running independently, the correlation decreased (walk, $r^2 = 0.13$, $P < 0.01$; run $r^2 = 0.30$, $P < 0.001$), but the slope of the regression line was similar

in all three conditions (Figs 7.2 and 7.3). The consistency of the slope lends confidence to the predicted relationship between COT and active muscle volume, therefore the contribution of individual muscle groups to locomotor cost could be estimated.

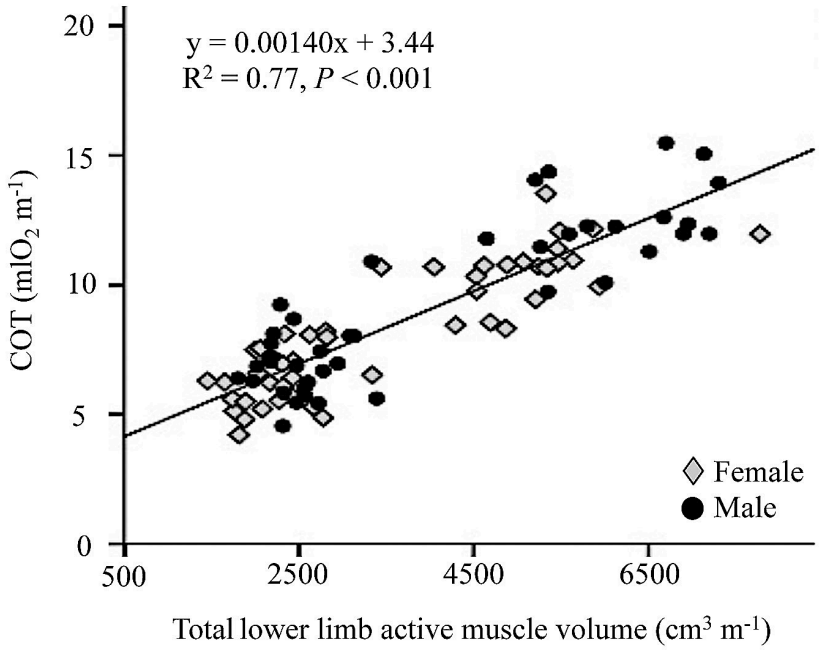

Figure 7.2. Whole body cost of transport (COT) versus total active muscle volume of the lower limb. Data pooled for all speeds and gaits (n = 88). Line indicates LSR.

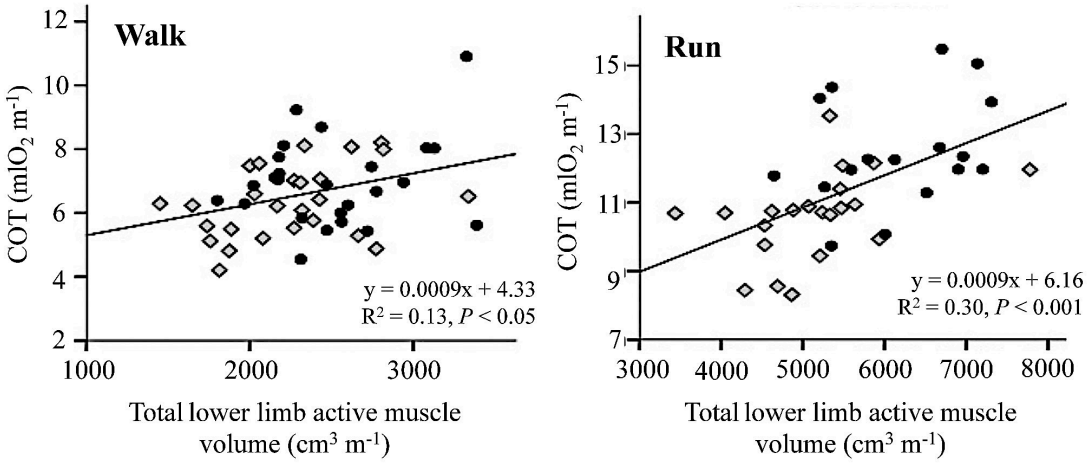

Figure 7.3. Whole body cost of transport (COT) versus active muscle volume of the lower limb at a walk (n = 50) and at a run (n = 37) independently. Line indicates LSR.

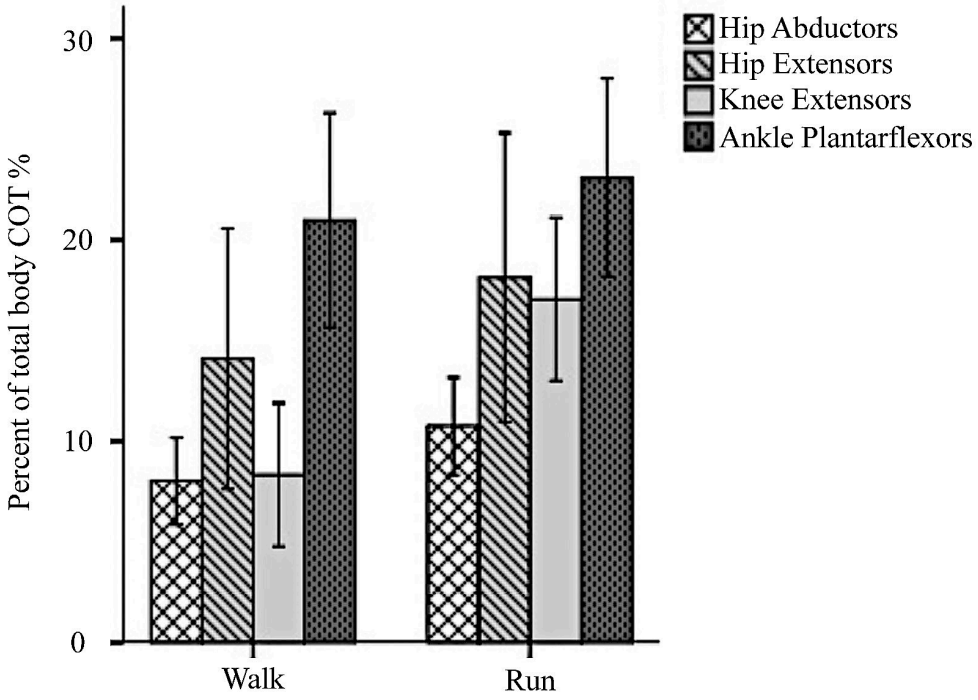

Figure 7.4. Percentage of cost of transport attributed to each muscle group of the lower limb. Data is for preferred walking and running gaits. Error bars indicate one standard deviation.

When preferred walking and running speeds are compared, the hip abductors

account for 7.7±2.3% of total body COT ($mlO_2\ m^{-1}$) during a walk and 10.7±2.5% at a run (Fig 7.4). The ankle plantarflexors are the largest contributor to total body COT of all the muscle groups, 19.8±6.5% at a walk and 22.8±4.6% at a run. Active muscle volume in the hip and knee extensors accounts for 11.4±2.9 and 8.5±2.9% of total body COT at a walk, and 16.8±8.1 and 16.6±4.3% at a run respectively (Fig 7.4).

Per kilogram body mass, cost attributable to hip abductor active muscle volume ($mlO_2\ kg^{-1}\ m^{-1}$) is higher in women than men during a preferred run, but not at a preferred walk (Fig 7.5). Female mass-specific hip abductor cost is 0.0083±0.0016 $mlO_2\ kg^{-1}\ m^{-1}$ at a walk, while in men the cost of activating the hip abductors is 0.0073±0.0020 $mlO_2\ kg^{-1}\ m^{-1}$ ($P = 0.20$, t = 1.31, Fig 7.5). At a run the cost associated with the hip abductors is 0.0218±0.0054 $mlO_2\ kg^{-1}\ m^{-1}$ in women and 0.0173±0.0041 $mlO_2\ kg^{-1}\ m^{-1}$ in men ($P < 0.05$, t = 2.16). These small differences account, in part, for the greater contribution of hip abductor active muscle volume to total cost in women during a walk (female mean = 8.8±2.4%, male mean = 7.1±2.4%, $P = 0.29$) and a run (female mean = 11.9±2.2%, male mean = 9.8±2.6%, $P = 0.11$), although neither comparison reaches statistical significance.

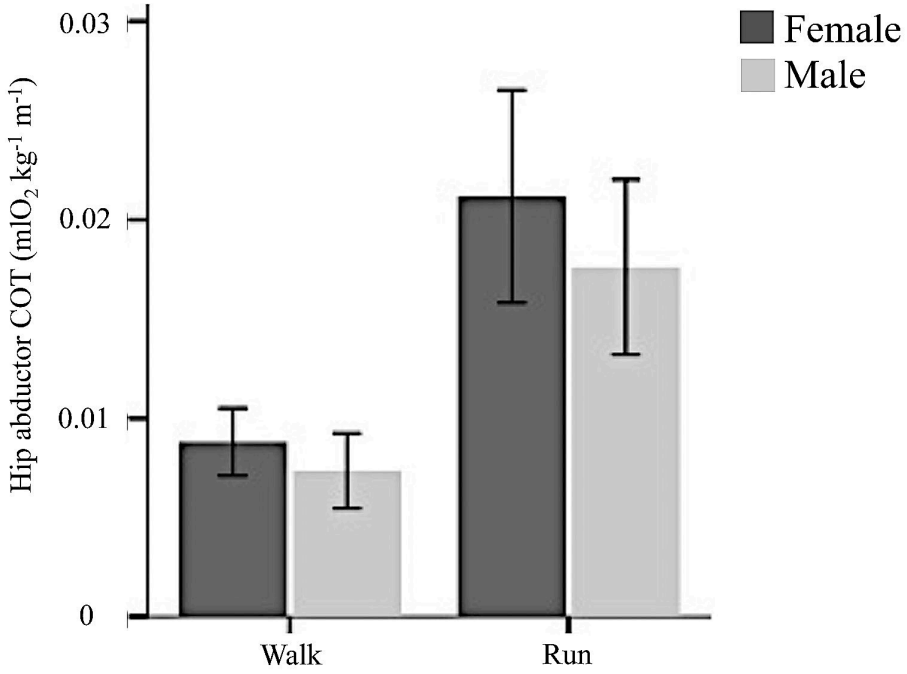

Figure 7.5. Mass-specific hip abductor contribution to COT in males and females. Data is for a preferred walk (female n = 13, male n = 14) and a preferred run (female n = 12, male n =10). Error bars are one standard deviation. Differences between men and women are significant at $P < 0.01$ at a walk and $P < 0.05$ at a run.

7.4 Hip abductor mechanics and locomotor cost

The effect of individual hip abductor mechanics on locomotor cost was estimated using a multiple regression model of whole body COT ($mlO_2\ m^{-1}$) on hip abductor EMA_{loc}, controlling for speed and body mass. When EMA_{loc} is added to the regression model, there is no significant increase in explained variance in COT ($mlO_2\ m^{-1}$) (r^2

change = 0.004, $P = 0.22$). The lack of relationship between EMA_{loc} and cost indicates that, although active muscle volume of the hip abductors makes up roughly 10% of COT ($mlO_2\ m^{-1}$), small changes in abductor mechanics have a negligible impact on total body cost during locomotion. This conclusion is reinforced when mass-specific COT ($mlO_2\ kg^{-1}\ m^{-1}$) is compared between men and women. Although women have slightly greater cost associated with hip abductor active muscle volume, overall locomotor cost is not different between the sexes (Fig. 7.7). At a preferred walk, average mass-specific COT was $0.1109 \pm 0.023 mlO_2\ kg^{-1}\ m^{-1}$ for women and $0.1051 \pm 0.015 mlO_2\ kg^{-1}\ m^{-1}$ for men ($P = 0.64$). At a preferred run, mass-specific COT was $0.1714 \pm 0.022 mlO_2\ kg^{-1}\ m^{-1}$ and $0.1782 \pm 0.017 mlO_2\ kg^{-1}\ m^{-1}$ in women and men respectively ($P = 0.51$).

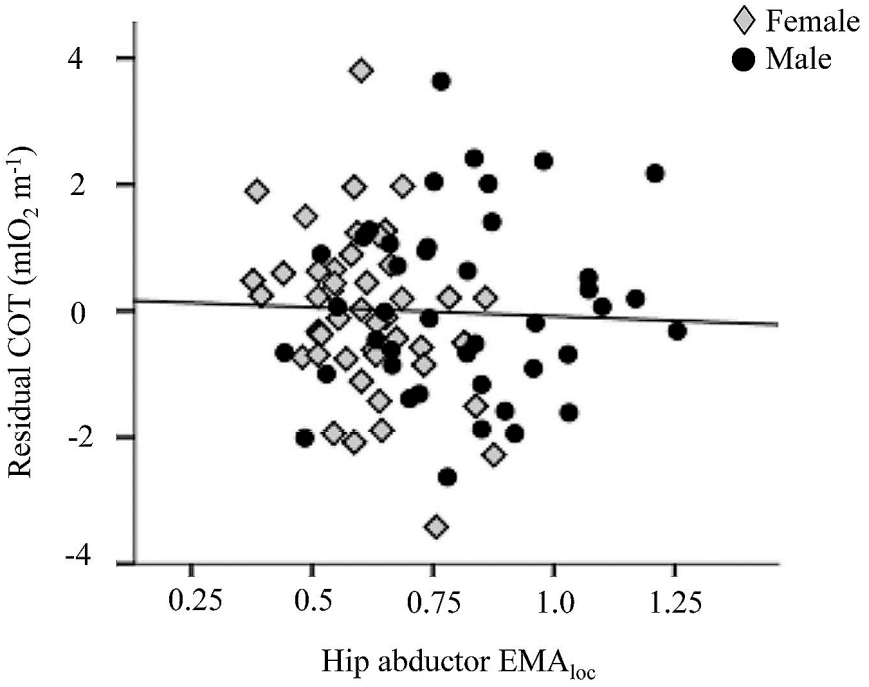

Figure 7.6. Residual COT versus hip abductor EMA_{loc}. Residuals are calculated from multiple regression of COT controlling for speed and body mass. When hip abductor EMA_{loc} is added to the multiple regression model, change $r^2 = 0.004$, $P = 0.22$. Line indicates LSR.

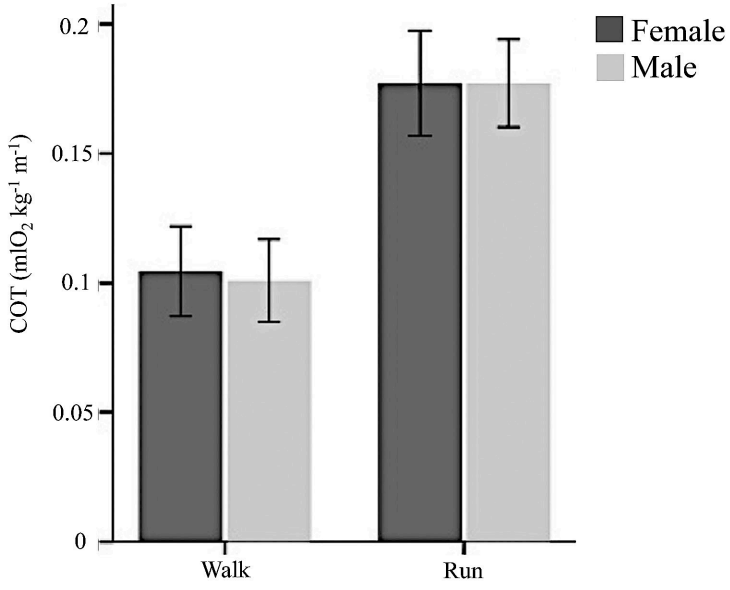

Figure 7.7. Mass-specific COT in women and men at a preferred walk (female n = 4, male n = 6) and a preferred run (female n = 21, male n = 9). Error bars indicate one standard deviation.

7.4 Discussion

The cost of producing force in the hip abductors via active muscle volume is approximately 10% of whole body COT. This cost is less than any of the extensor muscle groups of the lower limb, but still an important contributor to energetic demand during both walking and running. Although women show a slightly higher cost associated with the activation of the hip abductors, there is no significant relationship between hip abductor EMA_{loc} and COT once speed and body mass are accounted for, and there is no difference between men and women in mass-specific COT at either a walking or running gait. This suggests that the variability in active muscle volume of the hip abductors is small enough, at least in this sample, to be negligible. Although individual variation in COT associated with hip abductor function may not be predictive of individual locomotor efficiency, this analysis has shown when compared across muscle groups, the hip abductors are an important part of locomotor performance and should be included in future analyses of force generation and cost.

CHAPTER 8
DIFFERENCES BETWEEN MALES AND FEMALES IN JOINT MECHANICS

8.1 Introduction

Previous research has shown important kinematic differences between men and women during locomotion that are generally assumed to result from dimorphic aspects of body shape (Smith et al., 2002; Ferber et al., 2003; Cho et al., 2004). In particular women have been shown to walk and run with greater hip adduction, internal rotation of the thigh and increased valgus angle (Cho et al., 2004; Ferber et al., 2003). These differences are thought to contribute to the greater incidence of patellofemoral pain syndrome and iliotibial band injuries in women compared to men (Taunton et al., 2002; Ferber et al., 2003). While these studies have demonstrated kinematic variation in walking and running patterns between men and women, it is unclear how these differences affect joint mechanics and force production during locomotion. Few inverse dynamics studies of joint kinetics include women, and sample sizes for both sexes are often small (see Griffin et al., 2003 and Biewener et al., 2004).

This section compares joint moments, muscle force production and effective mechanical advantage in the joints of the lower limb to determine if any systematic differences between men and women are present. Because previous sections have already discussed the relationship between hip abductor EMA and sexual dimorphism of the pelvis, here I focus primarily on differences in joint moments and muscle force in this muscle group.

8.2 Anthropometrics

Men and women in this sample were significantly dimorphic in most aspects of body shape, including height ($P < 0.001$, t = 6.6), mass ($P < 0.01$, t = 2.9), total lower limb ($P < 0.01$, t = 3.9), thigh ($P < 0.01$, t = 3.3), shank ($P < 0.01$, t = 3.4), and and foot length ($P < 0.01$, t = 1.1), with males being absolutely larger in all measures (Table 8.1). As described in Chapter 4, several mediolateral dimensions of the true pelvis were significantly larger in females compared to males. In the false pelvis, there were no differences in either bi-ASIS or bi-iliac breadth between the sexes, but body breadth measured as the distance between the right and left greater trochanter was slightly but significantly larger in men ($P < 0.05$, t = 2.1, Table 8.1). Composite muscle moment arms of the hip and knee extensors and hip abductors were also significantly longer in men ($P < 0.01$), but ankle plantarflexor moment arms were nearly identical between the sexes (Table 8.1).

Table 8.1. Anthropometrics

	Male (n = 14)	Female (n = 13)	*P*-value
Body Shape			
Body Mass (kg)	70.0±8.7	60.9±7.4	0.007
Height (m)	1.77±0.05	1.64±0.03	< 0.001
Hip Height (cm)	88.6±4.8	82.7±2.6	0.001
Thigh Length (cm)	38.8±2.5	36.1±1.7	0.003
Shank Length (cm)	45.1±2.5	42.0±2.0	0.002
Foot Length (cm)	20.0±1.7	18.1±0.8	0.003
Bi-iliac (cm)	26.5±1.8	26.5±1.3	0.999
Bi-ASIS (cm)	22.8±1.7	21.8±1.7	0.128
Bi-trochanter (cm)	30.2±1.2	29.3±0.8	0.036
r, Composite Muscle Moment Arm			
r, Hip Abductors (cm)	5.9±0.7	5.2±0.4	0.007
r, Hip Extensors (cm)	6.5±0.5	5.9±0.4	0.008
r, Knee Extensors (cm)	4.6±0.6	4.0±0.8	0.042
r, Ankle Plantarflexors (cm)	3.9±0.3	3.9±0.4	0.868

8.3 Joint moments, muscle force and EMA in men and women

Comparisons between men and women for each variable were performed using ANOVA with a Bonferroni correction for multiple comparisons (Proschan and Waclawin, 2000). Because this approach is conservative and many comparisons were made, α was adjusted by the number of speeds tested (6) which yielded a *P*- value threshold of 0.008 for acceptance of significant differences.

Mass-specific joint moments were similar between men and women at all three joints, with a few exceptions (Figure 8.1). Men had larger mass-specific ankle plantarflexor moments at all speeds, but these were only statistically larger at slow and preferred walking speeds. Hip abductor moments per kilogram body mass tended to be greater in women at all speeds, but only the fastest walking speed was significantly higher for women. Figure 8.1 shows men also tend to have higher mass-specific hip extensor moments at faster speeds, but none of these differences reached significance. Knee moments in both the sagittal and coronal plane were very similar between men and women (Table 8.2)

Higher ankle moments in men resulted in consistently higher mass-specific ankle plantarflexor force at all walking speeds, but none of these differences reached the threshold significance level (Fig 8.2). Greater ankle muscle force in men appears to be the result of significantly lower EMA at the ankle at walking speeds when compared to women (Table 8.2, Figure 8.3). Average male female difference in ankle EMA at all walking speeds was 13.5% lower in men compared to women. Lower male ankle EMA resulted from significantly larger R at the ankle during a walk (Table 8.2). At a run, male

and female ankle EMA was very similar because R at the ankle increased in women, lowering their EMA to male averages (Table 8.2, Fig 8.3). This decrease in R suggests that women change their foot strike pattern during running, moving the COP farther forward on the foot, which increases the distance between the GRF vector and the joint COR.

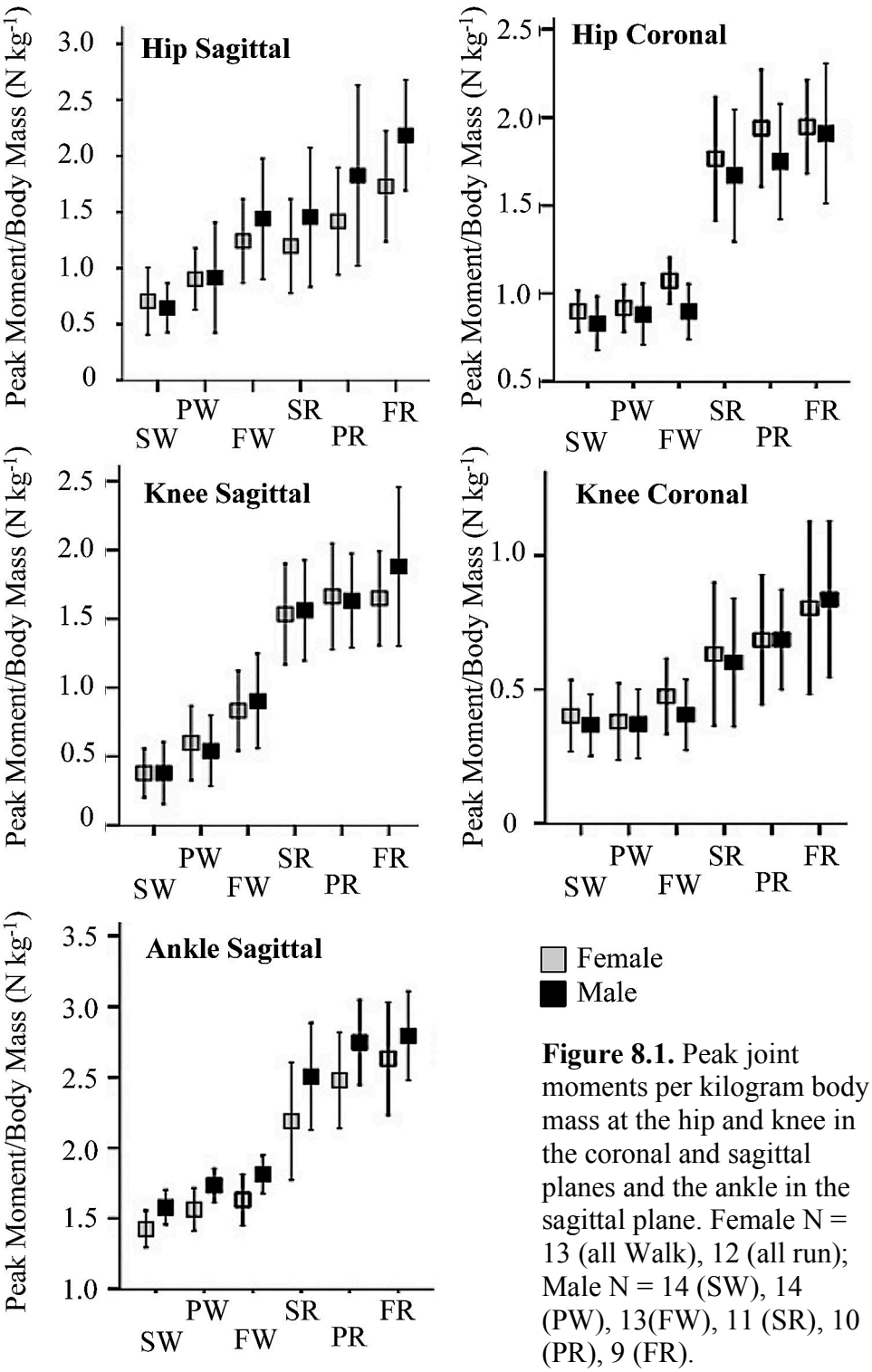

Figure 8.1. Peak joint moments per kilogram body mass at the hip and knee in the coronal and sagittal planes and the ankle in the sagittal plane. Female N = 13 (all Walk), 12 (all run); Male N = 14 (SW), 14 (PW), 13(FW), 11 (SR), 10 (PR), 9 (FR).

Table 8.2. Mass-specific joint moments and muscle force, EMA and R

	Sex	SW	PW	FW	SR	PR	FR
Moment/Body Mass (Nm kg^{-1})							
Hip ML	F	0.89±0.11	0.91±0.13	1.07±0.13*	1.76±0.35	1.93±0.33	1.94±0.26
	M	0.82±0.15	0.88±0.17	0.89±0.15	1.66±0.37	1.74±0.32	1.90±0.39
Hip AP	F	0.70±0.29	0.90±0.27	1.24±0.37	1.19±0.42	1.41±0.47	1.73±0.49
	M	0.64±0.21	0.91±0.49	1.43±0.53	1.45±0.62	1.82±0.80	2.18±0.49
Knee AP	F	0.37±0.17	0.59±0.27	0.83±0.29	1.53±0.36	1.66±0.38	1.64±0.34
	M	0.37±0.22	0.54±0.25	0.90±0.34	1.56±0.36	1.63±0.34	1.87±0.57
Knee ML	F	0.40±0.13	0.37±0.14	0.47±0.14	0.63±0.26	0.68±0.24	0.80±0.32
	M	0.36±0.11	0.37±0.12	0.40±0.13	0.60±0.23	0.68±0.18	0.83±0.29
Ankle AP	F	1.42±0.13	1.56±0.15	1.63±0.18	2.18±0.41	2.47±0.34	2.63±0.39
	M	1.57±0.12*	1.73±0.11*	1.81±0.13*	2.50±0.37	2.74±0.30	2.79±0.31
Muscle Force/Body Mass (N kg^{-1})							
Hip ML	F	17.0±3.5	17.3±3.8	20.3±4.0*	33.6±9.1	36.4±9.2	37.1±7.9
	M	14.1±3.4	15.1±4.2	15.4±4.2	27.6±7.0	30.4±7.4	31.7±8.7
Hip AP	F	11.9±5.1	15.1±4.6	20.9±6.3	20.2±7.5	23.9±8.7	29.0±7.6
	M	10.1±4.1	14.5±8.7	22.5±9.3	22.5±11.6	29.1±14.9	33.1±8.0
Knee AP	F	9.7±4.9	15.4±7.8	21.2±8.1	38.6±10.2	42.7±10.8	42.1±11.3
	M	8.2±4.6	11.9±5.6	19.9±7.5	34.2±9.3	35.6±8.7	41.5±13.7
Ankle AP	F	36.3±4.0	39.8±3.6	41.6±5.4	56.0±13.4	62.6±10.6	68.1±11.4
	M	39.9±3.9	43.9±4.5	46.0±3.3	61.7±8.7	69.1±5.4	69.3±5.7
EMA (r/R)							
Hip ML	F	0.60±0.11	0.63±0.13	0.60±0.14	0.62±0.12	0.60±0.12	0.60±0.11
	M	0.78±0.19*	0.76±0.18	0.77±0.17	0.79±0.19	0.74±0.19	0.82±0.21*
Hip AP	F	2.32±1.22	1.58±1.00	1.07±0.39	1.40±0.57	1.32±0.64	1.37±0.89
	M	2.48±0.99	1.94±1.01	1.13±0.39	1.78±0.95	1.73±1.49	1.05±0.42
Knee AP	F	1.08±0.86	0.81±0.39	0.69±0.30	0.41±0.12	0.40±0.10	0.47±0.15
	M	0.92±0.29	0.76±0.30	0.72±0.20	0.53±0.17	0.46±0.17	0.47±0.19
Ankle AP	F	0.40±0.05	0.39±0.04*	0.40±0.04*	0.35±0.03	0.34±0.03	0.33±0.04
	M	0.35±0.03	0.33±0.03	0.34±0.03	0.32±0.03	0.34±0.04	0.32±0.47
R (cm)							
Hip ML	F	8.8±1.3	8.4±1.2	8.9±1.5*	8.6±1.7	8.9±1.5	8.7±1.4
	M	7.8±1.4	8.0±1.3	7.8±1.2	7.9±1.3	8.1±1.3	7.7±1.5
Hip AP	F	3.6±1.4	5.2±2.3	7.0±3.4	5.0±1.8	6.3±4.1	5.8±3.0
	M	3.1±1.3	4.0±1.4	6.7±2.9	4.8±2.2	5.3±2.5	7.0±1.9
Knee AP	F	4.7±1.3	5.7±1.2	6.4±1.8	10.6±2.8	10.4±2.9	9.4±3.3
	M	5.5±2.1	6.9±2.4	6.9±1.5	9.6±2.0	11.3±3.8	10.8±3.3
Ankle AP	F	9.8±1.1	10.0±1.0	9.8±1.1	11.2±1.3	11.7±1.1	11.8±1.1
	M	11.3±1.3*	11.8±1.1*	11.4±1.1*	12.6±1.0	11.6±1.2	12.6±2.0

Values are means ± 1 standard deviation. ANOVA with Bonferroni correction for multiple analyses was used to test for significant differences between men and women. Corrections were made for each measure at a joint based on the number of speeds sampled (Proschan and Waclawin, 2000). Differences were significant when $P < 0.008$.

At the hip, mass-specific abductor forces were higher in females at all speeds, but these differences only reached statistical significance at the fastest walking speed. EMA of the hip abductors was lower in women during walking and running, but differences were only significant at slow walking and fast running speeds (Fig 8.3). As discussed in Chapter 4, the difference in EMA appears to be primarily related to shorter hip abductor r, which is size dependent (Wolpoff, 1978).

However, women also have slightly higher values of R at the hip in the coronal plane (Table 8.2), although this trend is not statistically significant in this sample. As in previous analyses of hip abductor function, one female subject (137) stands out as having the highest hip abductor muscle force and R at the hip in the coronal plane at all walking and running speeds. Values for R at the hip in the coronal plane in this subject are more than two standard deviations from the female mean at all speeds (R; preferred walk, 137 = 11.0cm, preferred run = 13.0 cm). When this individual is removed from the analysis of hip abductor EMA, the differences between men and women decrease.

Sagittal plane mass-specific muscle force produced by the hip and knee extensors was not statistically different between men and women at any walking or running speed, although a trend was apparent where women seem to have higher knee extensor force per kilogram body mass at most gaits. Despite slightly larger hip and knee extensor muscle moment arms in men, EMA of both the hip and knee extensors was similar between men and women with a large degree of overlap at most gaits (Figs 8.2 and 8.3).

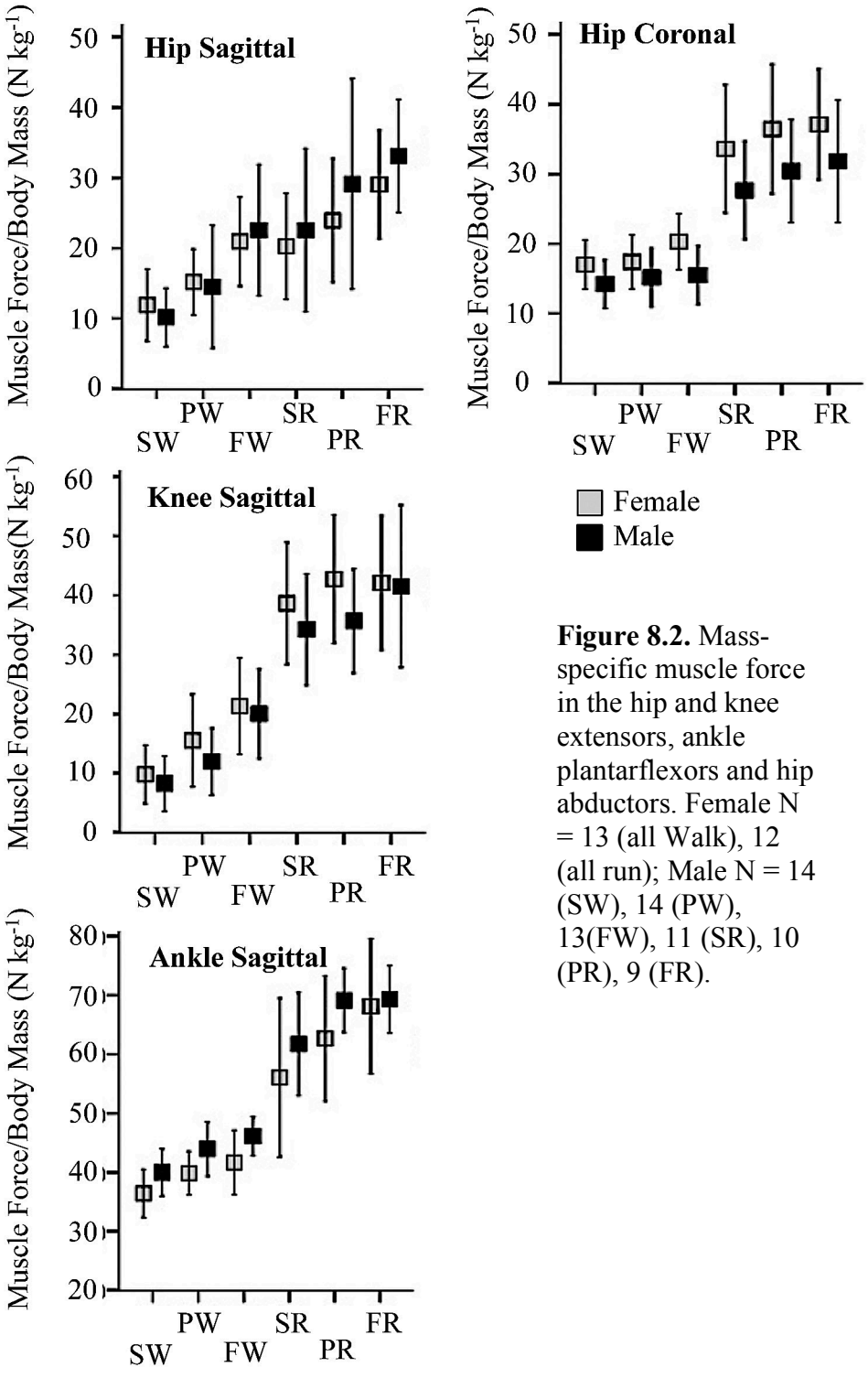

Figure 8.2. Mass-specific muscle force in the hip and knee extensors, ankle plantarflexors and hip abductors. Female N = 13 (all Walk), 12 (all run); Male N = 14 (SW), 14 (PW), 13(FW), 11 (SR), 10 (PR), 9 (FR).

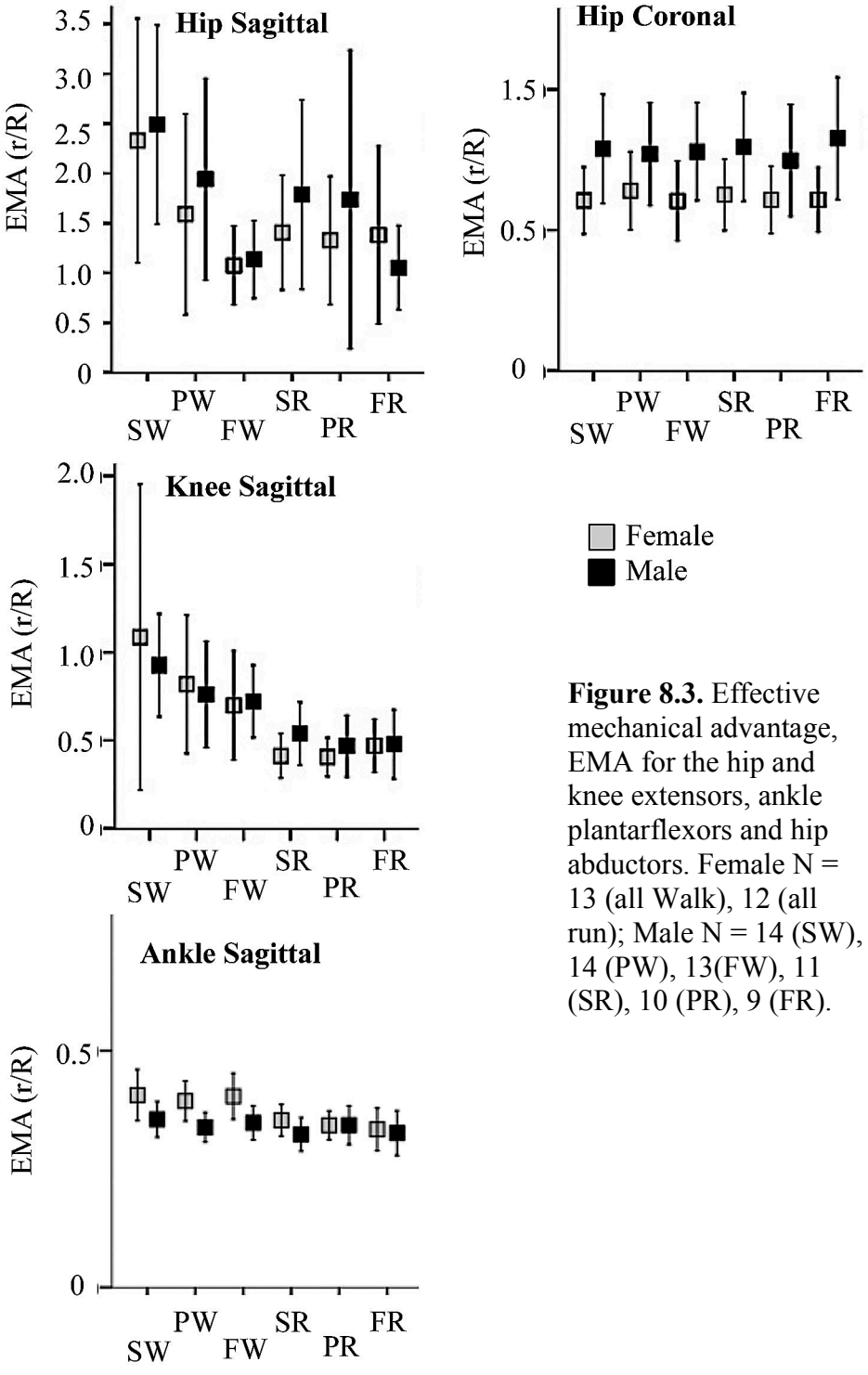

Figure 8.3. Effective mechanical advantage, EMA for the hip and knee extensors, ankle plantarflexors and hip abductors. Female N = 13 (all Walk), 12 (all run); Male N = 14 (SW), 14 (PW), 13(FW), 11 (SR), 10 (PR), 9 (FR).

8.4. Discussion

These results suggest overall similarity in joint moments, force production and EMA in the lower limb, with the exception of the ankle plantarflexors, and hip abductors at some speeds and gaits. At the ankle, men had higher mass-specific joint moments and muscle force, and lower EMA while walking. In the hip abductors, women tended to have greater mass-specific moments and muscle force, and lower EMA, although these trends only reached statistical significance in some instances. Knee mechanics and kinetics were broadly similar between the groups in both the sagittal and coronal planes, despite documented differences in valgus angle during locomotion (Cho et al., 2004; Ferber et al., 2003). Finally, while men showed slightly greater hip extensor moments at the faster speeds, higher EMA resulting from significantly longer hip extensor r appears to mitigate the effects on mass-specific muscle force, which were not higher than female values at any speed.

This analysis provides important baseline data on joint function in men and women, but only differences in hip abductor and extensor EMA can be reasonably linked to anatomical variation between the sexes, specifically femoral neck length and hip extensor moment arm length. Other kinematic patterns, or a more complex interaction between anatomy and movement profiles appear to underlie the differences observed in ankle plantarflexor moments and EMA, and possibly mediolateral force production as well, but larger samples are needed to confirm the trends in joint mechanics shown here.

CHAPTER 9
DISCUSSION AND CONCLUSIONS

9.1 Introduction

The adoption of habitual bipedal locomotion required major alterations in hominin pelvic morphology, particularly the shortening and reorientation of the ilia, which repositioned the minor gluteal muscles allowing them to act as thigh abductors and stabilize the pelvis during bipedal walking and running (Reynolds, 1931; Sigmon, 1971; Stewart, 1984a). These changes in pelvic morphology are clearly evident in the fossil record by at least 3.4Ma (Ward, 2002; Lovejoy, 2005), and recent analysis of the reconstructed pelvis of *Ardipithecus ramidus* suggests that some of the pelvic changes associated with pelvic stabilization may have originated shortly after the divergence of hominins from the last common ancestor with chimpanzees (Lovejoy et al., 2009).

The importance of the hip abductors to proper gait mechanics during bipedal locomotion is well understood, but there is a lack of consensus on how to interpret the influence of variation in pelvic morphology on hip abductor function (Lovejoy et al., 1973; McHenry, 1975; McHenry and Temerin, 1979; Stern and Susman, 1983; Lovejoy, 1988, 2005; Rak, 1991; Berge, 1994; Ruff, 1995, 1998; MacLatchy, 1996; Lovejoy et al., 2009). The mechanical model that has been used to link pelvic morphology and hip abductor mechanics is a static single leg stance model that assumes the GRF vector passes approximately vertically through the body COM. The model does not incorporate

the dynamics of movement during the support phase of walking and running. The accuracy of the static model in predicting hip abductor force production has important implications for reconstructing gait in fossil hominins and understanding the effect of sexual dimorphism on locomotor performance in modern humans. Additionally, the static hip abductor model is used in the design of prosthetic hip implants and to facilitate restoration of normal hip anatomy after replacement surgery (Sariali et al., 2008; Traina et al., 2009).

The purpose of this dissertation was to test the assumption that the mechanics of the hip abductors during locomotion could be predicted from dimensions of the pelvis and hip, as is implied by the static model of abductor function. Three research questions were addressed. First, how do hip abductor EMA and muscle force production compare to other muscle groups of the lower limb? Second, can R at the hip in the coronal plane and EMA of the hip abductors be predicted from skeletal dimensions of the pelvis and hip? Third, what is the relationship between active muscle volume of the hip abductors and locomotor cost, and how much do the abductors contribute to whole body cost during walking and running? The following section summarizes the results of this study. The relevance of these finding to the reconstruction of hip abductor function in extinct hominins will then be addressed, as well as implications for the 'obstetrical dilemma' and prosthetic design.

9.2 The hip abductors in context: EMA and muscle force production across the joints of the lower limb

In Chapter 3, mass-specific joint moments, muscle force and EMA of the hip abductors, hip and knee extensors and ankle plantarflexors were compared. The hip abductors accounted for up to 20% of total lower limb force production during locomotion, and mass-specific joint moments were equal to or greater than those at the hip and knee in the sagittal plane. EMA of the hip abductors remained constant across gaits. In contrast EMA at the hip, knee and ankle in the sagittal plane increased significantly when gait changed from a walk to a run.

When compared to previous studies of abductor force production based on a static single leg stance model (Merchant, 1965; McLeish and Charnley, 1970), hip abductor force was generally higher in this study for both walking and running gaits. The discrepancy results from an underestimation of the magnitude of both the mediolateral and vertical components of GRF in static models and also incorrect estimations of R at the hip in the coronal plane.

The results of this analysis demonstrate that hip abductor force production is an important component of overall force production in the lower limb and that the mechanics of the hip joint in the mediolateral plane are relatively stable between gaits. Additionally, in conjunction with results from other biomechanical analyses of gait (Griffin et al., 2003; Biewener et al., 2004), a clearer pattern of force production across the lower limb is shown. The ankle plantarflexors produce the largest portion of total lower limb force at both walking and running speeds. The contribution of knee extensor

force is gait dependent because of increasing knee flexion when gait transitions from a walk to a run, while hip extensor force increases gradually with greater speed regardless of gait. Taken together, this analysis depicts gait dynamics across the joints of the lower limb in a large sample of individuals, and demonstrates the importance of including the hip abductors in future biomechanical studies of locomotion.

9.3 Predicting hip abductor mechanics from skeletal dimensions

Chapter 4 tested the hypothesis that hip abductor mechanics can be determined from skeletal dimensions of the pelvis and hip, specifically that EMA_{skel} (femoral neck length/ 0.5 biacetabular width) predicts EMA_{loc} (r/R). The results suggest that dynamic changes in R over the course of stance phase cannot be accurately described by one-half biacetabular distance (the diameter between the centers of the femoral heads). When all subjects are included, one-half biacetabular distance explains 14% of the variation in R at the hip in the coronal plane during a walk and 7% during a run (walk $P = 0.05$, run $P = 0.21$). In contrast, femoral neck length is well correlated with hip abductor r, explaining 62% of the variation in the dependent variable ($R^2 = 0.62$, $P < 0.001$). Therefore the relationship between EMA_{loc} and EMA_{skel} primarily reflects the correlation between the two anatomical variables of the hip (femoral neck length and r), and not a relationship between biacetabular dimensions and R.

The cause of variability in R at the hip in the coronal plane is difficult to determine. Neither variation in the mediolateral component of GRF, nor pelvic inclination during walking and running appears to determine the length of R. The lack of

correlation between these variables suggests that additional factors are influencing the moments generated at the hip in the coronal plane. The double pendulum model presented by Pandy et al. (2010), which predicts hip abductor force production as a response to the lateral pull of the body COM during stance phase may help to clarify this issue in the future.

When men and women are compared, women have significantly lower hip abductor EMA than men at each walking and running speed. However, this appears to primarily reflect shorter average femoral neck length in women, which reduces the length of hip abductor r, thereby decreasing EMA. Because femoral neck length scales with femoral length (Wolpoff, 1978; Corruccini, 1980; Ruff, 1995), lower EMA in women is likely a reflection of smaller overall body size, and not a direct result of sexual dimorphism. R at the hip in the coronal plane is also slightly larger in women, but the differences are not significant at any speed. It is possible that with larger sample sizes, these small differences may become statistically, significant, but the low of correlation between biacetabular breadth and R indicates that lower hip abductor EMA in women is not a direct consequence of pelvic breadth.

In light of these findings, reconstructions of hip abductor function in extinct hominin species may need to be reconsidered. Although relative femoral neck length is greater in australopithecines and early *Homo*, suggesting higher hip abductor EMA, the low correlation between these variables limits the interpretation of hip abductor function in extinct hominins.

9.4 Hip abductor active muscle volume and contribution to locomotor cost

Wider pelves are thought to decrease locomotor economy by increasing the force required for the hip abductors to maintain the stability of the pelvis (Napier, 1964; Zihlman and Brunker, 1979; Stern and Susman, 1983; Meindl et al., 1985; Rosenberg, 1992; Berge, 1994; Hunt 1998; Arsuaga, 1999). Chapter 5 assessed the contribution of hip abductor active muscle volume to total lower limb active muscle volume and their contribution to overall locomotor cost. The hip abductors account for approximately 15% of active muscle volume of the lower limb during walking and running. Eight percent of total body COT ($mlO_2\ m^{-1}$) at a walk and 10% of total body COT ($mlO_2\ m^{-1}$) were attributable to hip abductor active muscle volume. Women had slightly higher metabolic cost ($mlO_2\ kg^{-1}\ m^{-1}$) associated with the activation of the hip abductors than men, but there was no statistical difference in overall COT ($mlO_2\ kg^{-1}\ m^{-1}$) between the sexes during walking or running. Furthermore, when body mass and speed where controlled for, hip abductor EMA_{loc} did not increase explained variance in cost per meter traveled across gaits.

These results suggest that while the hip abductors account for approximately 10% of COT, variation in this cost associated with hip abductor mechanics is small enough, at least within this sample, to be negligible when considering the overall COT. While not predictive of individual locomotor efficiency, the hip abductors are an important part of locomotor performance and should be included in future biomechanical studies of gait and energetics.

9.5 Implications for gait reconstructions in fossil hominins

The goal of biomechanical analyses in anthropology is ultimately to provide a validated model that links dynamic aspects of performance to anatomy that can be assessed from the fossil record. Although analyses of hip abductor function in australopithecines and later *Homo* have been performed many times using a static biomechanical model based on pelvic anatomy, this analysis suggests inherent difficulties in obtaining reliable estimates of hip abductor EMA from biacetabular width and femoral neck length. Although the hip abductor musculature likely obtained its human like orientation very early in our lineage (Lovejoy, 2005), disagreement over the effectiveness of the lateral stabilization mechanism, particularly in *Australopithecus*, has led some researchers to suggest that striding bipedal gait was not fully developed in early hominins (Stern and Susman, 1983; Berge, 1994; Ruff, 1998; Hunt, 1998). The analysis presented here is not able to directly address hip abductor function in early hominins if gait kinematics differed significantly from that of modern humans. However, conclusions that striding bipedal gait was not present in australopithecines because the hip abductors were at a mechanical disadvantage (Hunt, 1998) or because estimated hip abductor forces from a static mechanical model differ from those predicted for modern humans (Berge, 1994; Ruff, 1998) are not supported by these results.

9.6 The 'obstetrical dilemma' and locomotor efficiency in women

As first proposed by Washburn (1960), the 'obstetrical dilemma' refers to the narrowing of the pelvis to accommodate bipedal locomotion, while encephalization in the

hominin lineage demanded an increasingly larger birth canal through which the large brained fetus could pass successfully. These two competing selective forces are thought to be the basis of sexual dimorphism of the bony pelvis in modern humans. Wider pelves are presumed to increase locomotor cost in women compared to men (Zihlman and Brunker, 1979; Meindl et al., 1985; Rosenberg, 1992). However, tests of locomotor efficiency during walking and running have failed to confirm higher mass-specific cost in women (Bunc and Heller, 1989; Bourdin et al., 1993; Hall et al., 2004).

The analyses of hip biomechanics in relation to pelvic dimensions, as well as the comparisons of locomotor cost between men and women, suggest the parturition/locomotion tradeoff scenario that has been used to explain sexual dimorphism of the pelvis in modern humans may need to be revised. As described above, R at the hip in the coronal plane is not well correlated with biacetabular width at either walking or running gaits, and while women have lower EMA of the hip abductors, this is primarily a consequence of shorter femoral neck length, not greater pelvic width.

Additionally, while women in this sample had significantly greater bispinous and outlet dimensions, those aspects most closely associated with successful parturition (Abitbol, 1996), the biomechanically relevant dimension for locomotion, biacetabular width (measured as the distance between the centers of the right and left femoral heads) was not different between the sexes. The relative equality of biacetabular width (male average = 17.3±0.5cm; female mean = 17.6±0.6cm) can be attributed to significantly larger femoral head diameter in men. Finally, the analysis of locomotor cost in men and women shows that, although women have a slightly higher component of COT associated

with the activation of the hip abductors, the mass specific cost to travel a unit distance is not different between the sexes.

Determining the origins of pelvic sexual dimorphism in the genus *Homo* is difficult because of the general scarcity of pelvic remains, and particularly the lack of relatively complete female pelves of archaic *Homo* (Weaver and Hublin, 2009). If birthing encephalized infants was the primary factor placing differential selective pressure on the male and female pelvis, then we would expect reduced pelvic dimorphism in hominins through the Middle Pleistocene (Rosenberg, 1992). Recent discoveries of a male archaic *Homo* pelvis from Sima de los Huesos (Arsuaga et al., 1999) and a female pelvis from Gona (Simpson et al., 2008) support this hypothesis. However, both the male and female pelvis are broad mediolaterally throughout the pelvic planes and larger than comparative samples of modern humans for most mediolateral dimensions (Arsuaga et al., 1999; Simpson et al., 2008). Arsuaga et al. (1999) and Simpson et al. (2008) argue that the wide pelvis, long femoral neck and flaring ilia are the ancestral hominin condition, and that a narrow pelvis seen in modern males is the derived condition.

While the research presented here suggests that the stereotyped narrow male pelvis is probably not related to increases in locomotor economy, it is unclear what ultimate or proximate causes have produced this change in pelvic anatomy. Tague (2005) presents an interesting hypothesis of sexual dimorphism in the pelvis and femur based on analysis of a range of dimorphic and non-dimorphic anthropoid primates. His results indicate that species that are most dimorphic in overall body size (males being larger) also show the greatest dimorphism in pelvic shape (males being smaller). Because

testosterone is responsible for inducing differential growth on dimensions of the pelvis, Tague (2005) argues that the human male pelvis is also responding to the effects of testosterone, which produce enhanced dimorphism in the rest of the body. This explanation provides an interesting new approach to the analysis of human pelvic dimorphism, but significant challenges remain in determining when and why males and/or females departed from the ancestral form of pelvic anatomy.

9.7 Biomechanics of the hip and clinical applications

One important application of biomechanical data related to hip abductor function is in the design and implantation of prosthetic hip devices. This procedure is common and generally successful at relieving pain due to osteoarthritis (Traina et al., 2009). In an effort to improve the long-term performance of implants and to restore normal hip function, surgeons are increasingly using biomechanical principles in concert with patient specific anatomy to choose proper prosthetic design and surgical approaches (Sariali et al., 2008; Traina et al., 2009). However, in medical practice, the assessment of mechanical forces acting at the hip in the coronal plane is based on the static model of hip abductor mechanics that equates the distance from the center of the femoral head to the body mid-line with the GRF leaver arm, R (Sariali et al., 2008; Traina et al., 2009). While the research presented in this dissertation is not adequate to address the engineering process associated with hip replacement, it seems important to note that the static mechanical model is probably inappropriate for application to hip prosthetic design. This

is especially true in younger patients whose activities likely induce significantly higher forces at the hip than can be estimated through the static model.

9.8 Directions for future research

Although this analysis did not support a mechanical model of hip abductor force production that can be directly correlated to skeletal dimensions of the pelvis and hip, the double pendulum model of hip mechanics presented by Pandy et al. (2010) may improve predictability of hip abductor moments and mediolateral GRF. A more comprehensive model that incorporates the dynamic movement of the body center of mass as a function of lower limb and thigh orientation in the coronal plane, as well as step width and lower limb length, is needed. Biomechanical testing that incorporates multi-step sequences across a series of force platforms or on a force instrumented treadmill, and simultaneous recordings of the movement of the body center of mass and lower limb excursion angles in the coronal plane will be needed to further test such a model.

Additionally, continued exploration of the relationship between locomotor cost and active muscle volume of the lower limb is warranted. While the data presented here are likely strong enough to support conclusions regarding the average cost associated with the activation of muscle groups across the lower limb, precise matching of speed for both force and oxygen consumption data would improve the predictability of the active muscle volume-cost model. Additionally, inter-individual variation in cost will be better addressed if the external work to swing the contralateral limb and force required to lift and accelerate the body COM are accounted for (Pontzer, 2005, 2007).

Finally, from a methodological perspective, the development of a software application to quickly and accurately determine subject-specific muscle moment arms, joint center of rotation and structural anatomy is needed. Generic rescaled models of muscle and tendon anatomy are inaccurate causing errors in the calculation of joint and muscle moments (Scheys et al., 2008). While the wide availability of MRI makes attaining individual anatomical images relatively easy, analysis of such data using commercially available software requires extensive labor to calculate the needed dimensions (Arnold et al., 2000). Therefore, by partnering with medical software engineers, producing a software application with measurement tools that can be applied to anatomical images quickly will be particularly useful in clinical and research oriented biomechanical studies.

APPENDIX A

Table A1. Subject Anthropometrics. Measurements are in meters unless otherwise indicated

Subject	Sex	Age	BM (kg)	Height	Hip Height	Thigh Length	Shank Length	Foot Length
114	Male	31	73.60	1.85	0.970	0.435	0.475	0.220
115	Male	23	70.12	1.76	0.889	0.387	0.463	0.203
117	Male	23	69.80	1.72	0.850	0.380	0.430	0.190
118	Male	23	66.10	1.77	0.901	0.406	0.444	0.209
119	Female	22	47.00	1.66	0.838	0.381	0.412	0.184
120	Female	23	78.65	1.67	0.812	0.336	0.431	0.190
121	Female	22	67.40	1.67	0.850	0.381	0.438	0.171
122	Male	23	64.70	1.70	0.812	0.349	0.406	0.228
123	Male	23	58.78	1.67	0.838	0.368	0.425	0.177
124	Female	23	60.87	1.65	0.844	0.355	0.450	0.177
125	Female	24	57.87	1.58	0.793	0.349	0.412	0.171
126	Male	23	73.39	1.80	0.889	0.400	0.451	0.191
127	Female	26	63.50	1.66	0.850	0.362	0.445	0.197
128	Male	23	64.59	1.80	0.902	0.394	0.457	0.197
129	Male	23	59.51	1.75	0.845	0.368	0.438	0.197
130	Male	25	71.12	1.87	0.972	0.419	0.495	0.210
131	Female	24	58.10	1.66	0.838	0.394	0.394	0.184
132	Female	25	58.60	1.71	0.851	0.362	0.445	0.178
133	Male	23	64.50	1.72	0.844	0.368	0.438	0.196
134	Female	23	61.23	1.66	0.826	0.368	0.413	0.191
135	Female	24	63.23	1.60	0.845	0.343	0.406	0.184
136	Female	31	54.97	1.62	0.762	0.342	0.393	0.184
137	Female	23	64.50	1.68	0.832	0.356	0.432	0.191
139	Male	21	91.44	1.80	0.864	0.362	0.445	0.203
140	Male	24	70.30	1.85	0.933	0.387	0.495	0.228
141	Female	23	55.88	1.61	0.813	0.368	0.400	0.171
142	Male	34	82.73	1.80	0.910	0.420	0.455	0.215

Table A1 continued

Subject	Sex	Bi-iliac	Bi-ASIS	Biacetabular	Biomechanical Biacetabular	Bi-trochanter	Inlet ML	Inlet AP	Bi-spinous
114	Male	0.284	0.250	0.129	0.177	0.330	0.000	0.142	0.100
115	Male	0.284	0.257	0.114	0.170	0.301	0.126	0.122	0.092
117	Male	0.257	0.222	0.124	0.170	0.301	0.109	0.113	0.104
118	Male	0.262	0.213	0.116	0.170	0.294	0.111	0.117	0.099
119	Female	0.253	0.201	0.126	0.177	0.284	0.114	0.140	0.114
120	Female	0.281	0.233	0.124	0.168	0.291	0.123	0.112	0.100
121	Female	0.277	0.240	0.123	0.169	0.295	0.126	0.130	0.102
122	Male	0.231	0.201	0.116	0.167	0.289	0.104	0.116	0.095
123	Male	0.228	0.221	0.133	0.177	0.296	0.114	0.107	0.104
124	Female	0.261	0.221	0.133	0.180	0.292	0.122	0.113	0.111
125	Female	0.243	0.194	0.122	0.170	0.282	0.124	0.120	0.119
126	Male	0.272	0.228	0.126	0.185	0.315	0.122	0.131	0.094
127	Female	0.275	0.226	0.128	0.177	0.303	0.135	0.129	0.112
128	Male	0.281	0.219	0.126	0.174	0.301	0.122	0.124	0.087
129	Male	0.252	0.211	0.128	0.172	0.277	0.116	0.121	0.102
130	Male	0.275	0.238	0.128	0.177	0.301	0.114	0.134	0.094
131	Female	0.269	0.221	0.141	0.185	0.303	0.126	0.129	0.116
132	Female	0.250	0.201	0.158	0.182	0.291	0.126	0.137	0.129
133	Male	0.264	0.211	0.116	0.162	0.305	0.126	0.117	0.090
134	Female	0.291	0.213	0.131	0.182	0.303	0.131	0.127	0.111
135	Female	0.269	0.226	0.123	0.172	0.284	0.131	0.116	0.109
136	Female	0.257	0.214	0.123	0.170	0.287	x	0.140	0.116
137	Female	0.255	0.196	0.136	0.187	0.306	0.119	0.132	0.124
139	Male	0.274	0.247	0.119	0.172	0.299	0.121	0.114	0.083
140	Male	0.291	0.241	0.117	0.173	0.315	0.131	0.122	0.112
141	Female	0.276	0.252	0.124	0.172	0.291	0.134	0.142	0.111
142	Male	0.268	0.246	0.150	0.179	0.308	0.123	0.120	0.099

Table A1 continued

Subject	Sex	Midplane AP	Outlet ML	Outlet AP	Biomechanical Femoral Neck	Femoral Head
114	Male	0.168	0.111	0.099	0.079	0.047
115	Male	0.150	0.119	0.088	0.063	0.044
117	Male	0.135	0.112	0.097	0.065	0.046
118	Male	0.137	0.116	0.101	0.064	0.045
119	Female	0.144	0.145	0.107	0.055	0.040
120	Female	0.133	0.114	0.105	0.059	0.039
121	Female	0.153	0.109	0.137	0.065	0.043
122	Male	0.135	0.107	0.084	0.057	0.046
123	Male	0.123	0.112	0.099	0.059	0.040
124	Female	0.138	0.124	0.109	0.060	0.039
125	Female	0.136	0.146	0.089	0.056	0.041
126	Male	0.144	0.122	0.106	0.067	0.048
127	Female	0.150	0.116	0.093	0.060	0.041
128	Male	0.150	0.098	0.091	0.063	0.048
129	Male	0.142	0.117	0.092	0.056	0.043
130	Male	0.157	0.122	0.088	0.061	0.042
131	Female	0.144	0.131	0.107	0.061	0.185
132	Female	0.151	0.136	0.093	0.055	0.041
133	Male	0.129	0.097	0.106	0.072	0.048
134	Female	0.131	0.133	0.090	0.060	0.041
135	Female	0.135	0.138	0.099	0.060	0.041
136	Female	0.154	0.124	0.096	0.058	0.041
137	Female	0.150	0.145	0.094	0.060	0.043
139	Male	0.133	0.121	0.088	0.064	0.048
140	Male	0.141	0.114	0.090	0.073	0.046
141	Female	0.151	0.107	0.101	0.057	0.043
142	Male	0.135	0.106	0.099	0.065	0.048

Table A2. Joint center of rotation coordinates. Hip, from the left ASIS; knee, from right lateral femoral epicondyle, ankle from right lateral malleolus.

Subject	Acetabulum COR (mm)			Knee COR (mm)			Ankle COR (mm)		
	ML	AP	Vertical	ML	AP	Vertical	ML	AP	Vertical
114	42.5	-13.6	69.7	41.65	-13.6	0.85	17	-22.95	-8.5
115	45.9	-10.2	68	44.2	8.5	2.55	22.1	-16.15	-9.35
117	25.5	-6.8	68	38.25	5.1	0	22.95	-7.65	-9.35
118	18.7	-15.3	74.8	43.35	5.95	1.7	21.25	-17.85	-8.5
119	8.5	-10.2	66.3	37.4	0	-0.85	19.55	-17	-8.5
120	23.8	-8.5	78.2	42.5	3.4	-4.25	22.95	-14.45	-6.8
121	32.3	-17	47.6	39.1	7.65	2.55	19.55	-16.15	-7.65
122	18.7	-8.5	78.2	41.65	0.85	1.7	22.1	-6.8	-5.1
123	23.8	-11.9	66.3	38.25	7.65	1.7	23.8	-13.6	-6.8
124	20.4	-8.5	64.6	38.25	1.7	0	19.55	-11.9	-7.65
125	15.3	-11.9	73.1	37.4	0.85	4.25	19.55	-14.45	-4.25
126	18.7	-17	61.2	40.8	5.1	0	24.65	-14.45	-5.1
127	22.1	15.3	64.6	38.25	1.7	0	23.8	-12.75	-6.8
128	18.7	1.7	74.8	42.5	2.55	2.55	26.35	-12.75	-3.4
129	17	-13.6	76.5	41.65	1.7	2.55	17	-21.25	-6.8
130	28.9	5.1	71.4	44.2	5.1	0	25.5	-13.6	-11.05
131	17	-10.2	61.2	39.1	1.7	0.85	21.25	-15.3	-5.95
132	0	-8.5	78.2	37.4	2.55	-0.85	21.25	-14.45	-9.35
133	22.1	-15.3	56.1	40.8	2.55	-0.85	22.95	-16.15	-8.5
134	15.3	-3.4	73.1	38.25	9.35	1.7	25.5	-5.1	-5.1
135	28.9	-23.8	59.5	38.25	5.1	-0.85	20.4	-15.3	-7.65
136	23.8	-1.7	68	34.85	1.7	2.55	20.4	-12.75	-5.95
137	0	-10.2	68	39.1	0.85	2.55	19.55	-16.15	-5.95
139	39.1	-17	79.9	43.35	7.65	2.55	21.25	-21.25	-8.5
140	28.9	-18.7	66.3	42.5	6.8	5.1	23.8	-16.15	-7.65
141	37.4	-10.2	74.8	34.85	9.35	4.25	18.7	-15.3	-4.25
142	37.4	-3.4	73.1	45.05	8.5	0.85	19.55	-23.8	-8.5

Table A3. Subject muscle moment arms measured from MRI (cm)

Subject	(Gluteus Minimus	Gluteus Medius	Tensor Fascia Latae	Gluteus Maximus	Rectus Femoris at the hip	Semitendenosus at the hip	Semimembranosus at the hip	Biceps femoris Long head at the hip	Semitendinosus at the knee	Semimenbranosus at the knee	Biceps Feomris at the knee	Patellar Tendon	Medial Gastrocnemius at the knee	Lateral Gastrocnemius at the knee	Achilles Tendon	Flexor Hallicus Longus	Flexor Digitorum Longus	Tibialis Posterior
114	5.35	6.90	9.95	6.99	3.12	5.30	5.30	5.41	3.38	3.38	2.76	5.26	1.73	3.14	4.23	2.01	0.53	2.15
115	4.68	6.04	12.03	7.26	3.88	5.57	5.57	5.52	1.78	1.78	2.05	4.29	1.95	2.28	4.45	2.09	2.13	2.01
116	3.98	4.92	7.57	7.09	3.88	4.91	4.91	5.20	2.94	2.94	1.08	3.74	3.50	2.55	4.47	2.99	2.96	2.98
117	4.31	5.56	10.34	6.65	3.53	3.94	3.94	4.09	2.06	2.06	1.16	5.84	1.65	2.15	3.97	2.49	1.60	2.55
118	4.86	5.78	10.54	7.05	3.44	5.91	5.91	6.01	2.08	2.08	1.20	6.04	1.68	2.18	5.28	1.57	1.26	1.54
119	3.76	4.65	6.90	6.70	3.61	3.34	3.34	3.42	2.60	2.60	2.16	4.58	2.42	2.66	3.77	2.08	1.47	2.07
120	4.93	5.48	11.09	7.16	2.91	5.67	5.67	5.96	3.32	3.32	1.17	3.69	2.89	3.52	4.85	2.01	1.81	2.01
121	3.40	5.55	11.53	6.69	2.91	5.09	5.09	4.97	0.31	0.31	1.30	6.46	1.40	1.57	3.91	2.23	2.38	2.19
122	4.20	4.95	9.00	7.25	3.86	5.40	5.40	5.27	1.48	1.48	2.25	4.51	3.76	3.61	4.73	1.29	0.79	1.22
123	3.12	4.48	8.60	7.17	3.95	3.99	3.99	4.07	1.66	1.66	1.19	4.38	1.57	1.89	3.69	1.55	1.20	1.53
124	3.92	5.21	9.00	6.57	3.01	4.89	4.89	5.19	3.88	3.88	1.72	3.33	3.62	3.61	4.24	1.91	1.87	1.91
125	4.12	4.94	6.57	9.20	3.19	4.03	4.03	4.13	2.59	2.59	2.06	3.45	3.29	2.96	4.11	1.44	1.45	1.44
126	4.82	5.67	8.35	8.27	3.72	5.00	5.00	5.08	1.98	1.98	1.51	4.04	2.86	2.86	4.42	2.75	2.72	2.75
127	4.57	5.46	9.20	6.55	3.79	4.70	4.70	4.98	3.28	3.28	1.60	3.82	3.93	3.77	4.90	3.23	3.37	3.22
128	4.70	5.92	10.05	7.49	3.95	5.29	5.29	5.38	2.99	2.99	2.37	4.29	4.00	4.94	4.74	2.53	2.58	2.55
129	3.89	4.90	8.40	7.60	3.60	4.75	4.75	4.62	1.84	1.84	2.56	4.22	4.92	4.76	4.07	1.96	2.33	2.04
130	4.24	5.46	8.80	7.05	5.85	5.62	5.62	5.91	4.05	4.05	2.06	4.24	5.13	5.61	4.72	2.24	2.65	2.27
131	4.14	5.10	9.24	7.39	3.40	4.99	4.99	5.18	3.50	3.50	2.11	4.01	3.90	3.90	4.36	2.51	2.59	2.45

Table A3 continued

Subject	(Gluteus Minimus	Gluteus Medius	Tensor Fascia Latae	Gluteus Maximus	Rectus Femoris at the hip	Semitendenosus at the hip	Semimembranosus at the hip	Biceps femoris Long head at the hip	Semitendinosus at the knee	Semimenbranosus at the knee	Biceps Feomris at the knee	Patellar Tendon	Medial Gastrocnemius at the knee	Lateral Gastrocnemius at the knee	Achilles Tendon	Flexor Hallicus Longus	Flexor Digitorum Longus	Tibialis Posterior
132	3.49	4.56	6.71	6.93	4.18	4.93	4.93	5.17	4.09	4.09	2.70	3.42	4.06	3.87	4.32	1.67	1.86	1.47
133	4.52	6.21	10.73	7.54	3.72	4.92	4.92	5.15	3.42	3.42	2.01	3.89	3.23	3.10	4.25	2.21	2.44	2.12
134	4.04	5.44	6.87	6.85	3.21	5.25	5.25	5.42	2.96	2.96	1.26	3.87	4.17	3.71	4.59	3.11	3.42	3.05
135	3.95	5.07	10.00	6.86	3.20	4.10	4.10	4.51	2.81	2.81	0.74	3.43	3.36	3.51	4.81	2.34	2.60	2.40
136	3.47	4.94	7.93	5.87	4.25	4.77	4.77	5.04	3.54	3.54	1.73	4.37	1.42	1.70	3.43	2.39	1.27	2.44
137	3.35	5.18	8.22	6.80	3.03	4.39	4.39	4.32	1.26	1.26	1.71	3.54	3.46	3.46	5.02	2.16	2.41	2.23
139	5.06	5.83	12.11	8.70	3.53	4.83	4.83	4.81	2.02	2.02	2.16	4.70	3.40	3.70	4.96	2.08	2.23	2.11
140	5.65	6.59	12.61	8.01	3.96	5.69	5.69	5.72	2.39	2.39	2.20	4.75	2.10	2.43	4.91	2.42	2.63	2.40
141	3.82	5.05	10.10	5.65	3.66	5.78	5.78	5.73	0.55	0.55	1.03	4.34	2.09	2.11	4.32	2.89	3.09	2.94
142	4.58	5.99	10.14	9.30	3.88	6.19	6.19	6.27	1.77	1.77	1.17	4.57	3.86	4.03	4.82	1.58	1.30	1.56

Table A4. Subject maximum cross section area for muscle of the lower limb. Measurements are in cm^2

Subject	Gluteus Medius	Gluteus Minimus	Tensor Fasciae latae	Gluteus Maximus	Semitendinosus	Semimembranosus	Biceps Femoris Short Head	Biceps Femoris Long Head	Rectus femoris	Vastus Lateralis	Vastus Intermedius	Vastus Medialis	Gastrocnemius Lateralis	Gastrocnemius Medialis	Soleus	Tibialis Posterior	Flexor Halucus longus	Flexor digitorum Longus
114	37.07	18.94	11.61	53.30	12.30	16.89	12.07	19.75	20.30	38.52	33.12	28.50	12.39	17.09	29.80	4.22	7.59	2.48
115	34.73	16.63	10.22	48.02	9.87	15.16	7.82	12.76	15.27	32.77	30.00	25.09	9.85	15.56	23.59	3.52	4.53	2.71
117	31.09	20.44	7.80	60.17	10.71	12.30	6.06	13.63	17.32	31.44	23.27	27.17	9.33	15.25	21.68	3.64	7.33	2.54
118	37.56	25.67	11.66	63.41	10.74	16.17	7.91	14.93	17.44	34.47	24.74	28.73	8.72	13.31	22.23	4.80	7.07	2.36
119	24.54	14.64	5.54	42.18	6.27	8.84	5.08	10.63	9.70	18.25	19.00	21.51	6.70	8.52	15.59	3.29	4.56	1.33
120	22.67	16.05	6.73	55.52	7.56	13.31	6.61	14.18	11.41	33.15	27.49	26.45	13.77	19.84	29.57	5.60	5.95	1.93
121	29.19	20.15	6.81	48.88	8.72	13.92	5.60	13.46	11.35	26.56	21.77	19.69	7.88	12.44	19.81	6.15	4.59	1.15
122	28.27	20.90	5.77	55.18	8.86	15.36	5.51	12.56	12.68	31.85	26.19	24.48	9.56	15.01	27.26	6.53	5.66	1.91
123	28.35	19.72	4.79	48.71	8.60	14.00	6.47	12.53	17.73	30.32	20.79	19.92	9.64	14.55	22.46	4.24	5.89	2.60
124	30.95	13.97	7.00	44.98	8.95	15.65	6.01	11.55	12.62	32.80	25.15	26.04	9.70	14.55	23.79	4.71	4.48	1.93
125	30.49	14.32	4.39	46.00	8.29	13.17	5.83	13.46	12.50	27.52	15.71	20.36	9.67	13.05	19.66	4.94	3.98	1.70
126	35.83	21.08	9.96	63.03	10.89	17.01	8.75	16.95	15.36	39.44	34.62	32.14	9.85	18.94	22.75	6.81	5.57	3.58
127	25.70	17.76	6.53	45.97	8.34	12.65	5.31	14.96	12.73	27.37	17.81	18.28	8.84	17.24	19.72	5.02	4.62	2.71
128	35.89	16.37	9.36	67.36	11.09	14.44	7.82	16.78	16.60	32.83	25.50	26.71	10.68	15.51	22.17	4.30	6.55	2.66
129	24.57	14.93	5.37	55.15	6.27	11.66	7.31	11.81	12.50	31.73	23.68	29.39	9.21	13.25	26.13	5.17	4.33	2.77
130	31.39	21.16	9.47	57.43	10.37	12.24	7.05	12.99	14.84	44.29	29.51	28.44	12.07	17.67	25.67	5.26	5.28	2.63
131	32.97	14.00	6.24	47.76	6.96	9.15	6.47	13.80	9.36	30.72	20.53	20.62	7.22	12.36	22.38	4.94	5.11	2.77
132	27.34	15.48	6.81	45.76	9.21	10.37	6.01	13.22	11.78	27.72	20.93	20.53	10.77	14.84	27.14	4.30	3.96	1.50
133	34.94	19.37	6.93	56.56	11.12	13.43	8.40	14.32	16.40	34.68	29.83	25.64	7.07	14.44	17.44	5.43	6.29	2.66
134	28.09	14.44	4.45	44.29	6.50	11.32	5.60	10.60	10.22	27.14	16.31	20.79	7.25	13.80	17.56	4.68	4.27	2.02
135	27.52	16.34	5.31	36.27	6.96	10.97	4.19	13.80	9.73	25.03	17.73	16.40	9.59	16.80	24.11	4.53	4.91	2.17
136	25.47	13.80	4.24	44.00	6.03	12.53	4.88	13.11	6.96	19.29	17.06	16.17	7.31	14.58	19.84	2.69	5.17	1.33
137	37.30	16.34	4.71	57.89	7.97	13.63	4.79	12.65	10.89	32.54	20.85	23.53	9.01	17.70	30.46	6.24	4.16	2.05

Table A4 continued.

Subject	Gluteus Medius	Gluteus Minimus	Tensor Fasciae latae	Gluteus Maximus	Semitendinosus	Semimembranosus	Biceps Femoris Short Head	Biceps Femoris Long Head	Rectus femoris	Vastus Lateralis	Vastus Intermedius	Vastus Medialis	Gastrocnemius Lateralis	Gastrocnemius Medialis	Soleus	Tibialis Posterior	Flexor Halucus longus	Flexor digitorum Longus
139	44.29	21.02	12.05	78.33	19.09	25.29	11.09	22.58	23.30	49.03	31.07	39.18	16.20	27.52	32.60	5.89	6.90	3.78
140	29.48	22.32	7.56	56.39	9.93	13.02	7.16	11.26	17.15	34.10	22.90	21.74	9.04	17.06	24.05	5.11	7.82	2.17
141	23.45	15.71	7.82	46.43	6.53	14.75	4.91	14.41	12.44	27.78	16.57	18.45	7.71	12.18	20.30	4.48	4.45	1.93
142	37.33	20.18	10.60	65.28	12.39	19.84	10.16	14.84	19.98	48.16	30.69	31.33	12.42	20.18	25.61	6.44	5.89	3.46

Table A5. Subject fascicle length by muscle group weighted by muscle cross-sectional area. Measurements are in cm

Subject	Hip Abductor	Hip Extensor	Knee Extensor	Ankle Plantarflexor
114	6.49	10.85	7.88	6.54
115	5.94	10.82	7.91	6.06
117	5.67	10.67	7.31	5.74
118	5.66	11.04	7.75	5.89
119	5.27	10.18	6.95	5.54
120	5.28	10.93	7.36	5.92
121	5.39	10.40	7.79	5.67
122	4.99	11.09	6.84	5.25
123	5.28	9.80	7.08	5.89
124	5.54	10.10	7.27	5.75
125	5.03	9.78	6.97	5.06
126	6.28	11.71	8.11	5.94
127	5.62	10.57	7.53	5.51
128	6.08	10.71	7.80	6.62
129	5.44	10.66	7.31	5.88
130	6.19	11.75	7.85	6.54
131	5.93	10.97	7.68	5.43
132	5.79	9.93	4.55	5.47
133	5.42	10.34	7.45	5.95
134	4.92	10.46	7.34	5.63
135	4.80	9.82	7.08	5.44
136	5.07	10.06	7.23	5.28
137	4.97	11.01	7.16	5.59
139	5.95	11.76	7.84	6.36
140	5.86	12.72	7.97	6.77
141	5.49	11.08	7.30	5.37
142	6.30	10.68	7.62	6.27

APPENDIX B

Table B1. Force plate velocity, contact time, step length and Froude number for all trials

Subject	Sex	Gait	Contact Time (s)	Velocity (m/s)	Step Length (m)	Froude
114	M	SW	0.767	1.117	0.855	0.131
115	M	SW	0.79	0.886	0.7	0.088
117	M	SW	0.708	1.182	0.837	0.167
118	M	SW	0.874	0.824	0.714	0.076
119	F	SW	0.69	1.057	0.729	0.137
120	F	SW	0.853	0.936	0.795	0.104
121	F	SW	0.823	0.876	0.72	0.088
122	M	SW	0.68	1.097	0.746	0.147
123	M	SW	0.7	1.005	0.703	0.121
124	F	SW	0.825	0.904	0.746	0.099
125	F	SW	0.737	0.928	0.683	0.109
126	M	SW	0.763	1.044	0.797	0.122
127	F	SW	0.703	1.098	0.772	0.141
128	M	SW	0.692	1	0.692	0.11
129	M	SW	0.803	0.922	0.74	0.099
130	M	SW	0.873	0.902	0.787	0.086
131	F	SW	0.693	1.189	0.825	0.169
132	F	SW	0.578	1.243	0.718	0.182
133	M	SW	0.847	0.85	0.719	0.086
134	F	SW	0.765	1.006	0.769	0.125
135	F	SW	0.744	0.86	0.637	0.092
136	F	SW	1.024	0.636	0.651	0.052
137	F	SW	0.715	1.081	0.773	0.138
139	M	SW	0.813	0.868	0.706	0.086

Table B1 continued

Subject	Sex	Gait	Contact Time (s)	Velocity (m/s)	Step Length (m)	Froude
140	M	SW	0.853	0.933	0.796	0.091
141	F	SW	0.867	0.951	0.824	0.111
142	M	SW	0.645	1.276	0.823	0.181
114	M	NW	0.687	1.351	0.928	0.195
115	M	NW	0.655	1.22	0.797	0.169
117	M	NW	0.627	1.361	0.853	0.222
118	M	NW	0.685	1.202	0.823	0.161
119	F	NW	0.595	1.3	0.773	0.208
120	F	NW	0.711	1.162	0.825	0.16
121	F	NW	0.668	1.201	0.802	0.166
122	M	NW	0.565	1.367	0.773	0.229
123	M	NW	0.565	1.365	0.771	0.222
124	F	NW	0.658	1.139	0.75	0.156
125	F	NW	0.643	1.197	0.768	0.183
126	M	NW	0.648	1.459	0.946	0.241
127	F	NW	0.6	1.382	0.829	0.223
128	M	NW	0.609	1.296	0.789	0.185
129	M	NW	0.58	1.43	0.829	0.239
130	M	NW	0.681	1.296	0.882	0.18
131	F	NW	0.578	1.484	0.858	0.264
132	F	NW	0.496	1.689	0.838	0.339
133	M	NW	0.713	1.138	0.81	0.156
134	F	NW	0.613	1.385	0.849	0.239
135	F	NW	0.59	1.283	0.757	0.207
136	F	NW	0.768	0.913	0.701	0.108

Table B1 continued

Subject	Sex	Gait	Contact Time (s)	Velocity (m/s)	Step Length (m)	Froude
137	F	NW	0.573	1.498	0.858	0.266
139	M	NW	0.66	1.19	0.786	0.162
140	M	NW	0.658	1.348	0.885	0.191
141	F	NW	0.658	1.279	0.842	0.201
142	M	NW	0.608	1.366	0.83	0.208
114	M	FW	0.625	1.596	0.997	0.271
115	M	FW	0.598	1.421	0.85	0.229
117	M	FW	0.547	1.674	0.914	0.336
119	F	FW	0.507	1.627	0.824	0.327
120	F	FW	0.635	1.387	0.881	0.229
121	F	FW	0.528	1.673	0.883	0.325
122	M	FW	0.488	1.712	0.836	0.361
123	M	FW	0.479	1.747	0.836	0.367
124	F	FW	0.518	1.581	0.818	0.302
125	F	FW	0.551	1.407	0.775	0.252
126	M	FW	0.593	1.771	1.049	0.359
127	F	FW	0.513	1.702	0.873	0.341
128	M	FW	0.555	1.539	0.854	0.262
129	M	FW	0.468	1.843	0.863	0.399
130	M	FW	0.577	1.668	0.963	0.3
131	F	FW	0.53	1.668	0.884	0.334
132	F	FW	0.471	1.725	0.813	0.353
133	M	FW	0.611	1.392	0.851	0.233
134	F	FW	0.564	1.63	0.919	0.333
135	F	FW	0.497	1.49	0.74	0.277

Table B1 continued

Subject	Sex	Gait	Contact Time (s)	Velocity (m/s)	Step Length (m)	Froude
136	F	FW	0.592	1.285	0.761	0.215
137	F	FW	0.537	1.794	0.963	0.386
139	M	FW	0.558	1.538	0.857	0.273
140	M	FW	0.508	2.026	1.028	0.46
141	F	FW	0.577	1.542	0.889	0.295
142	M	FW	0.54	1.642	0.887	0.3
115	M	SR	0.312	2.142	0.668	0.525
117	M	SR	0.305	2.295	0.7	0.657
118	M	SR	0.292	1.816	0.53	0.366
119	F	SR	0.23	2.548	0.586	0.79
120	F	SR	0.423	1.604	0.678	0.301
121	F	SR	0.383	1.884	0.721	0.407
125	F	SR	0.307	1.566	0.48	0.313
126	M	SR	0.275	2.481	0.682	0.703
127	F	SR	0.34	2.144	0.728	0.544
128	M	SR	0.36	1.622	0.584	0.288
129	M	SR	0.37	1.854	0.686	0.395
130	M	SR	0.368	2.015	0.742	0.435
131	F	SR	0.375	1.883	0.706	0.42
132	F	SR	0.255	2.183	0.556	0.565
133	M	SR	0.359	1.942	0.696	0.452
134	F	SR	0.428	1.579	0.674	0.31
135	F	SR	0.368	1.607	0.591	0.322
136	F	SR	0.308	1.511	0.464	0.297
137	F	SR	0.283	2.479	0.703	0.746

Table B1 continued

Subject	Sex	Gait	Contact Time (s)	Velocity (m/s)	Step Length (m)	Froude
139	M	SR	0.318	1.908	0.606	0.418
140	M	SR	0.329	1.897	0.624	0.38
141	F	SR	0.28	2.317	0.648	0.677
142	M	SR	0.273	2.676	0.732	0.801
117	M	NR	0.275	2.655	0.73	0.881
118	M	NR	0.27	2.393	0.646	0.638
120	F	NR	0.307	2.082	0.633	0.531
121	F	NR	0.265	2.495	0.661	0.721
123	M	NR	0.265	2.739	0.726	0.925
124	F	NR	0.3	2.357	0.707	0.669
125	F	NR	0.248	2.149	0.534	0.598
126	M	NR	0.25	2.812	0.703	0.927
127	F	NR	0.28	2.604	0.729	0.924
128	M	NR	0.25	2.599	0.65	0.737
129	M	NR	0.223	3.212	0.715	1.215
130	M	NR	0.283	2.863	0.808	0.887
131	F	NR	0.285	2.437	0.694	0.725
132	F	NR	0.23	2.745	0.653	0.906
133	M	NR	0.29	2.288	0.663	0.642
134	F	NR	0.29	2.419	0.702	0.739
135	F	NR	0.333	1.988	0.66	0.502
136	F	NR	0.267	2.098	0.56	0.576
137	F	NR	0.25	2.961	0.739	1.071
139	M	NR	0.28	2.589	0.724	0.779
140	M	NR	0.263	2.876	0.755	0.891

Table B1 continued

Subject	Sex	Gait	Contact Time (s)	Velocity (m/s)	Step Length (m)	Froude
141	F	NR	0.248	2.168	0.537	0.602
114	M	FR	0.218	3.564	0.775	1.388
115	M	FR	0.22	3.063	0.674	1.073
118	M	FR	0.258	2.613	0.675	0.766
119	F	FR	0.205	3.213	0.659	1.283
120	F	FR	0.26	2.793	0.726	0.959
121	F	FR	0.235	2.796	0.657	0.925
124	F	FR	0.235	2.769	0.651	1.016
125	F	FR	0.225	2.703	0.608	1.006
126	M	FR	0.205	3.71	0.76	1.6
129	M	FR	0.203	3.721	0.753	1.625
130	M	FR	0.238	3.645	0.866	1.464
131	F	FR	0.277	2.667	0.737	0.881
132	F	FR	0.195	3.34	0.652	1.337
133	M	FR	0.245	2.495	0.611	0.819
134	F	FR	0.248	3.117	0.771	1.238
135	F	FR	0.281	2.338	0.651	0.711
136	F	FR	0.23	2.702	0.621	1.001
137	F	FR	0.238	3.385	0.801	1.427
139	M	FR	0.22	3.327	0.731	1.324
141	F	FR	0.23	3.459	0.796	1.64
142	M	FR	0.235	3.177	0.747	1.139

Table B2. Speed matched trials between force plate and treadmill data.

Subject	Gait	FP Velocity (m/s)	FP Step Length (m)	Treadmill Velocity (m/s)	Treadmill Step Length (m/s)
114	Walk	1.596	0.997	1.5	1.0894
114	Walk	1.117	0.855	1	0.9713
115	Walk	1.421	0.85	1.5	1.02
115	Walk	1.22	0.797	1	0.8038
117	Walk	1.674	0.914	1.5	1.0294
117	Walk	1.182	0.837	1	0.8338
118	Walk	1.202	0.823	1	0.96
119	Walk	1.627	0.824	1.5	0.9863
119	Walk	1.057	0.729	1	0.92
120	Walk	1.387	0.881	1.5	1.0238
120	Walk	0.936	0.795	1	0.9088
121	Walk	1.673	0.883	1.5	1.0631
121	Walk	0.876	0.72	1	0.8863
122	Walk	1.367	0.773	1.5	0.9581
122	Walk	1.097	0.746	1	0.8488
123	Walk	1.747	0.836	1.5	0.9469
123	Walk	1.005	0.703	1	0.8188
124	Walk	1.581	0.818	1.5	1.0088
124	Walk	0.904	0.746	1	0.9088
125	Walk	1.407	0.775	1.5	0.9863
125	Walk	0.928	0.683	1	0.7925
126	Walk	1.459	0.946	1.5	1.1156
126	Walk	1.044	0.797	1	0.9088
127	Walk	1.702	0.873	1.5	1.0425
127	Walk	1.098	0.772	1	0.8838

Table B2 continued

Subject	Gait	FP Velocity (m/s)	FP Step Length (m)	Treadmill Velocity (m/s)	Treadmill Step Length (m/s)
128	Walk	1.539	0.854	1.5	0.9919
128	Walk	1	0.692	1	0.7913
129	Walk	1.43	0.829	1.5	0.9806
129	Walk	0.922	0.74	1	0.9463
130	Walk	1.668	0.963	1.5	1.0556
130	Walk	0.902	0.787	1	0.8588
131	Walk	1.484	0.858	1.5	1.0331
131	Walk	1.189	0.825	1	0.8838
132	Walk	1.689	0.838	1.5	0.9225
132	Walk	1.243	0.718	1	0.7725
133	Walk	1.392	0.851	1.5	1.0425
133	Walk	0.85	0.719	1	0.8738
134	Walk	1.63	0.919	1.5	1.0256
134	Walk	1.006	0.769	1	0.8663
135	Walk	1.49	0.74	1.5	0.9713
135	Walk	0.86	0.637	1	0.845
136	Walk	1.285	0.761	1.5	0.96
136	Walk	0.913	0.701	1	0.7888
137	Walk	1.498	0.858	1.5	1.0481
137	Walk	1.081	0.773	1	0.935
139	Walk	1.538	0.857	1.5	1.0313
139	Walk	0.868	0.706	1	0.8338
140	Walk	1.348	0.885	1.5	1.0481
140	Walk	0.933	0.796	1	0.8988
141	Walk	1.542	0.889	1.5	0.9844
141	Walk	0.951	0.824	1	0.93

Table B2 continued

Subject	Gait	FP Velocity (m/s)	FP Step Length (m)	Treadmill Velocity (m/s)	Treadmill Step Length (m/s)
114	Run	3.564	0.775	3	0.8888
115	Run	3.063	0.674	3	1.0988
115	Run	2.142	0.668	2.5	1.0563
117	Run	2.655	0.73	3	1.0688
117	Run	2.295	0.7	2.5	1
118	Run	2.613	0.675	3	0.7425
118	Run	2.393	0.646	2.5	0.7188
119	Run	3.213	0.659	3	0.8025
119	Run	2.548	0.586	2.5	0.7656
121	Run	2.796	0.657	3	1.0463
121	Run	2.495	0.661	2.5	0.9625
123	Run	2.739	0.726	3	0.96
124	Run	2.769	0.651	3	0.9638
124	Run	2.357	0.707	2.5	0.875
125	Run	2.703	0.608	2.5	0.8156
126	Run	3.71	0.76	3	1.0875
126	Run	2.812	0.703	2.5	1.0125
127	Run	2.604	0.729	2.5	0.9969
128	Run	2.599	0.65	2.5	0.8125
129	Run	3.212	0.715	3	0.8138
130	Run	2.863	0.808	3	0.9863
131	Run	2.667	0.737	3	0.975
131	Run	2.437	0.694	2.5	0.9813
132	Run	3.34	0.652	3	0.6713
132	Run	2.745	0.653	2.5	0.6813
133	Run	2.495	0.611	2.5	0.9781

Table B2 continued

Subject	Gait	FP Velocity (m/s)	FP Step Length (m)	Treadmill Velocity (m/s)	Treadmill Step Length (m/s)
134	Run	3.117	0.771	3	0.99
134	Run	2.419	0.702	2.5	0.8969
135	Run	2.338	0.651	2.5	0.7438
136	Run	2.702	0.621	2.5	0.7031
137	Run	2.961	0.739	3	0.9263
137	Run	2.479	0.703	2.5	0.8313
139	Run	3.327	0.731	3	1.0163
139	Run	2.589	0.724	2.5	0.9375
140	Run	2.876	0.755	3	0.9788
141	Run	3.459	0.796	3	0.9263
141	Run	2.317	0.648	2.5	0.8813

BIBLIOGRAPHY

Abitbol, M. M. 1991. Ontogeny and evolution of pelvic diameters in anthropoid primates and in *Australopithecus afarensis* (AL 288-1). *Am J Phys Anthropol* 85:135-148.

Abitbol, M. M., F.A. Chervenah, and W.J. Ledger. 1996. *Birth and human evolution: anatomical and obstetrical mechanics in primates* Bergin & Garvey.

Aiello, L. C., and J.C.K. Wells. 2002. Energetics and the evolution of the genus Homo. *Annu Rev Anthropol* :323-338.

Albracht, K., A. Arampatzis, and V. Baltzopoulos. 2008. Assessment of muscle volume and physiological cross-sectional area of the human triceps surae muscle in vivo. *J Biomech* 41:2211-18.

Alexander, R. M. 2005. Models and the scaling of energy costs for locomotion. *J Exp Biol* 208:1645-652.

Ariëns, G. A., W. van Mechelen, H.C. Kemper, and J.W. Twisk. 1997. The longitudinal development of running economy in males and females aged between 13 and 27 years: the Amsterdam Growth and Health Study. *Eur J Appl Physiol Occup Physiol* 76:214-220.

Arnold, A. S., S. Salinas, D.J. Asakawa, and S.L. Delp. 2000. Accuracy of muscle moment arms estimated from MRI-based musculoskeletal models of the lower extremity. *Comput Aided Surg* 5:108-119.

Arsuaga, J. L., C. Lorenzo, J.M. Carretero, A. Gracia, I. Martínez, N. García, J.M. Bermúdez de Castro, and E. Carbonell. 1999. A complete human pelvis from the Middle Pleistocene of Spain. *Nature* 399:255-58.

Asano, T., M. Akagi, and T. Nakamura. 2005. The functional flexion-extension axis of the knee corresponds to the surgical epicondylar axis: in vivo analysis using a biplanar image-matching technique. *J Arthroplasty* 20:1060-67.

Beck, M., J.B. Sledge, E. Gautier, C.F. Dora, and R. Ganz. 2000. The anatomy and function of the gluteus minimus muscle. *J Bone Joint Surg Br* 82:358.

Berge, C. 1994. How did the australopithecines walk? A biomechanical study of the hip and thigh of *Australopithecus afarensis*. *J Hum Evol* 26:259-273.

Berge, C., and D. Goularas. 2010. A new reconstruction of Sts 14 pelvis (*Australopithecus africanus*) from computed tomography and three-dimensional modeling techniques. *J Hum Evol* 58:262-272.

Berge, C., R. Orban-Segebarth, and P. Schmid. 1984. Obstetrical interpretation of the australopithecine pelvic cavity. *J Hum Evol* 13:573-587.

Berger, L. R., D.J. de Ruiter, S.E. Churchill, P. Schmid, K.J. Carlson, P.H. Dirks, and J.M. Kibii. 2010. Australopithecus sediba: a new species of Homo-like australopith from South Africa. *Science* 328:195-204.

Bhambhani, Y., and M. Singh. 1985. Metabolic and cinematographic analysis of walking and running in men and women. *Med Sci Sports Exerc* 17:131-37.

Biewener, A. A. 1989. Scaling body support in mammals: limb posture and muscle mechanics. *Science* 245:45-48.

Biewener, A. A. 2003. *Animal locomotion* Oxford University Press, New York.

Biewener, A. A., C.T. Farley, T.J. Roberts, and M. Temaner. 2004. Muscle mechanical advantage of human walking and running: implications for energy cost. *J Appl Physiol* 97:2266-274.

Bischoff, J. L., R.W. Williams, R.J. Rosenbauer, A. Aramburu, J.L. Arsuaga, N. Garcia, and G. Cuenca-Bescós. 2007. High-resolution U-series dates from the Sima de los Huesos hominids yields: implications for the evolution of the early Neanderthal lineage. *J Archaeol Sci* 34:763-770.

Bourdin, M., J. Pastene, M. Germain, and J.R. Lacour. 1993. Influence of training, sex, age and body mass on the energy cost of running. *Eur J Appl Physiol Occup Physiol* 66:439-444.

Bramble, D. M., and D.E. Lieberman. 2004. Endurance running and the evolution of *Homo*. *Nature* 432:345-352.

Brown, F., J. Harris, R. Leakey, and A. Walker. 1985. Early *Homo erectus* skeleton from west Lake Turkana, Kenya. *Nature* 316:788-792.

Bull, A. M. J., and A.A. Amis. 1998. Knee joint motion: description and measurement. *P I Mech Eng H* 212:357-372.

Bunc, V., and J. Heller. 1989. Energy cost of running in similarly trained men and women. *Eur J Appl Physiol Occup Physiol* 59:178-183.

Burr, D. B., D.P. Van Gerven, and B.L. Gustav. 1977. Sexual dimorphism and mechanics of the human hip: a multivariate assessment. *Am J Phys Anthropol* 47:273-78.

Caldwell, W., H.C. Moloy, and P. Swenson. 1939. The anatomical variations in the female pelvis and their classification according to morphology. *Am J Roentgenol Radium Ther* 41:505-06.

Caldwell, W. E., H.C. Moloy, and D.A. D'Esopo. 1934. Further studies on the pelvic architecture. *Am J Obstet Gynecol* 28:482.

Cerling, T. E., J.G. Wynn, S.A. Andanje, M.I. Bird, D.K. Korir, N.E. Levin, W. Mace, A.N. Macharia, J. Quade, and C.H. Remien. 2011. Woody cover and hominin environments in the past 6 million years. *Nature* 476:51-56.

Cho, S. H., J.M. Park, and O.Y. Kwon. 2004. Gender differences in three dimensional gait analysis data from 98 healthy Korean adults. *Clin Biomech (Bristol, Avon)* 19:145-152.

Chumanov, E. S., C. Wall-Scheffler, and B.C. Heiderscheit. 2008. Gender differences in walking and running on level and inclined surfaces. *Clin Biomech (Bristol, Avon)* 23:1260-68.

Churchill, P. h. D., M.D. Incavo, B.S. Johnson, and P.h.D. Beynnon. 1998. The transepicondylar axis approximates the optimal flexion axis of the knee. *Clin Orthop Relat R* 365:111-18.

Clark, J. M., and D.R. Haynor. 1987. Anatomy of the abductor muscles of the hip as studied by computed tomography. *J Bone Joint Surg Am* 69:1021-031.

Correia, H., S. Balseiro, and M. De Areia. 2005. Sexual dimorphism in the human pelvis: testing a new hypothesis. *HOMO* 56:153-160.

Corruccini, R. S., and H.M. McHenry. 1980. Hominid femoral neck length. *Am J Phys Anthropol* 52:397-98.

Dart, R. A. 1949. Innominate fragments of *Australopithecus prometheus*. *Am J Phys Anthropol* 7:301-334.

Day, M. H. 1971. Postcranial remains of Homo erectus from bed IV, Olduvai Gorge, Tanzania. *Nature* 232:382-87.

Dejaeger, D., P.A. Willems, and N.C. Heglund. 2001. The energy cost of walking in children. *Eur J Appl Physiol* 441:538-543.

Doke, J., J.M. Donelan, and A.D. Kuo. 2005. Mechanics and energetics of swinging the human leg. *J Exp Biol* 208:439-445.

Donelan, J. M., R. Kram, and A.D. Kuo. 2001. Mechanical and metabolic determinants of the preferred step width in human walking. *Proc Biol Sci* 268:1985-992.

Donelan, J. M., R. Kram, and A.D. Kuo. 2002. Mechanical work for step-to-step transitions is a major determinant of the metabolic cost of human walking. *J Exp Biol* 205:3717-727.

Drake, R. L., W. Vogl, et al. 2005. *Gray's anatomy for students* Elsevier/Churchill Livingstone: Philadelphia.

Eng, J. J., and D.A. Winter. 1995. Kinetic analysis of the lower limbs during walking: what information can be gained from a three-dimensional model? *J Biomech* 28:753-58.

Fedak, M. A., L. Rome, and H.J. Seeherman. 1981. One-step N2-dilution technique for calibrating open-circuit VO2 measuring systems. *J Appl Physiol* 51:772-76.

Ferber, R., I.M. Davis, and D.S. Williams. 2003. Gender differences in lower extremity mechanics during running. *Clin Biomech (Bristol, Avon)* 18:350-57.

Fetto, J., A. Leali, and A. Moroz. 2002. Evolution of the Koch model of the biomechanics of the hip: clinical perspective. *J Orthop Sci* 7:724-730.

Folland, J. P., and A.G. Williams. 2007. The adaptations to strength training: morphological and neurological contributions to increased strength. *Sports Med* 37:145-168.

Friederich, J. A., and R.A. Brand. 1990. Muscle fiber architecture in the human lower limb. *J Biomech* 23:91-95.

Gabunia, L., A. Vekua, D. Lordkipanidze, C.C. Swisher, R. Ferring, A. Justus, M. Nioradze, M. Tvalchrelidze, S.C. Antón, and G. Bosinski. 2000. Earliest Pleistocene hominid cranial remains from Dmanisi, Republic of Georgia: taxonomy, geological setting, and age. *Science* 288:1019.

Gottschalk, F., S. Kourosh, and B. Leveau. 1989. The functional anatomy of tensor fasciae latae and gluteus medius and minimus. *J Anat* 166:179-189.

Gottschall, J. S., and R. Kram. 2003. Energy cost and muscular activity required for propulsion during walking. *J Appl Physiol* 94:1766-772.

Gottschall, J. S., and R. Kram. 2005. Energy cost and muscular activity required for leg swing during walking. *J Appl Physiol* 99:23-30.

Griffin, T. M., T.J. Roberts, and R. Kram. 2003. Metabolic cost of generating muscular force in human walking: insights from load-carrying and speed experiments. *J Appl Physiol* 95:172-183.

Grün, R., and C.B. Stringer. 1991. Electron spin resonance dating and the evolution of modern humans. *Archaeometry* 33:153-199.

Haeusler, M. 2002. New insights into the locomotion of *Australopithecus africanus* based on the pelvis. *Evol Anthropol* 11:53-57.

Haile-Selassie, Y., B.M. Latimer, M. Alene, A.L. Deino, L. Gibert, S.M. Melillo, B.Z. Saylor, G.R. Scott, and C.O. Lovejoy. 2010. An early *Australopithecus afarensis* postcranium from Woranso-Mille, Ethiopia. *Proc Natl Acad Sci U S A* 107:12121-26.

Hall, C., A. Figueroa, B. Fernhall, and J.A. Kanaley. 2004. Energy expenditure of walking and running: comparison with prediction equations. *Med Sci Sports Exerc* 36:2128-134.

Häusler, M., and L. Berger. 2001. Stw 441/465: a new fragmentary ilium of a small-bodied *Australopithecus africanus* from Sterkfontein, South Africa. *J Hum Evol* 40:411-17.

Häusler, M., and P. Schmid. 1995. Comparison of the pelves of Sts 14 and AL288-1: implications for birth and sexual dimorphism in australopithecines. *J Hum Evol* 29:363-383.

Hsin, J., R. Saluja, R.E. Eilert, and J.D. Wiedel. 1996. Evaluation of the biomechanics of the hip following a triple osteotomy of the innominate bone. *J Bone Joint Surg Am* 78:855-862.

Hunt, K. D. 1998. Ecological morphology of *Australopithecus afarensis*: traveling terrestrially, eating arboreally. In *Primate locomotion. New York: Plenum Press*.

Inman, V. T. 1947. Functional aspects of the abductor muscles of the hip. *J Bone Joint Surg Am* 29:607.

Johanson, D. C., C.O. Lovejoy, W.H. Kimbel, T.D. White, S.C. Ward, M.E. Bush, B.M. Latimer, and Y. Coppens. 1982. Morphology of the Pliocene partial hominid skeleton (AL 288-1) from the Hadar Formation, Ethiopia. *Am J Phys Anthropol* 57:403-451.

Johnston, R. C., R.A. Brand, and R.D. Crowninshield. 1979. Reconstruction of the hip. A mathematical approach to determine optimum geometric relationships. *J Bone Joint Surg Am* 61:639-652.

Jordaan, H. V. 1976. The differential development of the hominid pelvis. *S Afr Med J* 50:744-48.

Kawai, A., S.I. Backus, J.C. Otis, H. Inoue, and J.H. Healey. 2000. Gait characteristics of patients after proximal femoral replacement for malignant bone tumour. *J Bone Joint Surg Br* 82:666-69.

Kellis, E., N. Galanis, K. Natsis, and G. Kapetanos. 2010. Muscle architecture variations along the human semitendinosus and biceps femoris (long head) length. *J Electromyogr Kinesiol* 20:1237-243.

Kibii, J. M., and R.J. Clarke. 2003. A reconstruction of the Stw 431 *Australopithecus* pelvis based on newly discovered fragments: news and views. *S Afr J Sci* 99:225-26.

Kimbel, W. H., and L.K. Delezene. 2009. "Lucy" redux: a review of research on *Australopithecus afarensis*. *Am J Phys Anthropol* 140 Suppl 49:2-48.

Konje, J. C., and O.A. Ladipo. 2000. Nutrition and obstructed labor. *Am J Clin Nutr* 72:291S.

Kram, R., and C.R. Taylor. 1990. Energetics of running: a new perspective. *Nature* 346:265-67.

Kramer, P. A., and G.G. Eck. 2000. Locomotor energetics and leg length in hominid bipedality. *J Hum Evol* 38:651-666.

Krevolin, J. L., M.G. Pandy, and J.C. Pearce. 2004. Moment arm of the patellar tendon in the human knee. *J Biomech* 37:785-88.

Krogman, W. M. 1951. The scars of human evolution. *Sci Am* :54-57.

Kumagai, M., N. Shiba, F. Higuchi, H. Nishimura, and A. Inoue. 1997. Functional evaluation of hip abductor muscles with use of magnetic resonance imaging. *J Orthop Res* 15:888-893.

LaVelle, M. 1995. Natural selection and developmental sexual variation in the human pelvis. *Am J Phys Anthropol* 98:59-72.

Leutenegger, W. 1982. Encephalization and obstetrics in primates with particular reference to human evolution. Ed. M Armstrong and E Armstrong. *Primate brain evolution: Methods and concepts* Plenum, New York.

Leutenegger, W. 1987. Neonatal brain size and neurocranial dimensions in Pliocene hominids: implications for obstetrics. *J Hum Evol* 16:291-96.

de Leva, P. 1996. Adjustments to Zatsiorsky-Seluyanov's segment inertia parameters. *J Biomech* 29:1223-230.

Lieberman, D. E., D.A. Raichlen, H. Pontzer, D.M. Bramble, and E. Cutright-Smith. 2006. The human gluteus maximus and its role in running. *J Exp Biol* 209:2143-155.

Liselele, H. B., C.K. Tshibangu, and S. Meuris. 2000. Association between external pelvimetry and vertex delivery complications in African women. *Acta Obstet Gynecol Scand* 79:673-78.

Lovejoy, C. O. 1988. Evolution of human walking. *Sci Am* 259:82-89.

Lovejoy, C. O. 2005. The natural history of human gait and posture. Part 1. Spine and pelvis. *Gait Posture* 21:95-112.

Lovejoy, C. O., G. Suwa, L. Spurlock, B. Asfaw, and T.D. White. 2009. The pelvis and femur of *Ardipithecus ramidus*: the emergence of upright walking. *Science* 326:71.

Lovejoy, C. O., K.G. Heiple, and A.H. Burstein. 1973. The gait of *Australopithecus*. *Am J Phys Anthropol* 38:757-779.

Lundberg, A., O.K. Svensson, G. Nemeth, and G. Selvik. 1989. The axis of rotation of the ankle joint. *J Bone Joint Surg Br* 71:94.

MacLatchy, L. M. 1996. Another look at the australopithecine hip. *J Hum Evol* 31:455-476.

McHenry, H. M. 1975. Biomechanical interpretation of the early hominid hip. *J Hum Evol* 4:343-355.

McHenry, H. M., and L.A. Temerin. 1979. The evolution of hominid bipedalism: evidence from the fossil record. *Yearb Phys Anthropol* 22:105-131.

McLeish, R. D., and J. Charnley. 1970. Abduction forces in the one-legged stance. *J Biomech* 3:191-209.

Meindl, R. S., C.O. Lovejoy, R.P. Mensforth, and L. Don Carlos. 1985. Accuracy and direction of error in the sexing of the skeleton: implications for paleodemography. *Am J Phys Anthropol* 68:79-85.

Merchant. 1965. Hip abductor muscle force; an experimental study of the influence of hip position with particular reference to rotation. *J Bone Joint Surg Am* 47:462.

Merchant, K. M., J. Villar, and E. Kestler. 2001. Maternal height and newborn size relative to risk of intrapartum caesarean delivery and perinatal distress. *BJOG* 108:689-696.

Nagano, A., B.R. Umberger, M.W. Marzke, and K.G. Gerritsen. 2005. Neuromusculoskeletal computer modeling and simulation of upright, straight-legged, bipedal locomotion of *Australopithecus afarensis* (A.L. 288-1). *Am J Phys Anthropol* 126:2-13.

Napier, J. R. 1964. The evolution of bipedal walking in the hominids. *Arch Biol* 75:673-708.

Neilson, J. P., T. Lavender, S. Quenby, and S. Wray. 2003. Obstructed labour. *Brit Med Bull* 67:191.

Pandy, M. G., Y.C. Lin, and H.J. Kim. 2010. Muscle coordination of mediolateral balance in normal walking. *J Biomech* 43:2055-064.

Pauwels, F., R. Furlong, and P. Maquet. 1976. *Biomechanics of the normal and diseased hip: theoretical foundation, technique, and results of treatment: an atlas* Springer-Verlag.

Perron, M., F. Malouin, H. Moffet, and B.J. McFadyen. 2000. Three-dimensional gait analysis in women with a total hip arthroplasty. *Clin Biomech* 15:504-515.

Ponce de León, M. S., L. Golovanova, V. Doronichev, G. Romanova, T. Akazawa, O. Kondo, H. Ishida, and C.P. Zollikofer. 2008. Neanderthal brain size at birth provides insights into the evolution of human life history. *Proc Natl Acad Sci U S A* 105:13764-68.

Pontzer, H. 2005. A new model predicting locomotor cost from limb length via force production. *J Exp Biol* 208:1513-524.

Pontzer, H. 2007. Predicting the energy cost of terrestrial locomotion: a test of the LiMb model in humans and quadrupeds. *J Exp Biol* 210:484-494.

Pontzer, H., C. Rolian, G.P. Rightmire, T. Jashashvili, M.S. Ponce de León, D. Lordkipanidze, and C.P. Zollikofer. 2010. Locomotor anatomy and biomechanics of the Dmanisi hominins. *J Hum Evol* 58:492-504.

Pontzer, H., D.A. Raichlen, and M.D. Sockol. 2009. The metabolic cost of walking in humans, chimpanzees, and early hominins. *J Hum Evol* 56:43-54.

Proschan MA, Waclawiw MA. 2000. Practical guidelines for multiplicity adjustment in clinical trials. Controlled clinical trials 21: 527-539.

Rak, Y. 1990. On the differences between two pelvises of Mousterian context from the Qafzeh and Kebara caves, Israel. *Am J Phys Anthropol* 81:323-332.

Rak, Y. 1991. Lucy's pelvic anatomy: its role in bipedal gait. *J Hum Evol* 20:283-290.

Rak, Y., and B. Arensburg. 1987. Kebara 2 Neanderthal pelvis: First look at a complete inlet. *Am J Phys Anthropol* 73:227-231.

Reynolds. 1931. The evolution of the human pelvis in relation to the mechanics of the erect posture. *Papers of the Peabody Museum of American Archaeology and Ethnology* 11:255-334.

Richmond, B. G., and W.L. Jungers. 2008. *Orrorin tugenensis* femoral morphology and the evolution of hominin bipedalism. *Science* 319:1662-65.

Roberts, T. J., R. Kram, P.G. Weyand, and C.R. Taylor. 1998a. Energetics of bipedal running. I. Metabolic cost of generating force. *J Exp Biol* 201:2745-751.

Roberts, T. J., M.S. Chen, and C.R. Taylor. 1998b. Energetics of bipedal running. II. Limb design and running mechanics. *J Exp Biol* 201:2753-762.

Robertson, D. G. E. 2004. *Research methods in biomechanics* Human Kinetics Publishers.

Robinson, J. T., and J.T. Robinson. 1972. *Early hominid posture and locomotion* University of Chicago Press.

Rodman, P. S., and H.M. McHenry. 1980. Bioenergetics and the origin of hominid bipedalism. *Am J Phys Anthropol* 52:103-06.

Rolian, C., D.E. Lieberman, J. Hamill, J.W. Scott, and W. Werbel. 2009. Walking, running and the evolution of short toes in humans. *J Exp Biol* 212:713-721.

Rose, M. D. 1984. A hominine hip bone, KNM-ER 3228, from East Lake Turkana, Kenya. *Am J Phys Anthropol* 63:371-78.

Rosenberg, K., and W. Trevathan. 1995. Bipedalism and human birth: the obstetrical dilemma revisited. *Evol Anthropol* 4:161-68.

Rosenberg, K., and W. Trevathan. 2002. Birth, obstetrics and human evolution. *BJOG* 109:1199-1206.

Rosenberg, K. R. 1992. The evolution of modern human childbirth. *Am J Phys Anthropol* 35:89-124.

Rosenberg, K. R. 1998. Morphological variation in west Asian postcrania. In *Neandertals and modern humans in Western Asia* Edited by T Akazawa, K Aoki and O Bar-Yosef. Springer.

Rosenberg, K. R., C.L. Brace, D.W. Frayer, M.C. Geise, D.L. Greene, R.G. Tague, N.C. Tappen, W.R. Trevathan, and E. Trinkaus. 1988. The functional significance of neandertal public length [and comments and reply]. *Curr Anthropol* 29:595-617.

Rosenberg, K. R., L. Zuné, and C.B. Ruff. 2006. Body size, body proportions, and encephalization in a Middle Pleistocene archaic human from northern China. *Proc Natl Acad Sci U S A* 103:3552.

Ruff, C. B. 1994. Morphological adaptation to climate in modern and fossil hominids. *Am J Phys Anthropol* 37:65-107.

Ruff, C. B. 1995. Biomechanics of the hip and birth in early *Homo*. *Am J Phys Anthropol* 98:527-574.

Ruff, C. B. 1998. Evolution of the hominid hip. In *Primate locomotion: recent advances. New York: Plenum Press.*

Ruff, C. B. 2010. Body size and body shape in early hominins - implications of the Gona pelvis. *J Hum Evol* 58:166-178.

Rugg, S. G., R.J. Gregor, B.R. Mandelbaum, and L. Chiu. 1990. In vivo moment arm calculations at the ankle using magnetic resonance imaging (MRI). *J Biomech* 23:495-97.

Sariali, E., V. Veysi, and T. Stewart. 2008. Biomechanics of the human hip-consequences for total hip replacement. *Curr Orthopead* 22:371-75.

Saunders, J. B., V.T. Inman, and H.D. Eberhart. 1953. The major determinants in normal and pathological gait. *J Bone Joint Surg Am* 35-A:543-558.

Scheys, L., A. Spaepen, P. Suetens, and I. Jonkers. 2008. Calculated moment-arm and muscle-tendon lengths during gait differ substantially using MR based versus rescaled generic lower-limb musculoskeletal models. *Gait Posture* 28:640-48.

Schultz, A. H. 1949. Sex differences in the pelves of primates. *Am J Phys Anthropol* 7:401-424.

Sharma, K. 2002. Genetic basis of human female pelvic morphology: a twin study. *Am J Phys Anthropol* 117:327-333.

Sheehan, F. T. 2007. The finite helical axis of the knee joint (a non-invasive in vivo study using fast-PC MRI). *J Biomech* 40:1038-047.

Sheehan, F. T. 2010. The instantaneous helical axis of the subtalar and talocrural joints: a non-invasive in vivo dynamic study. *J Foot Ankle Res* 3:13.

Sibley, L. M., G.J. Armelagos, and D.P. Van Gerven. 1992. Obstetric dimensions of the true pelvis in a Medieval population from Sudanese Nubia. *Am J Phys Anthropol* 89:421-430.

Sigmon, B. A. 1971. Bipedal behavior and the emergence of erect posture in man. *Am J Phys Anthropol* 34:55-60.

Simpson, S. W., J. Quade, N.E. Levin, R. Butler, G. Dupont-Nivet, M. Everett, and S. Semaw. 2008. A female *Homo erectus* pelvis from Gona, Ethiopia. *Science* 322:1089-1092.

Smith, L. K., J.L. Lelas, and D.C. Kerrigan. 2002. Gender differences in pelvic motions and center of mass displacement during walking: stereotypes quantified. *J Womens Health Gend Based Med* 11:453-58.

Sockol, M. D., D.A. Raichlen, and H. Pontzer. 2007. Chimpanzee locomotor energetics and the origin of human bipedalism. *Proc Natl Acad Sci U S A* 104:12265-69.

Spoor, F., M.G. Leakey, P.N. Gathogo, F.H. Brown, S.C. Antón, I. McDougall, C. Kiarie, F.K. Manthi, and L.N. Leakey. 2007. Implications of new early *Homo* fossils from Ileret, east of Lake Turkana, Kenya. *Nature* 448:688-691.

Stern Jr, J. T., and R.L. Susman. 1983. The locomotor anatomy of *Australopithecus afarensis*. *Am J Phys Anthropol* 60:279-317.

Steudel-Numbers, K. L. 2006. Energetics in *Homo erectus* and other early hominins: the consequences of increased lower-limb length. *J Hum Evol* 51:445-453.

Steudel-Numbers, K. L., and M.J. Tilkens. 2004. The effect of lower limb length on the energetic cost of locomotion: implications for fossil hominins. *J Hum Evol* 47:95-109.

Stewart, D. B. 1984. The pelvis as a passageway. I. Evolution and adaptations. *Br J Obstet Gynaecol* 91:611-17.

Stewart, D. B. 1984. The pelvis as a passageway. II. The modern human pelvis. *Br J Obstet Gynaecol* 91:618-623.

Tague, R. G. 1989. Variation in pelvic size between males and females. *Am J Phys Anthropol* 80:59-71.

Tague, R. G. 1992. Sexual dimorphism in the human bony pelvis, with a consideration of the Neandertal pelvis from Kebara Cave, Israel. *Am J Phys Anthropol* 88:1-21.

Tague, R. G. 1994. Maternal mortality or prolonged growth: age at death and pelvic size in three prehistoric Amerindian populations. *Am J Phys Anthropol* 95:27-40.

Tague, R. G. 2005. Big-bodied males help us recognize that females have big pelves. *Am J Phys Anthropol* 127:392-405.

Tague, R. G., and C.O. Lovejoy. 1986. The obstetric pelvis of AL 288-1 (Lucy). *J Hum Evol* 15:237-255.

Taunton, J. E., M.B. Ryan, D.B. Clement, D.C. McKenzie, D.R. Lloyd-Smith, and B.D. Zumbo. 2002. A retrospective case-control analysis of 2002 running injuries. *Br J Sports Med* 36:95-101.

Taylor, C. R., K. Schmidt-Nielsen, and J.L. Raab. 1970. Scaling of energetic cost of running to body size in mammals. *Am J Physiol* 219:1104-07.

Taylor, C. R., N.C. Heglund, and G.M. Maloiy. 1982. Energetics and mechanics of terrestrial locomotion. I. Metabolic energy consumption as a function of speed and body size in birds and mammals. *J Exp Biol* 97:1.

Traina, F., M. De Clerico, F. Biondi, F. Pilla, E. Tassinari, and A. Toni. 2009. Sex differences in hip morphology: is stem modularity effective for total hip replacement? *J Bone Joint Surg Am* 91 Suppl 6:121-28.

Trevathan, W. R. 1996. The evolution of bipedalism and assisted birth. *Med Anthropol Q* 10:287-290.

Trinkaus, E. 1976. The morphology of European and Southwest Asian Neandertal pubic bones. *Am J Phys Anthropol* 44:95-103.

Trinkaus, E. 1984. Neandertal pubic morphology and gestation length. *Curr Anthropol* 25:509-514.

van den Bogert, A. J., C. Reinschmidt, and A. Lundberg. 2008. Helical axes of skeletal knee joint motion during running. *J Biomech* 41:1632-38.

Walker, A. 1993. Perspectives on the Nariokotome discovery. Ed. A Walker and R Leakey. *Nariokotome Homo erectus Skeleton*, Harvard University Press, Cambridge.

Walker, A., and C.B. Ruff. 1993. The reconstruction of the pelvis. Ed. A Walker and R Leakey. *Nariokotome Homo erectus Skeleton*, Harvard University Press, Cambridge.

Wall, L. L. 2006. Obstetric vesicovaginal fistula as an international public-health problem. *Lancet* 368:1201-09.

Ward, C. V. 2002. Interpreting the posture and locomotion of *Australopithecus afarensis*: where do we stand? *Am J Phys Anthropol* Suppl 35:185-215.

Ward, C. V., W.H. Kimbel, and D.C. Johanson. 2011. Complete fourth metatarsal and arches in the foot of *Australopithecus afarensis*. *Science* 331:750-53.

Washburn, S. L. 1960. Tools and human evolution. *Scientific American* 203:63-75.

Weaver, T. D., and J.J. Hublin. 2009. Neandertal birth canal shape and the evolution of human childbirth. *Proc Natl Acad Sci U S A* 106:8151.

White, T. D., B. Asfaw, Y. Beyene, Y. Haile-Selassie, C.O. Lovejoy, G. Suwa, and G. WoldeGabriel. 2009. *Ardipithecus ramidus* and the paleobiology of early hominids. *Science* 326:64.

Wiesman Jr, H. J., S.R. Simon, F.C. Ewald, W.H. Thomas, and C.B. Sledge. 1978. Total hip replacement with and without osteotomy of the greater trochanter. Clinical and biomechanical comparisons in the same patients. *J Bone Joint Surg Am* 60:203.

Williams, K. R., P.R. Cavanagh, and J.L. Ziff. 1987. Biomechanical studies of elite female distance runners. *Int J Sports Med* 8 Suppl 2:107-118.

Winter, D. A. 2005. *Biomechanics and motor control of human movement* John Wiley & Sons Inc.

Wittman, A. B., and L.L. Wall. 2007. The evolutionary origins of obstructed labor: bipedalism, encephalization, and the human obstetric dilemma. *Obstet Gynecol Surv* 62:739-748.

Wolpoff, M. H. 1978. Some implications of relative biomechanical neck length in hominid femora. *Am J Phys Anthropol* 48:143-47.

Zihlman, A. L., and L. Brunker. 1979. Hominid bipedalism: then and now. *Yearb Phys Anthropol* 22:132-162.